

**Plant morphology, environment, and leaf area growth
in wheat and maize**

Promotor: dr. ir. P.C. Struik
hoogleraar in de gewasfysiologie

Co-promotor: dr. ir. J. Vos
universitair hoofddocent bij het Departement Plantenteelt

1171 1999 2 11

**Plant morphology, environment, and leaf area growth
in wheat and maize**

H.J. Bos

Proefschrift
ter verkrijging van de graad van doctor
op gezag van de rector magnificus
dr. C.M. Karssen
in het openbaar te verdedigen
op vrijdag 5 februari 1999
des namiddags te vier uur in de Aula
van de Landbouwniversiteit te Wageningen

wa 962145

CIP-DATA KONINKLIJKE BIBLIOTHEEK, DEN HAAG

Bos, H.J.

Plant morphology, environment, and leaf area growth
in wheat and maize. / H.J. Bos. - [S.l. : s.n.].

Thesis Landbouw Universiteit Wageningen. - With ref. -

With summary in Dutch.

ISBN 90-5808-003-x

Subject headings: wheat; maize.

Cover design: Linda van Leeuwen

The research described in this thesis was part of the research programme of the C.T. de Wit
Graduate School Production Ecology

BIBLIOTHEEK
LANDBOUWUNIVERSITEIT
WAGENINGEN

Stellingen

1. De stelling van Kemp (1981) dat verschillen in bladmorfologische kenmerken binnen een tarweplant bepaald worden door verschillen in het tijdstip van verschijning, is voor juveniele planten onjuist.

Kemp DR. 1981. Comparison of growth rates and sugar and protein concentrations of the extension zone of main shoot and tiller leaves of wheat. *Journal of Experimental Botany* 32: 151-158.

Dit proefschrift.

2. De gemeenschappelijkheid van de morfologische kenmerken van grasachtigen maakt één basismodel voor waarneming en simulatie van bladoppervlaktegroei mogelijk.

Dit proefschrift.

3. Voor de verklaring van effecten van omgevingsfactoren op bladoppervlaktegroei per plant is voor grasachtigen de hoeveelheid bladeren belangrijker dan individuele bladgroottes.

Dit proefschrift.

4. Met de lineaal kan de studie naar gewasmorfologie nog heel ver vooruit, ook al geeft het gebruik van ingewikkelde meetapparatuur meer status.

Dit proefschrift.

5. Object-georiënteerde technieken zijn goed toepasbaar voor simulatiemodellen in de biologie.

6. Plantmorfologie dient een belangrijk aspect te zijn van elk onderzoek naar concurrentie tussen verschillende plantensoorten.

7. Investeren in communicatielijnen is rendabeler dan investeren in de Betuwelijn.

8. Alphanumerieke toetsen op telefoons vergroten de markt voor servicenummers.

9. Voor de grote stern heeft de aanwezigheid van kokmeeuwen bij zijn broedkolonie blijkbaar een voordeel dat groter is dan het nadeel van visroof door de kokmeeuw, aangezien de grote stern er zelf voor kiest naast deze kleptoparasiet te broeden.

Stienen EWM, Brenninkmeijer A, Geschiere CE. 1993. De relatie tussen de fourageermogelijkheden van de grote stern Sterna sandvicensis en het doorzicht van water, alsmede de invloed van kleptoparasitisme door de kokmeeuw Larus ridibundus op de visaanvoer en het broedsucces van de grote stern. Intern Verslag DLO-Instituut voor Bos- en Natuuronderzoek, Arnhem.

10. Een Bos lijkt van een afstand geslotener dan dat hij van dichtbij blijkt te zijn.

Stellingen behorend bij het proefschrift:

Plant morphology, environment, and leaf area growth in wheat and maize.

Bert Bos

Wageningen, 5 februari 1999

Abstract

Leaf area expansion of wheat (*Triticum aestivum* L.) and maize (*Zea mays* L.) plants, as contrasting representatives of the *Gramineae* family, was analysed. Seven variables were identified that together completely determine leaf area expansion of the plant: leaf appearance rate per tiller, specific site usage (fraction of buds that ultimately develop into a visible tiller at a specific site), Haun Stage-delay (indicating the timing of tiller appearance relative to the parent tiller), leaf elongation rate, leaf elongation duration, maximum leaf width and a leaf shape variable.

Experiments with spaced plants in growth chambers yielded equations in which the effects of leaf and tiller position, temperature and photosynthetic photon flux density (PPFD) were quantified for each leaf area variable. In non-tillering species maize, leaf appearance rate and leaf elongation rate were higher, and leaf elongation duration was shorter at higher temperatures. At higher PPFD values, leaf appearance rate and maximum leaf width were higher and leaf elongation rate was lower. In wheat, the effects of temperature and PPFD were qualitatively equal to those in maize, except that there was no effect of PPFD on maximum leaf width. In the tillering species wheat, specific site usage was higher at lower temperatures and higher PPFD values. Equations were developed for the effects of leaf position on leaf elongation rate and maximum leaf width.

This knowledge was used in the analysis of effects of plant density in growth chamber and field experiments. Plant density mainly affected leaf appearance rate in maize and specific site usage in wheat. For both species, the effects of plant density on these variables seemed well related to local assimilate availability.

Based upon the morphological framework presented, a simulation model was developed for wheat using the principles of object orientation. Plant related processes were strictly simulated at organ level. The simulation results showed clear differences in leaf area expansion for leaves at different positions in the plant.

The morphological framework can be used for experimental analysis of leaf area growth, revealing mechanisms regulating leaf area growth of plants. The simulation model is flexible and can be easily extended for different environmental conditions and plant species.

Key words: leaf area, wheat, maize, photosynthetic photon flux density, temperature, plant density, modelling, object orientation.

Woord vooraf

Dit proefschrift is tot stand gekomen met de hulp van vele personen. Enkele (groepen van) personen wil ik hier in het bijzonder vermelden.

Ten eerste wil ik mijn team van begeleiders bedanken. Allereerst Jan Neuteboom, die met zijn immer kritische blik met name hoofdstukken 2 en 3 heeft helpen vorm en inhoud te geven. Vervolgens Jan Vos, die dit onderzoek initieerde en op een breed vlak dit onderzoek begeleidde. Last but not least mijn promotor Paul Struik, die telkens weer met een verbazingwekkende combinatie van snelheid en nauwgezetheid de manuscripten van commentaar voorzag.

Met mijn collega's van de vakgroep Agronomie heb ik immer prettig samengewerkt. TUPEA-beheer zorgde ervoor dat het netwerk bijna altijd in de lucht bleef en zorgde voor snelle hulp bij allerlei problemen. In de personeelsvereniging heb ik met veel plezier allerlei activiteiten helpen organiseren, zoals bowlings, dagjes uit en kerstlunches. De sfeer en samenwerking binnen de pv was altijd bijzonder prettig. Hennie Halm wil ik bedanken voor het uitvoeren van chemische analyses en Klaas Scholte voor statistische adviezen. Hans Romberg wil ik bedanken voor de leuke sfeer die hij creëerde op de onderste verdieping van de halve cirkel. Wampie van Schouwenburg wil ik bedanken voor het gereed maken van enige manuscripten voor verzending naar tijdschriften. In het bijzonder wil ik mijn kamergenoot Jeroen Groot bedanken voor de gezellige sfeer in de kamer en de vele discussies die we voerden op vakmatig en ander vlak. Ik ben blij dat we elkaar nog regelmatig bij Panfox treffen.

Bij de uitvoering van de experimenten ben ik veel dank verschuldigd aan de mensen van UNIFARM. Door de goede verzorging van de proeven en de vele hulp bij zaai- en oogstwerkzaamheden kon de omvangrijke dataset die ten grondslag ligt aan dit proefschrift worden verzameld.

Veel inspiratie heb ik opgedaan bij de lunchsessies van de zogenaamde 'Morvoos'-groep. De inbreng van Marcel van Ooijen, Jacco Wallinga, Jeroen Groot en Jan Neuteboom leidde tot vele nieuwe ideeën.

Furthermore I would like to thank the following students for their contribution to this thesis during their graduation projects: Arend Biewenga, Aliye Hussen, Muktar Hassan Hussein, Asefa Táa and Hassan Tijani-Eniola.

De onderzoeksschool Produktie Ecologie wil ik bedanken voor het onderwijs dat ik dankzij hun heb kunnen volgen. Verder heeft de onderzoeksschool mij in staat gesteld dit onderzoek te presenteren op twee congressen: Fifth International Wheat Conference (Ankara, 10-14 juni 1996) en Fourth Congress of the European Society for Agronomy (Veldhoven, 7-11 juli 1996). Binnen het kader van de onderzoeksschool waren de tweewekelijkse sessies, waarin een groep promovendi elkaars manuscripten beoordeelden, bijzonder leerzaam. Ik wil alle promovendi die deze vrijdagochtenden inhoud gaven bedanken. Voor het begeleiden van deze sessies wil ik Rudy Rabbinge, Jan Goudriaan en Louise Fresco hartelijk danken.

Tenslotte wil ik Karin bedanken voor haar steun en geduld met name tijdens de voltooiing van dit proefschrift.

Contents

Chapter 1	General introduction	1
Part I: Effects of temperature and photosynthetic photon flux density on spaced plants		
Chapter 2	Growth of individual leaves of spring wheat (<i>Triticum aestivum</i> L.) as influenced by temperature and photosynthetic photon flux density	9
Chapter 3	Morphological analysis of leaf and tiller number dynamics of wheat (<i>Triticum aestivum</i> L.): responses to temperature and photosynthetic photon flux density	29
Chapter 4	Morphological analysis of leaf growth of maize: responses to temperature and photosynthetic photon flux density	45
Part II: Analysis of plant density effects		
Chapter 5	Morphological analysis of plant density effects on leaf area growth in wheat	65
Chapter 6	Morphological analysis of plant density effects on early leaf area growth in maize	85
Part III: Simulation		
Chapter 7	An object-oriented morphological model of leaf area expansion in wheat	101
Chapter 8	General discussion	119
Summary		133
Samenvatting		137
References		141
Curriculum Vitae		149

Chapter 1

General introduction

Importance of plant leaf area for plant growth

The production of crops can be described by the product of two factors:

- i) the amount of intercepted radiation;
- ii) radiation use efficiency, i.e. the increase in dry matter per amount of intercepted radiation.

The first component, the amount of intercepted radiation, is determined by incoming radiation characteristics, and by canopy characteristics such as leaf area index and the spatial arrangement of leaves. Leaf characteristics are important factors in understanding plant and crop growth, as they determine the amount of intercepted radiation at given radiation characteristics.

Gramineae species: importance and morphological aspects

In this thesis, analysis of plant leaf area expansion is limited to an important monocot plant family: *Gramineae*. *Gramineae* species comprise the most important crops in agriculture. Rice, wheat, sorghum and maize are examples of major food crops in the world from this family. Also livestock production is heavily dependent on *Gramineae* species such as perennial ryegrass and (forage) maize.

Gramineae species differ in their morphology from most other species. The first leaf of a tiller is a prophyll, a small non-photosynthesizing leaf. Every leaf, including the prophyll, has an axillary bud which can grow out into a new tiller. Based on these morphological rules, Klepper *et al.* (1982) have made an identification method which uniquely identifies every leaf and tiller on a *Gramineae* plant (Fig. 1). Full-grown leaves consist of a tube-shaped sheath and a blade, which are separated by the ligule. New leaves develop within the encircling sheath bundle, which means that emerging leaf parts are full-grown when pushed out of the enveloping sheath bundle. Leaves are therefore elongating in a relatively dark and humid environment, which is clearly different from dicot leaves, that elongate in the free air with its rapidly changing light, temperature and humidity environment. These aspects are important in the analysis of plant leaf area expansion of *Gramineae* species.

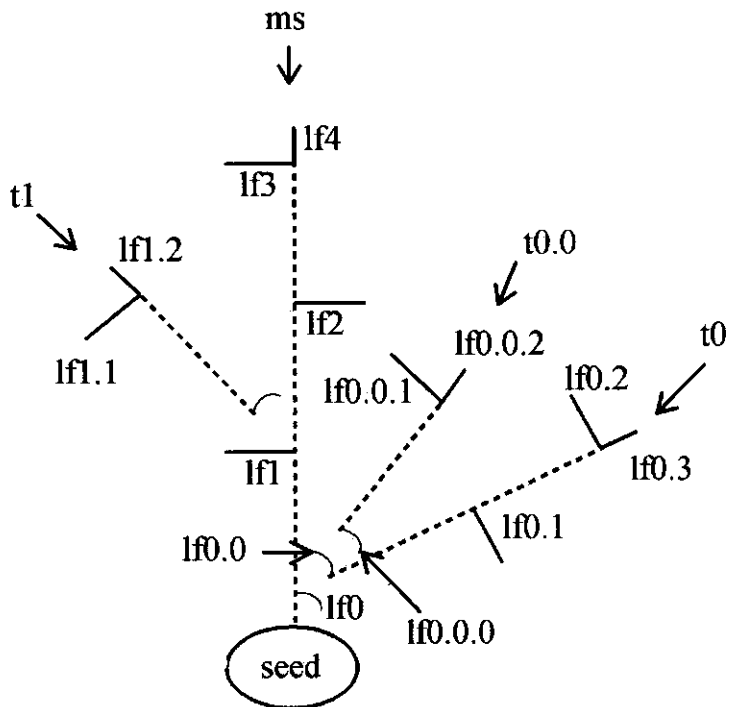


Figure 1. Morphological representation of a *Gramineae* seedling (redrawn from Klepper *et al.*, 1982). lf = leaf, t = tiller, ms = main stem.

Simulation of leaf area expansion

While crop growth is the result of a complex interaction between genotype, soil, climate, and cultural practices, computer simulation models are used to explain these interactions (Van Keulen and Seligman, 1987). Models are also quantitative summaries of the understanding of crop functioning. The more accurately insights are incorporated in the model, the more likely the information can be used to solve practical problems.

Leaf area expansion is a crucial factor for understanding plant and crop growth, but it is simulated in very different ways. These include the exponential growth method, a method in which leaf area expansion depends on assimilate availability and a third approach which takes account of the specific morphology of each species. These three methods are described in detail below.

Simulation based on exponential growth

The most simple assumption is that plant leaf area expansion is an exponential function of accumulated degree days above a threshold temperature (Goudriaan and Van Laar, 1994). In this method, there is no effect of assimilates, nutrients or water on plant leaf area expansion. Therefore, it can only be used when assimilates, nutrients or water do not limit plant leaf area expansion. The advantage of this method is that only three parameters need to be estimated: (i) the initial plant leaf area at emergence, (ii) the base temperature for leaf area expansion, and (iii) relative growth rate of leaf area, expressed in degree days. The method is suitable for models that predict yield of homogeneous crops with only one plant species involved. However, while the method is descriptive and does not include vertical or horizontal distribution of leaves or characterisation of individual leaves, the method is not suitable for heterogeneous crops, canopies with more than one species, or for crops with special management practices (e.g. cutting). The only way to deal with stresses is by inserting reduction factors on the relative growth rate of leaf area.

Assimilate-based simulation

When growth is source-limited, the availability of assimilates (partly) determines plant leaf area expansion. In SUCROS (Goudriaan and Van Laar, 1994), it is assumed that the expansion of leaf area is a function of the plant growth rate, the fraction of the dry matter that is allocated to the leaves and the specific leaf weight (SLW). The plant growth rate depends on the rate of photosynthesis and respiration. The fraction of the dry matter that is allocated to the leaves is assumed to depend on the plant development stage, while the SLW is assumed to be constant or to depend on LAI or plant development stage. The method fits in easily in a model that is based upon dry matter production and distribution. However, plant SLW is difficult to use as an input variable, while SLW of individual leaves depends on leaf position on the plant. Also, environmental factors have effects on dry matter growth of leaves on the plant which are different from those on plant leaf area expansion. Furthermore, plant leaf area expansion is a very complex process, because plant leaf area expansion is determined by tillering, leaf appearance rate per tiller, and individual leaf area expansion. These underlying processes are affected by environmental factors in very different ways. Therefore, the method is suited for simulation of plant growth under relatively stable environmental conditions, using descriptive empirical functions of the change of plant SLW in time.

Morphology-based simulation

Morphological models include some degree of morphological information (tillers, individual leaves). Number of leaves can be calculated from leaf appearance rate and site filling (Davies, 1974; Neuteboom and Lantinga, 1989). To calculate leaf area with the site filling method (Van Loo, 1993), it must be assumed that leaf area expansion per tiller is constant, because the site filling method does not differentiate between different tiller types. Other morphological models (e.g. Amir and Sinclair,

1991; Wilhelm *et al.*, 1993) also include processes of tillering and individual leaf growth. The lack of good experimental data on leaf area expansion of individual leaves on separate tillers necessitates some crude assumptions in the model, making it less suitable for good predictions. However, to a certain degree these models give a better insight in the mechanisms that control leaf area expansion. These models have the potential to analyse more complex problems, such as the expansion of leaf area in mixed species (Lotz *et al.*, 1996), because these models can simulate area expansion of leaves situated at different positions in the canopy. A general morphological framework for leaf area expansion is lacking and more and better experimental data are needed, for example on timing of appearance of individual tillers and expansion of individual leaves at different positions on a plant. In this thesis data will be collected with the aim to arrive at a general morphology-based simulation model, applicable to different *Gramineae* species.

Objectives and basic approach in this thesis

Experimental research on the analysis of plant and crop leaf area characteristics is scarce. Most experimental research has been devoted to the analysis of growth of a few individual leaves, or to measurement of the increase of leaf area of the whole plant or crop. Therefore, in this thesis the mechanisms of leaf area expansion in *Gramineae* species will be analysed. The approach for the analysis is the following:

1. determine general morphological variables for leaf area expansion of *Gramineae* species;
2. in experiments, compare two *Gramineae* species that clearly differ in their morphology (wheat: tillering plant; maize: non- or rarely-tillering plant);
3. perform the first basic experiments at constant environmental conditions (growth chambers, spaced plants), to avoid complexity in the basic analysis;
4. analyse the effects of some important environmental conditions (temperature, radiation, and plant density) on the morphological variables;
5. summarise the knowledge in a simulation model, which should be easily extendable to other species or environmental conditions.

Outline of this thesis

The thesis has been divided into four parts.

In Part I the general morphological variables for leaf area expansion of *Gramineae* species are determined. Furthermore, effects of temperature and photon flux density on spaced wheat and maize

plants are analysed in a growth chamber environment.

In Part II the effects of plant density are analysed, using the variables derived in Part I. The factors that are responsible for the effects of plant density effects on wheat and maize are also identified.

In Part III a simulation model is developed based upon the morphological variables of part I.

In the general discussion the results obtained in the current study are discussed. Possible applications and limitations of the approach followed are evaluated and conclusions are drawn.

Part I

Effects of temperature and photosynthetic photon flux density on spaced plants

Chapter 2

Morphological analysis of leaf and tiller number dynamics of wheat (*Triticum aestivum* L.): responses to temperature and photosynthetic photon flux density

with J. H. Neuteboom

Abstract

In recent literature on *Gramineae* species, leaf and tiller number dynamics have been studied by analysing site filling and the phyllochron of the main stem. However, site filling is influenced by three components: (i) the phyllochron of the main stem and daughter tillers, (ii) specific site usage (i.e. fraction of buds that ultimately develop into a visible tiller at a specific site) and (iii) HS-delay (i.e. difference in Haun Stage (HS) between the parent tiller and daughter tiller above the point where the daughter tiller appears). These three morphological components affecting site filling were studied under different environmental conditions in a growth chamber experiment with spring and winter wheat (*Triticum aestivum* L.). Treatments were temperature (daily average 10.5, 15.5 or 20.5 °C) and photosynthetic photon flux density (PPFD) (111, 191 or 286 $\mu\text{mol m}^{-2} \text{s}^{-1}$). Effects of temperature and PPFD on phyllochron were well described by equations already reported in literature. Specific site usage was higher at lower temperatures and higher PPFD values and was related to tiller position. It is proposed that these effects on specific site usage reflect differences in availability of local assimilate for tiller appearance. HS-delay of a tiller was lower if the expected tiller appearance was later and was only slightly affected by PPFD or temperature. This new concept, combining HS-delay and specific site usage, can be useful in the construction of more general models of the effects of environmental factors on the dynamics of leaf number and leaf area of *Gramineae* species.

Introduction

For the modelling of crop growth and potential dry matter production an adequate simulation of leaf area dynamics is a prerequisite (Goudriaan and Van Laar, 1994), particularly in the early stages of crop development when the canopy is still open. An adequate simulation of leaf area dynamics is also needed for realistic simulation of crop-weed competition (Kropff, 1993; Lotz *et al.*, 1996), since especially during early development, the rate of leaf area increase can be very decisive for establishment and growth of weeds.

Leaf number dynamics are determined by the birth and death rates of leaves (Harper, 1989). In early crop growth, leaf number dynamics are determined predominantly by the appearance of new leaves, which is a function of tiller appearance and leaf appearance per tiller. To model leaf production successfully, both processes should be analysed.

In some models for cereal crop growth, tillering has been calculated from the leaf appearance rate of the main stem, using a fixed pattern of tiller production, based on the Fibonacci series (Porter, 1985; Boone *et al.*, 1990). However, in recent literature on grasses for productive grassland (Van Loo, 1992), tillering is calculated from leaf appearance rate and site filling (Davies, 1974; Neuteboom and Lantinga, 1989). Site filling, expressed in tillers per tiller per day, varies under the influence of environmental conditions and is therefore more appropriate for dynamic simulation. Since, in this approach, leaf appearance rate is measured on the main stem only, and site filling is calculated from the total tiller number increase per plant, a third, and even more detailed approach is possible and, for some applications, also desirable. In this approach the presence, appearance time and leaf appearance rate should be measured for each individual tiller.

This paper presents data on tillering and leaf number dynamics of wheat from an experiment with spaced plants at different combinations of temperature and photosynthetic photon flux density (PPFD) (in a companion paper (Chapter 3) areas of individual leaves are analysed). The time of appearance, length and width of every leaf on a plant were recorded and the data were used to determine the time course of leaf and tiller numbers per plant according to (i) a fixed pattern according to the Fibonacci series, (ii) the site filling approach, and (iii) a detailed approach for tillering based on the presence, time of appearance and leaf appearance rate of individual tillers. Temperature effects were analysed because temperature has large effects on both phyllochron and tillering (Mitchell, 1953; Cao and Moss, 1989) and it varies greatly under field conditions. Effects of PPFD were analysed because a reduction in PPFD below the saturation level for photosynthesis reduces the rate of dry matter production per time interval, and relatively low PPFD values could also be responsible for variation in tillering when plants are competing for light. The focus of this study was on spring wheat. Since the initiation of reproductive development of spring wheat could possibly reduce tillering, some unvernialized winter wheat plants were also examined.

Materials and methods

Spring and winter wheat plants were grown in three growth chambers, each with a different temperature (T) regime. Within each growth chamber, three compartments were created with different light levels (L).

Plant material and growing conditions

Spring wheat cv. Minaret (average seed weight 0.045 g) and winter wheat cv. Ritmo (average seed weight 0.042 g) were sown at 3 cm depth in square 18×18 cm (4.5 l) pots filled with a mixture of 33 % sandy soil and 67 % quartz sand. Three seeds were sown per pot. The pots (540 for spring wheat; 108 for winter wheat) were placed on trolleys in three growth chambers (constant relative humidity 70 %; daily photoperiod 7.00-21.00 h; day temperature (9.00 - 21.00 h) 18 °C, night temperature 13 °C).

One day after 50 % emergence, plant number per pot and pot number were reduced to obtain a homogeneous population of plants (one plant per pot; 120 pots of spring wheat and 24 of winter wheat per growth chamber). Using white curtains, each growth chamber was divided into three equal compartments (3.20×1.50 m) for the L treatments. Each compartment contained 40 spring wheat and 8 winter wheat plants, chosen randomly, and arranged uniformly, resulting in an initial plant density of 31 m⁻². T and L treatments were started on the same day, but the photoperiod and relative humidity remained the same as in the pre-emergence period.

During growth, trolleys were rotated within a compartment at intervals of approximately 0.75 main stem phyllochrons to minimize variation in conditions for individual plants. The pots were irrigated with tap water at least once a day and a Steiner's nutrient solution (Steiner, 1984) was supplied at intervals of two main stem phyllochrons in quantities sufficient to meet the expected growth rate and desired high nutrient concentration in the plant material.

Treatments

The following temperature (T) treatments were imposed at the intermediate PPFD (L2):

T1: day: 13 °C, night: 8 °C;

T2: day: 18 °C, night: 13 °C;

T3: day: 23 °C, night: 18 °C.

These temperatures ensured large differences in the rate of increase of leaf area. The change-over from day to night temperature and *vice versa* occurred within half an hour.

Light treatments (L) were established as follows (values with s.e.):

L1: 111±7 μmol m⁻² s⁻¹ = 5.6±0.35 mol m⁻² d⁻¹;

L2: 191±10 μmol m⁻² s⁻¹ = 9.6±0.50 mol m⁻² d⁻¹;

L3: 286±12 μmol m⁻² s⁻¹ = 14±0.60 mol m⁻² d⁻¹.

In each compartment, the light ceiling contained 6 metal halide (Philips HPI 400 W) and 6 high pressure sodium (Philips AGROSON-T 400 W) lamps. For L3, all lamps were switched on, for L2, 8 lamps, and for L1, 4 lamps. The metal halide lamp/high pressure sodium lamp ratio was 1:1 for every L treatment. Photosynthetic photon flux density was measured using a LI-190 SA Quantum Sensor at nine points per compartment, just above the pots. The heights of the trolleys were adjusted to ensure the required PPFD values.

On average, the air temperature was 0.5 °C higher in L3 and 0.5 °C lower in L1 than in L2 during the light period. During the dark period air temperatures were the same.

Measurements

Destructive measurements were done only on spring wheat plants. Eight plants per treatment were harvested at intervals of one main stem phyllochron, starting from tip appearance of leaf 4 up to tip appearance of leaf 8 (five harvests). After each harvest, the remaining pots were rearranged to minimize interplant competition (plant density at last harvest 10 m⁻²). At each harvest, 7 plants were separated into roots and shoots, the shoot into individual tillers, and each tiller into separate visible leaves and internodes/sheaths. The dry weight of each component was measured after drying to constant weight at 70 °C.

For winter wheat, the number of leaves and the length of the youngest and second youngest visible leaves were measured non-destructively for each tiller in the T2 treatments on the same day that the spring wheat plants were harvested in that treatment (five times). Unintentionally, these measurements were not made at the first harvest of treatment T2L2, and, in the T1 and T3 treatments, they were made only at the last harvest of the spring wheat plants.

Definitions and calculations

General outline of calculations: To compare the tiller numbers per plant according to the three models, leaf stages have to be defined, and a leaf- and tiller-identification system is needed. The leaf stage of a tiller was measured as the Haun Stage (Haun, 1973) and tillers and leaves were identified according to the system of Klepper *et al.* (1982). The equation of Volk and Bugbee (1991) was used to calculate the effects of PPFD on the interval between the appearance of successive leaves on a tiller (the phyllochron). For the site filling model, the maximum number of tillers can be calculated, and the theoretical total leaf number per plant (all stems) can be calculated from an equation developed by Neuteboom and Lantinga (1989) and amplified by Van Loo (1992). In discussing leaf and tiller identification, two patterns of tillering (plant types 1 and 2) are referred to (see below).

Phyllochron. Phyllochron for each tiller was expressed in degree days using a base temperature of 0 °C, and was calculated by linear regression of thermal time vs. HS_t . The effects of PPFD were evaluated using the equation (Volk and Bugbee, 1991):

$$Phyllochron = Phyllochron_{min} \times \frac{(PPFD_{hf} + PPFD - 2 \times PPFD_{min})}{(PPFD - PPFD_{min})} \quad (2)$$

where PPFD is the daily photosynthetic photon flux ($\text{mol m}^{-2} \text{d}^{-1}$), $PPFD_{min}$ the minimum PPFD for leaf appearance ($= 2 \text{ mol m}^{-2} \text{d}^{-1}$ (Volk and Bugbee, 1991)), $PPFD_{hf}$ the PPFD for half-saturation of leaf appearance rate ($\text{mol m}^{-2} \text{d}^{-1}$) and $Phyllochron_{min}$ is the minimum phyllochron for $PPFD \rightarrow \infty$ ($^{\circ}\text{C d}$). $PPFD_{hf}$ and $Phyllochron_{min}$ were estimated by non-linear regression.

Site filling method. The total number of tillers per plant was estimated from the leaf appearance rate of the main stem, and site filling, which is defined as the number of new tillers per tiller per phyllochron (Davies, 1974). Since Neuteboom and Lantinga (1989) showed that a minimum of one phyllochron separates the appearance of a tiller and its first daughter tiller, maximum site filling is 0.69. Such a maximally-tillering plant is illustrated in Fig. 1 (plant type 1). Site filling was calculated by linear regression of $\ln(\text{number of tillers per plant})$ vs. HS_{ms} .

Leaf number per plant (L_p) can be calculated from site filling (F_s) and Haun Stage of the main stem (HS_{ms}) using the equation (Neuteboom and Lantinga, 1989):

$$L_p = e^{n F_s} T_{p,0} (e^{HS_{ms} F_s} - 1) + L_{p,0} \quad (3)$$

where n is the mean number of inhibited buds per tiller and $T_{p,0}$ and $L_{p,0}$ are the numbers of tillers and leaves, respectively, per plant at day = 0. Van Loo (1992) has shown that n depends on F_s :

$$n = 1 - \frac{\ln(e^{F_s} - 1)}{F_s} \quad (4)$$

Combining eqns. 3 and 4 yields a new equation:

$$L_p = e^{F_s - \ln(e^{F_s} - 1)} T_{p,0} (e^{HS_{ms} F_s} - 1) + L_{p,0} \quad (5)$$

Fibonacci series method. This method assumes that tiller number increases with leaf number on the main stem according to the Fibonacci series (1, 1, 2, 3, 5, 8 etc.), because two phyllochrons separate the appearance of a tiller and its first daughter tiller. Site filling for such a plant is 0.49 (Neuteboom and Lantinga, 1989). Plant type 2 in Fig. 1 shows such a plant schematically.

Detailed method. This method requires estimates of the phyllochron of individual tillers, the presence of tillers, and the timing of appearance of tillers. Presence of tillers was expressed as ‘specific site usage’, defined as the fraction of the buds in a specific axil that have ultimately grown out into visible tillers, and was calculated as the number of plants that possessed this tiller divided by the number of plants that possessed its parent tiller, determined at least one phyllochron after the tiller was expected to appear. Data of specific site usage were transformed using a logistic link function, assuming a binomial distribution (McCullagh and Nelder, 1989). To analyse quantitative effects of tiller type for each individual treatment, one of the five quantitative parameters for tiller type (Table 1) was used as independent variable in the regression with the transformed specific site usage as dependent variable.

The timing of appearance of a tiller t was expressed as ‘HS-delay’, which is the difference between the HS of tiller t and the HS of its parent tiller above the leaf from which axil tiller t appears

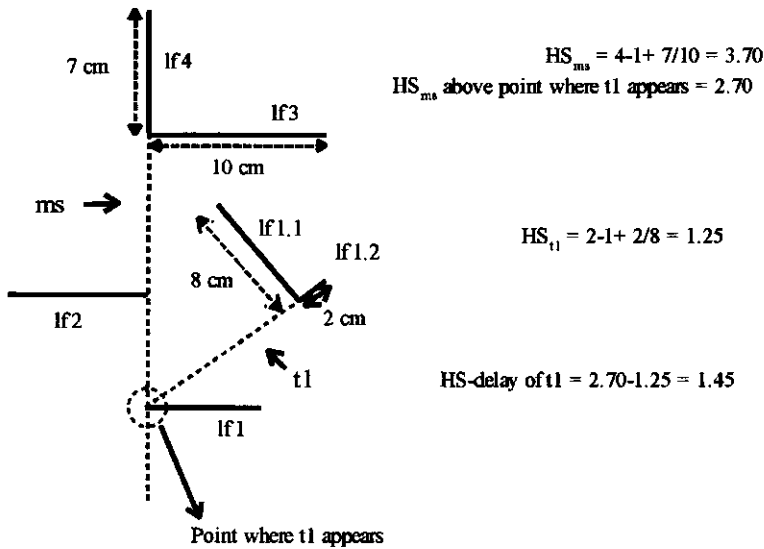


Figure 2. Illustration of the calculation of HS_t and $HS\text{-delay}$. Leaf sheaths are indicated by dashed lines, leaf blades by solid lines and the lengths of the two youngest leaf blades per tiller are given.

Table 1. Parent tiller and quantitative parameters for selected tiller types.

Tiller type	Parent tiller	Parameters related to plant development stage		Parameters related to position in a plant		
		HS _{ms} at tiller appearance (according to plant type 1)	HS _{ms} at tiller appearance (according to plant type 2)	Tiller order	Tiller position on parent tiller	Summed tiller position
t0	ms	1	2	1	0	0
t0.0	t0	2	4	2	0	0
t0.0.0	t0.0	3	6	3	0	0
t0.1	t0	3	5	2	1	1
t1	ms	2	3	1	1	1
t1.0	t1	3	5	2	0	1
t2	ms	3	4	1	2	2

(= 'NLAT' in Skinner and Nelson, 1992) (Fig. 2). HS-delay of tiller t was determined between HS₁ and 2. The observed values were compared with the values for plant type 1 and 2 (HS-delay is 1 and 2 respectively (Neuteboom and Lantinga, 1989)). To analyse quantitative effects of tiller type on HS-delay, a simple equation was assumed:

$$HS\text{-delay} = HS\text{-delay}_{\min} + (HS\text{-delay}_0 - HS\text{-delay}_{\min}) e^{-RDR \times x} \quad (6)$$

where x is one of the five quantitative parameters for tiller type (Table 1), $HS\text{-delay}_{\min}$ the HS-delay for $x \rightarrow \infty$, $HS\text{-delay}_0$ the HS-delay for $x=0$ and RDR the relative decline rate. Two values of $HS\text{-delay}_{\min}$ were evaluated: 1 (plant type 1) and 2 (plant type 2). This equation assumes that HS-delay declines with x , which is based on indications from literature (Ito *et al.*, 1987). $HS\text{-delay}_0$ and RDR were estimated by non-linear regression.

In the detailed method, leaf number per plant was calculated simply by daily summation of the number of leaves of all tillers present.

Results

Leaf death

Under the particular conditions of this experiment (relatively low irradiance; no competition between plants), there was no leaf death under any treatment by the time of appearance of the tip of leaf 8.

Phyllochron

For spring wheat, the phyllochron of the main stem was well fitted by eqn. 2 ($P < 0.05$), using values of 91 ± 5 °C d for $Phyllochron_{\min}$, and 3.5 ± 0.3 mol m⁻² d⁻¹ for $PPFD_{lr}$ (values with s.e.m.) (Fig. 3). Temperature did not have a significant effect on this relationship. The phyllochrons of tillers t_0 , t_1 and t_2 , also well fitted by eqn. 2, were between 0 and 14 % longer than the main stem phyllochron. However, the phyllochron of $t_{0.0}$ could not be fitted by eqn. 2, and the observed values were very high, between 150 and 350 °C d. The phyllochron of the winter wheat main stem was, on average, 17 % longer than that of spring wheat (data not shown).

Site filling

In spring wheat, site filling was always below the value for plant type 2 (Fig. 4a) and linear, quadratic or interaction terms of temperature and PPFD did not change site filling significantly ($P < 0.05$). The standard error of the individual points in Fig. 4a is relatively large, owing to the irregular increase of tiller number per plant with HS_{ms} , as illustrated for four treatments in Fig. 4b. In winter wheat, site filling values reached 0.67, which is close to the value for plant type 1.

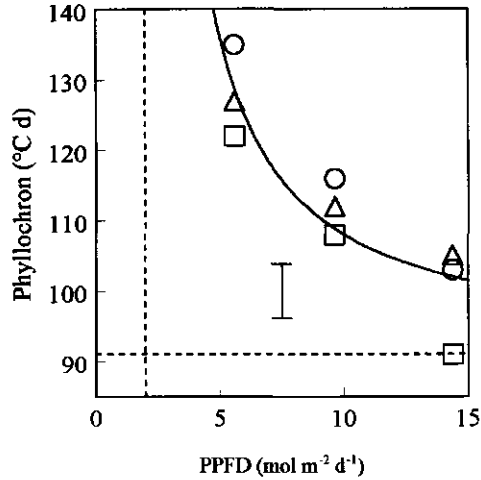


Figure 3. The phyllochron of the main stem of spring wheat as a function of PPFD, for the three temperature treatments (□: T1; ○: T2; Δ: T3). Dashed lines indicate asymptotes, and the vertical bar indicates twice the mean standard error of the phyllochron values.

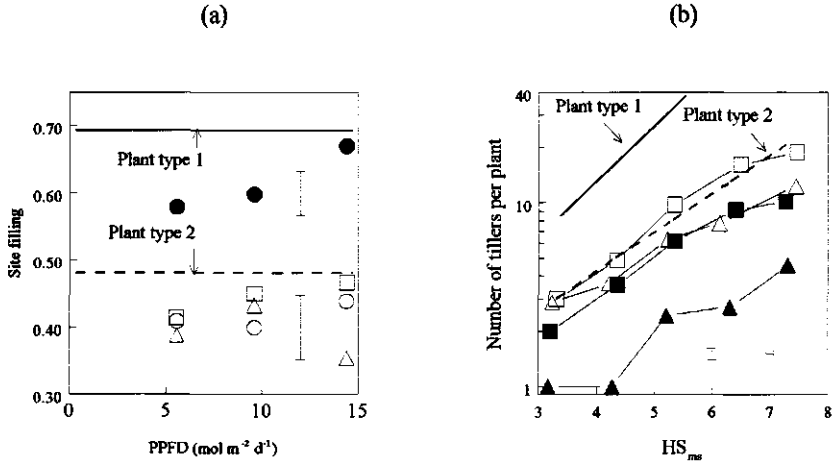


Figure 4. (a) Site filling in spring wheat (symbols as in Fig. 3) and winter wheat (●: T2) as a function of PPFD. (b) Number of tillers per plant (log scale) as a function of HS_m for treatments T1L1 (■), T1L3 (□), T3L1 (▲) and T3L3 (Δ) in spring wheat. The maximum tillering patterns of plant type 1 and 2 are indicated, and the vertical and horizontal bars indicate twice the mean standard error of the data points.

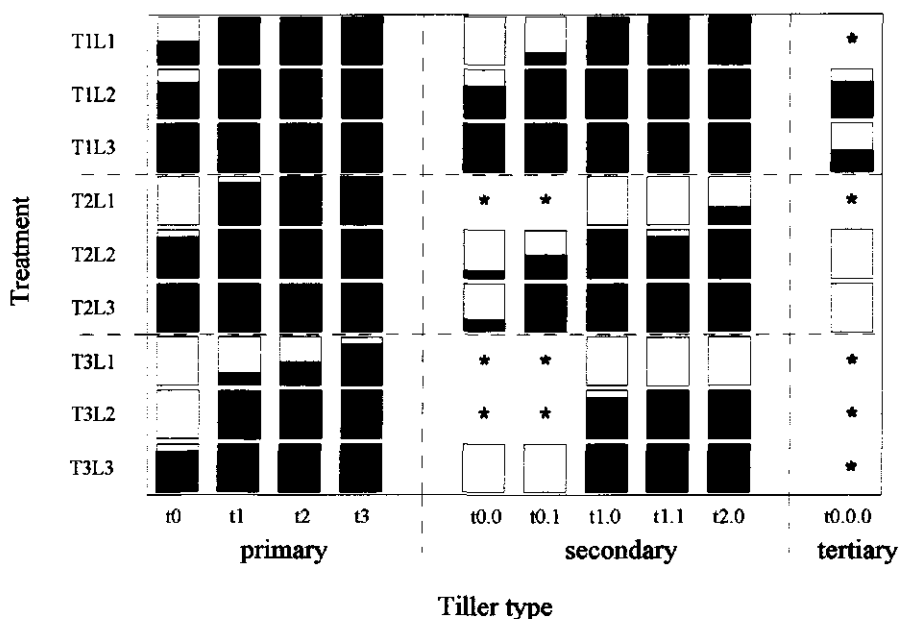


Figure 5. Specific site usage of different tiller types (primary, secondary and tertiary) for the nine treatments in spring wheat. The proportional filling of each box represents the specific site usage, e.g. specific site usage of t0 is 0 for T2L1 and 1 for T1L3. Asterisks indicate that specific site usage could not be calculated (parent tiller not present).

Detailed method: specific site usage

Tiller type, temperature and PPFD each had a significant and important effect on specific site usage in spring wheat (Fig. 5) and in winter wheat (data not shown). In general, a high specific site usage was observed for low temperatures, high PPFD values, high tiller position on the ms ($t_3 > t_2 > t_1 > t_0$) and low tiller order (primary > secondary > tertiary). The five parameters in Table 1 were used as independent variables to quantify tiller type effects per treatment. For each of the nine treatments, one of the 'position' parameters (tiller order, tiller position on parent tiller or summed tiller position) accounted for most of the variation. For winter wheat, specific site usage of t0, t0.0, t0.1 and t1 was lower than for spring wheat, while for the other tillers specific site usage was higher or equal.

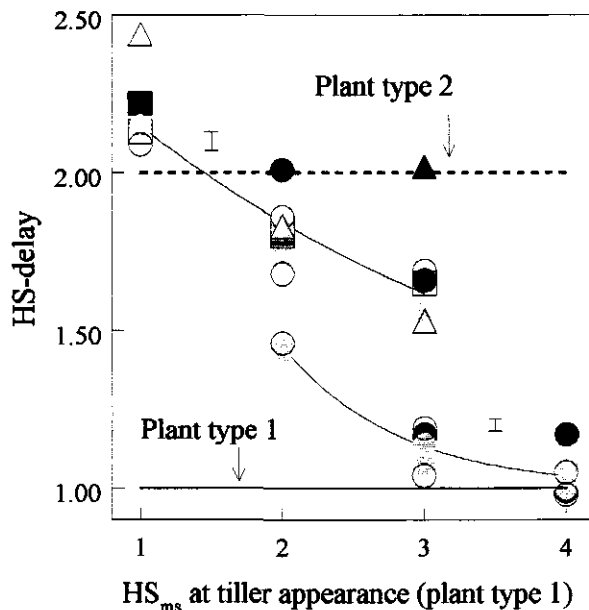


Figure 6. HS-delay as a function of the quantitative tiller parameter 'HS_{ms} at tiller appearance (plant type 1)' calculated for tillers t0, t0.0, t1 and t2 (spring wheat: upper line) or tillers t1, t1.0, t2 and t3 (winter wheat: lower line) for the nine treatments. Symbols for the three temperature treatments are as in Fig. 3, and PPFD treatments are represented by marker colour: L1 = black; L2 = grey; L3 = white. Vertical bars indicate twice the mean standard error of the data points.

Detailed method: HS-delay

There was a large and significant effect of tiller type on HS-delay for both spring and winter wheat with a clear trend of a reduction in HS-delay with higher placement of the tiller on the main stem, and with higher tiller order. Of the five tiller parameters tested (Table 1), HS_{ms} at the time the tiller appears (plant type 1) with a HS-delay_{min} = 1 accounted best for most of the variation in HS-delay using eqn. 6 (HS-delay = 2.2±0.05 and RDR = 0.31±0.038 (spring, P<0.05); 2.5±0.32 and 1.2±0.17 (winter, P<0.05)) (Fig. 6). RDR was much higher for winter wheat than for spring wheat, indicating a quick decline of HS-delay to 1 for winter wheat. Most of the data in Fig. 6 fell below HS-delay = 2, the absolute minimum for plant type 2.

For spring wheat, temperature and PPFD showed small but significant effects on HS-delay. These effects were due to three clearly deviating data points, i.e. T3L3 for tiller t0, T2L1 for tiller t1 and T3L1 for tiller t2.

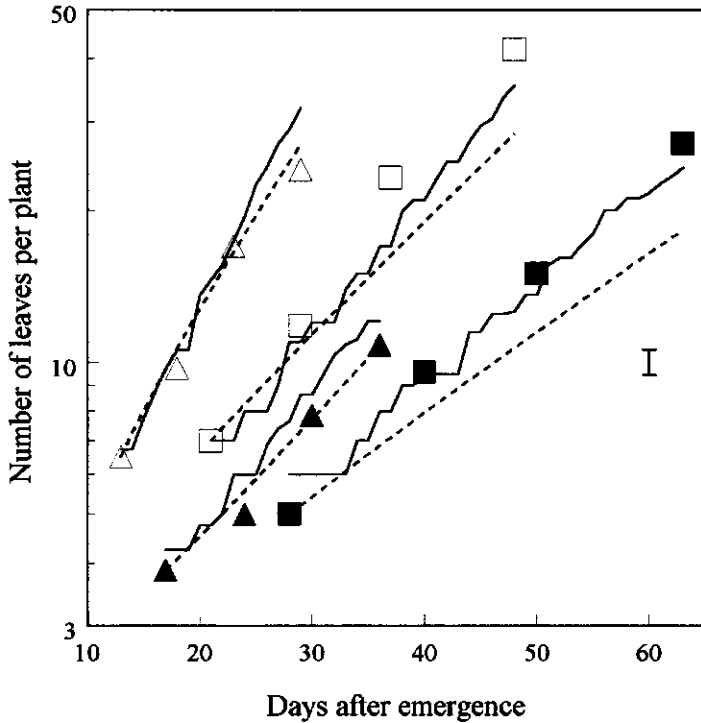


Figure 7. Increase in number of leaves per plant (log scale) of spring wheat observed for treatments T1L1 (■), T1L3 (□), T3L1 (▲) and T3L3 (△), and predicted by the site filling (dashed line) and the detailed methods (solid line) (see text). The first harvest was taken as starting point. The vertical bar indicates twice the mean standard error of the data points.

Leaf number per plant

To calculate leaf number per plant of spring wheat by the site filling method, eqns. 2 and 5 were used with $\text{Phyllochron}_{\text{min}} = 91 \text{ } ^\circ\text{C d}$, $\text{PPFD}_{\text{hr}} = 3.5 \text{ mol m}^{-2} \text{ d}^{-1}$ and the measured site filling values for each treatment (Fig. 4a). In the detailed method, leaf number per plant was calculated using eqns. 2 and 6, with $\text{Phyllochron}_{\text{min}} = 91 \text{ } ^\circ\text{C d}$ and $\text{PPFD}_{\text{hr}} = 3.5 \text{ mol m}^{-2} \text{ d}^{-1}$ for all tillers, $\text{RDR} = 1.22$, $\text{HS-delay}_{\text{min}} = 1$, $\text{HS-delay}_0 = 2.15$, and specific site use values as observed for each treatment and tiller type (Fig. 5). Initial values were taken from the first harvest for each treatment.

Fig. 7 compares the resulting lines for each method with experimental data on leaf number per plant on a log scale. The site filling method gives a smooth curve with a decreasing slope for treatments T1L1, T1L3 and T3L3. For treatment T3L1 the slope increases owing to a relatively low initial number of tillers compared with initial number of leaves (eqn. 5). The detailed method shows a

discontinuous increase, reflecting the discrete events (leaf and tiller appearance) that are included in this method.

Discussion

Differences between spring and winter wheat

Both spring and winter wheat plants formed new tillers up to the end of the observation period, and showed an increased specific site usage with higher placement of tillers on their parent tiller. It is, therefore, unlikely that the initiation of reproductive development in spring wheat affected the tillering process. However, there were clear differences between the two wheat types: spring wheat had shorter phyllochrons, a higher HS-delay and a lower specific site usage, except for the t_0 tiller and its daughter tillers. This shows that genotype effects on leaf and tiller number parameters can be substantial.

Does the Fibonacci series represent the maximum tillering pattern?

This research has shown that plant type 2 (Fibonacci series; HS-delay = 2) does not represent the type with the maximum possible number of tillers. Spring wheat and, more clearly, winter wheat showed much lower HS-delay values, down to 1 (Fig. 6). Therefore, as in perennial ryegrass (Neuteboom and Lantinga, 1989) plant type 1 is more representative of the maximum tillering pattern for wheat. This conclusion seems to conflict with a site filling for spring wheat that was never higher than 0.49 (plant type 2) (Fig. 4a), but site filling is affected by tiller type effects on phyllochron, specific site usage and HS-delay. For example, a decrease of site filling from 0.69 to 0.49 can be due to (i) a rise in HS-delay from 1 to 2, (ii) a decrease of specific site usage of all buds from 1 to 0.63, or (iii) an increase from 1 to 2 in the phyllochron of tillers relative to the main stem. It was shown that tiller type indeed has an effect on all these three parameters. These confounding effects of tiller type on phyllochron, specific site usage and HS-delay, all three affecting site filling, may have led to the incorrect conclusion that the Fibonacci series represent the maximum site filling pattern for wheat (Boone *et al.*, 1990).

Comparison between the site filling and detailed methods

Both the site filling and detailed methods described the trend of the experimental data on number of leaves per plant well (Fig. 7) and both methods can deal with an increasing and a decreasing relative growth rate of leaf number in time. Compared with the detailed method, site filling has the strong advantage that the effects of environmental factors need only be measured for two parameters: phyllochron of the main stem and site filling. However, the site filling method has a number of limitations: (i) site filling is not constant (Fig. 4b); (ii) differences in site filling are difficult to

interpret, since they can be due to effects on the phyllochron of tillers relative to the main stem, specific site usage and HS-delay of appearing tillers; and (iii) because the site filling method does not give information on which tiller types appear, leaf area growth can be included only if leaf area growth is equal for every tiller. Since this is certainly not true (Chapter 3), the detailed method is preferred if the regulation of the parameters involved in this method is sufficiently understood.

Regulation of phyllochron

The degree-day concept, adjusted for PPFD effects (eqn. 2), fitted the data on phyllochron well, and estimates of $\text{Phyllochron}_{\text{min}}$ and PPFD_{fr} were close to what has previously been found (Volk and Bugbee, 1991; McMaster *et al.*, 1991). At higher temperatures, the degree-day concept will fail and other equations (e.g. Volk and Bugbee (1991), Yin *et al.* (1995)) should be used. Tillers t0, t1, t2 had longer phyllochrons than the main stem, although differences were small, but tiller t0.0 had a much longer phyllochron, which could be related to the unfavourable positions of prophyll and coleoptile tillers, as also found by Kirby *et al.* (1985) and Skinner and Nelson (1992).

Regulation of specific site usage

Specific site usage increased significantly with higher primary tiller position, as also observed for wheat by Rickman *et al.* (1985), for barley by Cannell (1969) and for ryegrass by Mitchell (1953). Lower PPFD values reduced specific site usage of lower primary tillers in the current experiment, as was also found by Mitchell (1953) and Rickman *et al.* (1985), and higher temperatures reduced site usage, in agreement with the findings of Mitchell (1953) and Cannell (1969). It appears that environmental factors have their greatest impact on specific site usage during early growth. Generally, the following factors have been found to reduce specific site usage: (i) low nutrient availability (Van Loo *et al.*, 1992); (ii) low carbohydrate availability (Davies, 1965); and (iii) a low red/far-red ratio (Casal *et al.*, 1990). In the current experiment, nutrients were adequately supplied at fixed HS_{ms} and the red/far-red ratio was high (>2). Carbohydrate availability could therefore have been responsible for the observed differences between light and temperature treatments.

Since one of the three 'position' parameters (Table 1) always accounted for most of the variation in specific site usage, plant carbohydrate availability can not explain differences in specific site usage between different tiller types. If carbohydrate availability is the key factor involved, two mechanisms could be responsible for tiller type effects on specific site usage: (i) sinks (e.g. tiller buds) close to the source for carbohydrates (visible leaf blades) have highest priority; (ii) the amount of carbohydrates needed for a bud to grow out into a visible tiller differs between buds.

There is evidence that, in wheat, assimilates are translocated preferentially to the sink closest to the assimilating leaf (Rawson and Hofstra, 1969; Cook and Evans, 1978). Based on this evidence, the following simple hypothesis is proposed: only the parent tiller supplies carbohydrates for the appearance of its daughter tiller, and the relative sink strength of the tiller bud (i.e. the sink strength

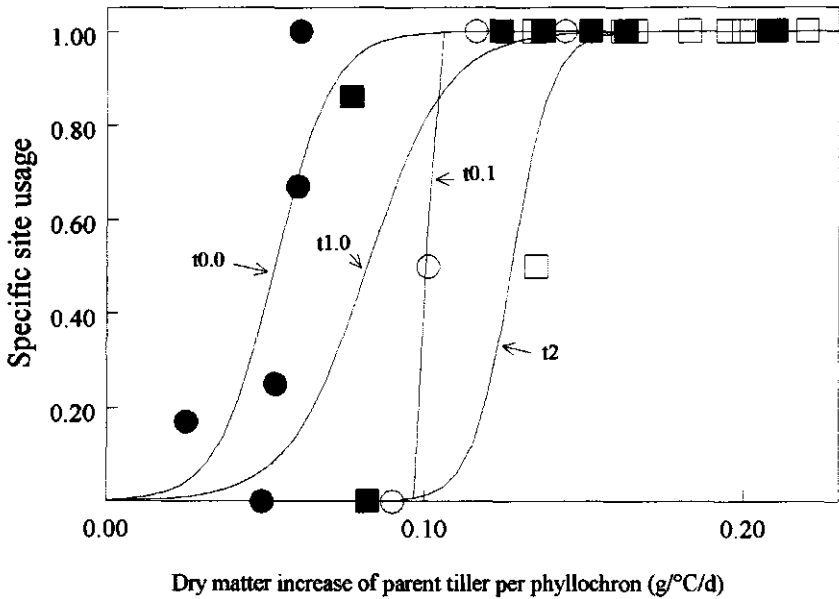


Figure 8. Specific site usage of four daughter tillers as a function of the total dry matter increase of the parent tiller per phyllochron (see text). For a given tiller, one data point represents a treatment. (●) t0.0; (○) t0.1; (■) t1.0; (□) t2. Fitted logistic curves are shown for each tiller type.

of the tiller bud divided by the sum of the sink strengths on the parent tiller) is independent of temperature and PPFD. If so, a positive relation must exist between the dry matter increase of the parent tiller per phyllochron at the time of appearance of the daughter tiller and the specific site usage of that daughter tiller. In the current experiment root weight per tiller was not measured, but was calculated by assuming that each tiller type had a share in root weight proportional to its above-ground weight. Fig. 8 shows that there is a positive relation between the specific site usage and the dry matter production (leaves, sheaths and roots) per phyllochron of the parent tiller. The relationship varied with tiller type: e.g. t0.0 appeared at a lower dry matter production per phyllochron of its parent tiller than the other tillers.

This mechanism of carbohydrate availability could explain differences in specific site usage between different PPFD and temperature conditions. Differences between tiller types could occur owing to bud size: e.g. t0.0 buds are relatively small and need a smaller amount of assimilates to grow out, as reflected in the small size of the first leaves of this tiller compared with other tillers (Chapter 3).

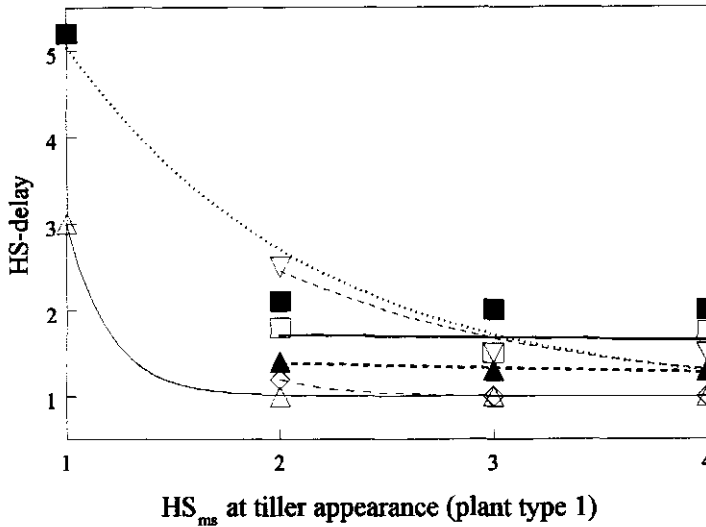


Figure 9. Published values of HS-delay as a function of quantitative tiller parameter 'HS_{ms} at tiller appearance (plant type 1)' for several *Gramineae* species: (■) winter wheat (Klepper *et al.*, 1982, their table 1 (field)); (□) winter wheat (Masle-Meynard and Sebillotte, 1981, their figure 1: pots treatment (growth chamber)); (▲) winter wheat (Rickman *et al.*, 1985, their figure 5 (growth chamber)); (Δ) ryegrass (Mitchell, 1953, his figure 6, treatment S.R. 2000-50 (growth chamber)); (▽) orchardgrass (Ito *et al.* (1987), their table 1 (growth chamber)); (◇) tall fescue (Ito *et al.* (1987), their table 1 (growth chamber)). Data were fitted with eqn. 6; each curve starts within the marker of the matching data set.

Regulation of HS-delay

The HS-delay of both spring and winter wheat depended mainly on the tiller timing parameter: 'HS_{ms} calculated from plant type 1', and much less on tiller position parameters, PPFD or temperature. This implies that HS-delay does not depend primarily on specific effects of light or temperature, nor on assimilate availability of the whole plant or at the tillering site. Apparently, HS-delay is determined principally by stage of plant development.

Spring and winter wheat showed large difference in HS-delay for equal tiller positions. Fig. 9 shows values of HS-delay for primary tillers of grasses and cereals, which could be calculated from literature. In two experiments, the HS-delay was as low as 1, for ryegrass (*Lolium* spp.) (Mitchell, 1953) and tall fescue (*Festuca arundinacea* Schreb.) (Ito *et al.*, 1987), indicating that variation in HS-delay among species of *Gramineae* is large.

Fig. 6 and 9 show a clearly decreasing HS-delay with plant development stage, which is at variance with the constant HS-delay often assumed (Davies, 1974; Masle-Meynard and Sebilotte, 1981; Neuteboom and Lantinga, 1989). Why tillers are delayed at an early plant development stage independent of environmental conditions is unknown. At later stages plants seem to reach a more constant HS-delay.

PPFD showed little effect on HS-delay, as also shown by data for orchardgrass (*Dactylis glomerata* L.) and tall fescue (Ito *et al.*, 1987), and winter wheat for tiller t0 (Peterson *et al.*, 1982); temperature had a small effect on HS-delay. Tillers with a specific site usage of less than 1 showed a markedly higher HS-delay (Fig. 5 and 6), indicating that the HS-delay increases with higher temperatures or lower PPFD values only when conditions are only just satisfactory for tiller appearance.

Towards a dynamic mechanistic model

Phyllochron has been studied extensively, and existing models (e.g. Volk and Bugbee, 1991) can be used for simulation. In a dynamic model, the HS-delay can be seen as a 'window of opportunity', which opens after the parent tiller has reached a certain HS. Then the assimilate production of the parent tiller, the relative sink strength of the tiller bud, and the amount of assimilate needed to grow out into a visible tiller, determine whether the bud develops into a visible tiller (specific site usage). As can be seen in Fig. 10, phyllochron, HS-delay, and specific site usage have an important effect on leaf number per plant. This concept could be the basis for modelling leaf and tiller dynamics of *Gramineae* species in which effects of PPFD and temperature, and probably also other factors (CO₂, plant density) could be included. We are currently developing such a model.

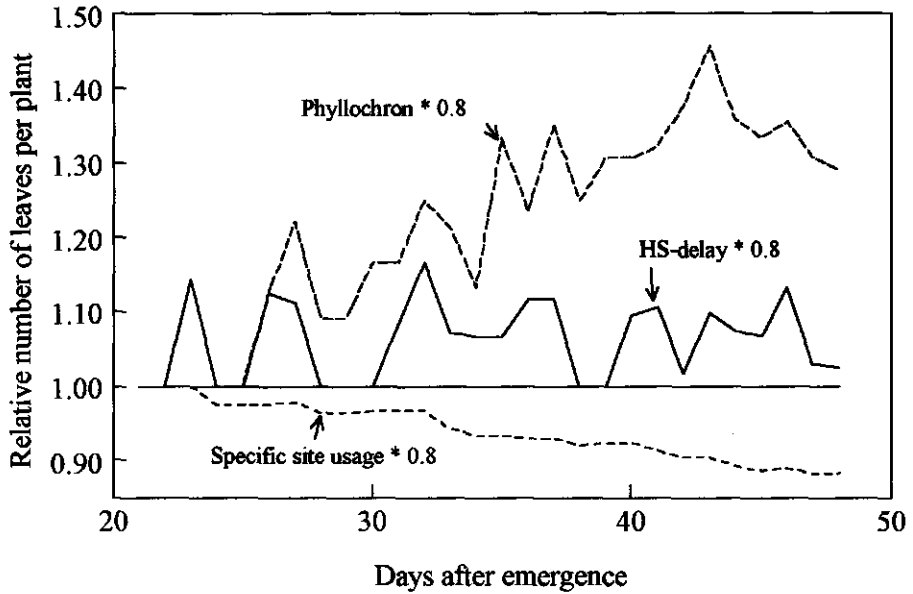


Figure 10. Effect of a 20 % reduction in phyllochron, HS-delay or specific site usage of each tiller on the number of leaves per plant relative to the original values for treatment T1L3. Day 21 (first harvest) was considered as starting point.

Chapter 3

Growth of individual leaves of spring wheat (*Triticum aestivum* L.) as influenced by temperature and photosynthetic photon flux density

with J. H. Neuteboom

Abstract

Existing models of leaf area expansion of *Gramineae* species based on individual leaf growth are descriptive and assume that there is no effect of tiller type on individual leaf area. However, sound experimental data on the growth of individual leaves on a plant are lacking. A growth chamber experiment was carried out with young spring wheat (*Triticum aestivum* L.) plants, and individual leaf area variables were measured. Treatments were temperature (daily mean 10.5, 15.5 and 20.5 °C) and photosynthetic photon flux density (PPFD) (111, 191 and 286 $\mu\text{mol m}^{-2} \text{s}^{-1}$). Effects of leaf position and tiller type on maximum leaf width and leaf elongation rate (LER) could be explained by a new assumption, that maximum leaf width, and LER, of a leaf depend on the values for the previous foliar leaf on the same tiller, or on the parent tiller. LER increased linearly with temperature and was not affected by PPFD, whereas maximum leaf width was not influenced by temperature or PPFD. Leaf elongation duration was closely related to phyllochron expressed in days, although this relation was slightly modified by PPFD. Equations formulated for each leaf area variable accounted for 90% of the variation in leaf area between different leaf types, temperatures and PPFD values. The results give a better general understanding of individual leaf growth of *Gramineae* species and can be used in the development of more mechanistic models for the simulation of leaf area expansion.

Introduction

In the early stages of development, leaf area largely determines the rate of crop growth (Goudriaan and Van Laar, 1994). Therefore, an accurate simulation of leaf area is a prerequisite for the modelling of dry matter production. In a companion paper, the leaf number dynamics of spaced wheat (*Triticum aestivum* L.) plants from an experiment involving the variation of temperature and light conditions were discussed (Chapter 2). The current paper discusses data, from the same experiment, on area expansion of individual leaves at different leaf positions.

The expanding leaf blades of dicotyledonous species increase both in length and width, whereas the visible leaf of monocotyledonous species increases only in length, because the width remains unchanged once it has emerged from the sheath bundle (Dale, 1988). Consequently, four variables must be estimated to analyse the area expansion of individual leaves of monocotyledonous species: (i) leaf elongation rate (LER; a list of abbreviations is given in Appendix I), (ii) leaf elongation duration (LED), (iii) maximum leaf width, and (iv) a constant, k , relating fully-expanded leaf length and maximum leaf width to fully-expanded leaf area.

In the literature, LER, LED, maximum leaf width and k have been assessed for one or more leaves of the main tiller (e.g. Kirby, 1973; Schnyder and Nelson, 1989). The interactions with tiller type and environmental factors are largely unknown, and rough generalisations have been made in the construction of simulation models of leaf area expansion based on the growth of individual leaves and tillers (e.g. Amir and Sinclair, 1991; Wilhelm *et al.*, 1993). In the current experiment, these interactions are quantified with the objective of providing a better basis for the simulation of leaf area expansion of *Gramineae* species.

In the experiment, temperature was varied because it has large effects on the rate of leaf area expansion (Hay and Tunnicliffe Wilson, 1982; Reid *et al.*, 1990) and it varies greatly under field conditions. Effects of photosynthetic photon flux density (PPFD) were studied because reduction in PPFD below the saturation level for photosynthesis reduces the rate of dry matter production and relatively low PPFD values could also cause differences in area expansion between individual leaves when plants compete for light. Spaced plants were used, to keep the measured effects of temperature and PPFD free from interactions with crop shading. Spring wheat was chosen as a representative of the *Gramineae*, because it is easy to grow and to measure. Moreover, it is a well-documented species, cultivated world-wide.

Materials and methods

Experimental setup

The design of the experiment has been described in Chapter 2. In brief, spaced spring wheat plants were grown in pots, filled with sand, in growth chambers differing in day (12 h) / night (12 h) temperature (T1: 13/8 °C; T2: 18/13 °C; T3: 23/18 °C). Sufficient nutrients and water were supplied to meet growth requirements. Within each growth chamber, three compartments were established, with photosynthetic photon flux densities of 111 (L1), 191 (L2), and 286 (L3) $\mu\text{mol m}^{-2} \text{s}^{-1}$ immediately above the plants. Daylength was set at 14 h d^{-1} .

Tiller and leaf identification

Tillers and leaves were identified using the system of Klepper *et al.* (1982), counting the leaves acropetally, with the coleoptile or prophyll named lf0 and the first foliar leaf lf1. The seedling stem was the main stem (ms). Other tillers were named after their parent leaf, e.g. t0 was the tiller from the axil of lf0. Higher-order tillers were indicated by additional digits; for example, t1.0 was the tiller from the axil of lf1.0 (i.e. the prophyll of t1). Tiller t1.0 was the “daughter” tiller of t1, which in turn was its “parent” tiller.

Measurements and calculation of variables

Plants were harvested at consecutive Haun stages (HS; Haun, 1973) of the main stem: i.e. eight plants per treatment at mean HS_{ms} of 3.2, 4.2, 5.2, 6.2 and 7.2. The lengths and maximum widths of the emerged part of all leaves, and the lengths of the fully-expanded sheaths of seven plants were measured and the dry weights of the various organs were obtained, after drying at 70 °C to constant weight. The eighth plant of each sample was used to measure the length, maximum width, and width at six or seven equidistant places over the entire length of each new fully-expanded leaf. Leaf area was calculated from leaf length and leaf widths using numerical rectangular integration, and the leaf shape factor k was calculated for each leaf using:

$$k = \frac{\text{Leaf area}}{\text{Leaf length} \times \text{Maximum leaf width}} \quad (1)$$

For the analysis of final leaf area and maximum leaf width, data were used from leaves, from the destructive harvests, which had just reached full expansion.

Plants reserved for the last harvest were used throughout growth for the collection of data on LER and LED by measuring the visible lengths (i.e. from the tip to the youngest visible ligule) of all growing leaves at a fixed time of the day four times per phyllochron. According to Gallagher (1979),

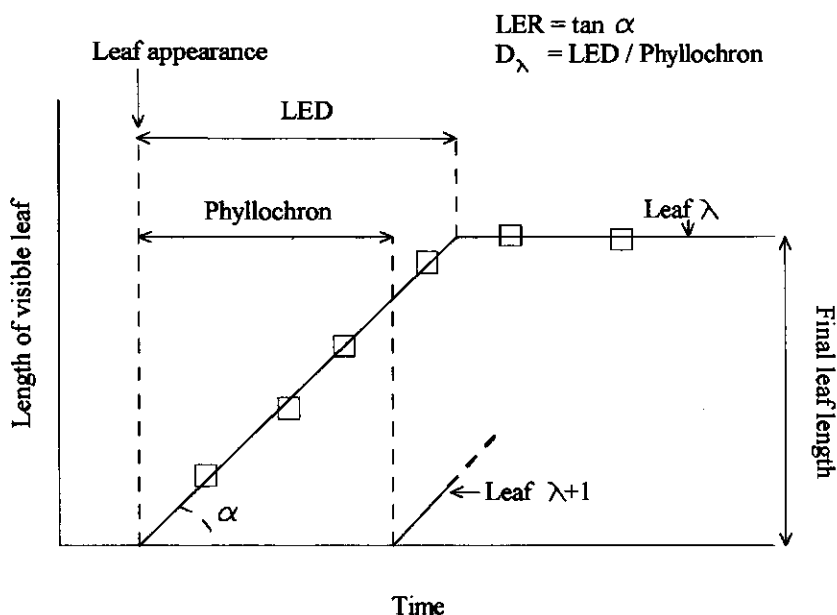


Figure 1. Estimation of time of leaf appearance, leaf elongation rate (LER), leaf elongation duration (LED), phyllochron and D_{λ} . The number of data points used in fitting the two lines for leaf λ was varied, and the solution with the least residual sum of squares was chosen. Data points of a representative leaf are given; in this case, a fit of the first line using the first four data points and the second line using the remaining two data points yielded the best solution.

the LER of visible leaf blades is relatively constant for wheat until it abruptly drops to zero. Therefore, these data could be used to estimate LER, LED and the time of leaf appearance from a two-fold regression as shown in Fig. 1.

Data analysis

Three hypotheses which give quantitative expression of the effects of leaf type on LER and maximum leaf width were tested for each treatment. Hypothesis A assumes that LER, or maximum width, of a leaf is determined by leaf appearance day (Kemp, 1981b). Hypothesis B assumes that LER, or maximum width, is determined by leaf position on the tiller (Amir and Sinclair, 1991; McMaster *et al.*, 1991; Van Loo, 1993). A new hypothesis, C, assumes that LER, or maximum width, of a leaf is determined by the value of the previous foliar leaf on the same tiller, or on the parent tiller. To test hypothesis C, a new parameter 'summed leaf position' was used as a quantifier for leaf type effects. Summed leaf position is equal to the sum of all the numbers in the designation of

Table 1. Three quantitative parameters calculated for seven selected leaf types.

Leaf type (see text)	Leaf appearance day ¹ (Hypothesis A)	Leaf position on tiller (Hypothesis B)	Summed leaf position (Hypothesis C)
lf1	-	1	1
lf2	-	2	2
lf3	-	3	3
lf0.1	-	1	1
lf1.3	-	3	4
lf2.1	-	1	3
lf3.0.2	-	2	5

¹ = observed values were used

the leaf (e.g. for lf3.0.1 this is 3+0+1=4; Table 1). C is quite different from the other two hypotheses: e.g. lf2 appears at an early plant stage (hypothesis A), and both its position on the tiller (hypothesis B) and its summed leaf position (hypothesis C) are equal to 2, whereas lf1.0.0.1 appears at a later plant stage, its position on the tiller is equal to 1 but its summed leaf position is equal to 2. Observed appearance day (hypothesis A), leaf position on the tiller (hypothesis B) and summed leaf position (hypothesis C) were used as independent parameters, and the best independent variable was selected which accounted for the most variation in LER, or maximum leaf width, using a biologically realistic equation (Appendix II).

Since LED is strongly related to phyllochron (Van Loo, 1993; Yin and Kropff, 1996), it was evaluated using the following equation (see Fig. 1):

$$LED \text{ leaf } \lambda = (\text{Time of appearance leaf } (\lambda + 1) - \text{Time of appearance leaf } \lambda) * D_{\lambda} \quad (2)$$

where λ is the acropetally counted position of a leaf on a tiller, and D_{λ} the LED of leaf λ expressed in phyllochrons.

Linear, quadratic and interactive effects of temperature and PPFd were analysed by a stepwise regression (McCullagh and Nelder, 1989). The term which accounted for most of the variation was included if its contribution was significant ($P < 0.05$). The percentage of variance accounted for was expressed as the adjusted R^2 statistic:

$$R^2_{adj} = 100 \times \left(1 - \frac{\text{Residual mean square}}{\text{Total mean square}} \right) \quad (3)$$

Results

LER

For six out of the nine treatments, summed leaf position (Table 1) accounted for most of the variation in LER. Since careful examination of the data showed that leaves which had appeared after $HS_{ms} = 4.7$ always had lower LER than fitted (e.g. Fig. 2a), the analysis was repeated for leaves that had appeared before $HS_{ms} = 4.7$ only. For eight treatments, summed leaf position accounted for most of the variation, and only LER in treatment T3L1 was better predicted using leaf position on the tiller. Averaging over all treatments, R^2_{adj} was 69% using summed leaf position as the independent variable (hypothesis C), and 37% for both leaf appearance day (hypothesis A) or leaf position on a tiller (hypothesis B) as independent variables. Averaging over all treatments, with summed leaf position as the independent variable, the negative exponential function (eqn. a, Appendix II) accounted for most of the variation.

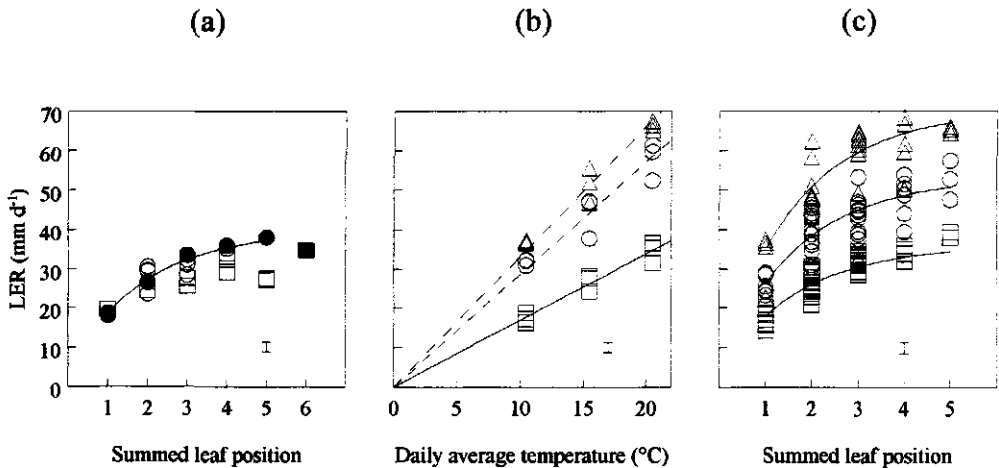


Figure 2. (a) LER in treatment T1L3 as a function of summed leaf position. The negative exponential equation (eqn. a, Appendix II) was fitted to data of leaves that appeared before $HS_{ms} = 4.7$ (circles) ($R^2_{adj} = 90\%$). Data of leaves that appeared after $HS_{ms} = 4.7$ are also drawn (squares). Filled symbols indicate main stem leaves, open symbols on other tillers. (b) LER₁ (□; i.e. LER at summed leaf position = 1 as fitted by the negative exponential equation), LER₃ (○) and LER₅ (Δ) for each treatment as linear functions of temperature with base temperature = 0 °C, including only leaves appearing before $HS_{ms} = 4.7$ ($R^2_{adj} = 97\%$). (c) LER as a function of summed leaf position for leaves appearing before $HS_{ms} = 4.7$ fitted by equation 4 ($R^2_{adj} = 83\%$). Data points are means of leaf type for each treatment (T1: (□); T2: (○); T3: (Δ)). The vertical bar indicates twice the mean standard error.

The effects of variation in temperature and PPFD on fitted LER₁ (LER at summed leaf position = 1; explained in Appendix II), LER₃ (LER at summed leaf position = 3), and LER₅ (LER at summed leaf position = 5) were examined. Stepwise regression showed for all three leaf variables, only a linear effect of temperature was significant, and there were no significant PPFD, quadratic or interaction effects. Since the estimated intercept with the temperature-axis did not vary significantly between leaf positions, and was not significantly different from 0 °C, a base temperature of 0 °C was used and the slopes estimated for LER₁, LER₃ and LER₅ (Fig. 2b). Combining the linear effects of temperature on LER₁, LER₃ and LER₅ with a base temperature of 0 °C, and the effects of summed leaf position on LER, yielded the following equation:

$$LER = (gT_d - fT_d) (1 - e^{-c(\text{Summed leaf position} - 1)}) + fT_d \quad (4)$$

where LER is in mm d⁻¹, c is a fitted constant, T_d is the mean daily temperature, fT_d is the LER for summed leaf position = 1, and gT_d is the LER for summed leaf position → ∞. This three-parameter (c, f and g) equation predicts LER in terms of leaf position and temperature before HS_{ms} = 4.7. The full data set (all treatments and leaf types appearing before HS_{ms} = 4.7) was used to estimate c, f and g, and the results are shown in Fig. 2c (c = 0.60±0.055; f = 1.7±0.04 mm °C d⁻¹; g = 3.4±0.07 mm °C d⁻¹; values with s.e.).

LED

LED was closely correlated with phyllochron (expressed in days; Fig. 1). Careful examination of the data showed that the relation between LED and phyllochron was different for main stem leaf 1. For this leaf, temperature and PPFD had no significant effect on the relationship (Fig. 3a). For the other leaves, increase in PPFD caused a significant increase in D_λ (Fig. 3bcd), although the differences were not large. The following equation set was obtained (values with s.e.):

$$\begin{aligned} LED &= 0.96 \pm 0.013 \times \text{Phyllochron} && \text{for leaf 1 on the ms} \\ LED &= (1.10 \pm 0.01 + 0.0071 \pm 0.00142 \times \text{PPFD}) \times \text{Phyllochron} && \text{for other leaves} \end{aligned} \quad (5)$$

where LED and phyllochron are in days and PPFD in mol m⁻² d⁻¹. Combining the relationship between phyllochron (expressed in thermal time with base temperature of 0 °C) and PPFD in Chapter 2 with eqn. 5 in the current paper gives LED values of 147, 127 and 123 °C d for treatments L1, L2 and L3 respectively.

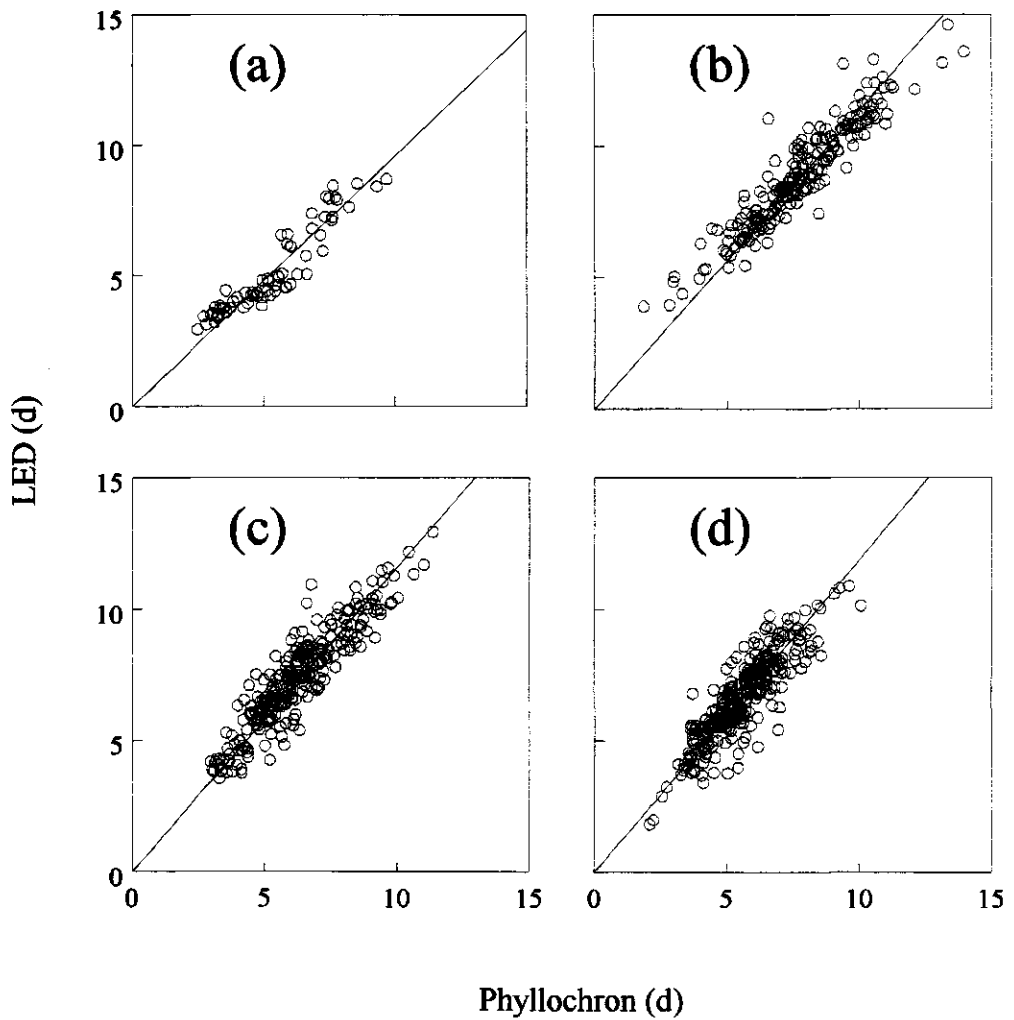


Figure 3. LED as linear function of phyllochron (eqn. 5). Data points are per leaf (not means per treatment): (a) relationship independent of temperature and PPFD for main stem leaf 1 ($R^2_{\text{adj}} = 86\%$); and relationships dependent on PPFD (eqn. 5) for all other leaves combined: (b) L1; (c) L2; (d) L3 ($R^2_{\text{adj}} = 84\%$).

Maximum width

Summed leaf position (Table 1) accounted for most of the variation in maximum leaf width, except for treatment T3L1. Since examination of the data showed that most of the unaccounted variation was caused by leaves that had appeared after $HS_{ms} = 4.7$ (e.g. Fig. 4a), the data were reanalysed including only those leaves that had appeared before $HS_{ms} = 4.7$. Again, summed leaf position accounted for most of the variation except for treatment T3L1. Averaging over all treatments, R^2_{adj} was 86% using summed leaf position as the independent variable (hypothesis C), and 60 and 63% using leaf appearance day (hypothesis A) or leaf position on a tiller (hypothesis B) respectively; the logistic function (eqn. c, Appendix II), using summed leaf position, accounted for most of the variation. Maximum widths of leaves appearing after $HS_{ms} = 4.7$ were larger than predicted by the fitted equation if the leaf position on a tiller was greater than 1 and lower than predicted if leaf position on a tiller was equal to 1.

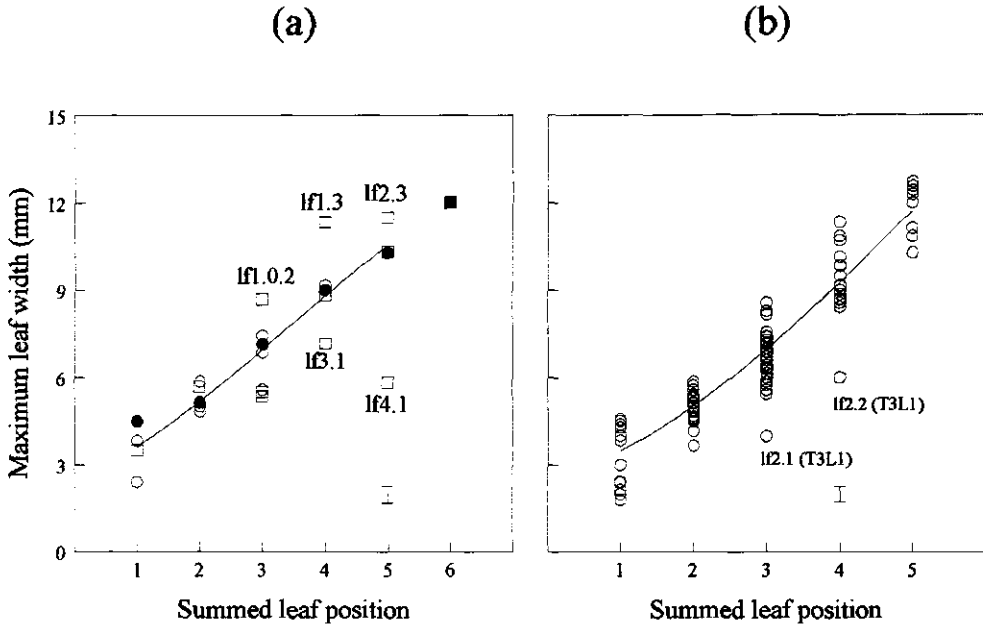


Figure 4. (a) Maximum leaf width in treatment T1L3 as a function of summed leaf position. The logistic equation (eqn. c, Appendix II) was fitted to data of leaves that appeared before $HS_{ms} = 4.7$ (circles) ($R^2_{adj} = 92\%$). Data of leaves that appeared after $HS_{ms} = 4.7$ are also given (squares). Filled symbols indicate main stem leaves, open symbols on other tillers. (b) Maximum width as a function of summed leaf position of leaves appearing before $HS_{ms} = 4.7$ fitted using the logistic function (eqn. 6; $R^2_{adj} = 84\%$). Data points are means of leaf type for each treatment. The vertical bars indicate twice the mean standard error.

The effects of variation in temperature and PPFD on fitted maximum width at summed leaf position = 1, 3 and 5 were examined (explained in Appendix II). Linear, quadratic and interaction terms of temperature and PPFD had no significant effect on any of the three variables. Therefore, the full data set (all treatments and leaf types appearing before $HS_{ms} = 4.7$) was used to give a single logistic equation (values with s.e.):

$$\text{Maximum leaf width} = \frac{22 \pm 2.5}{1 + e^{2.1 \pm 0.09 - 0.45 \pm 0.03 \times \text{Summed leaf position}}} \quad (6)$$

where maximum leaf width is in mm. The widths two leaf types (i.e. lf 2.1 and lf 2.2 in treatment T3L1 (Fig. 4b)) were clearly underestimated using this model.

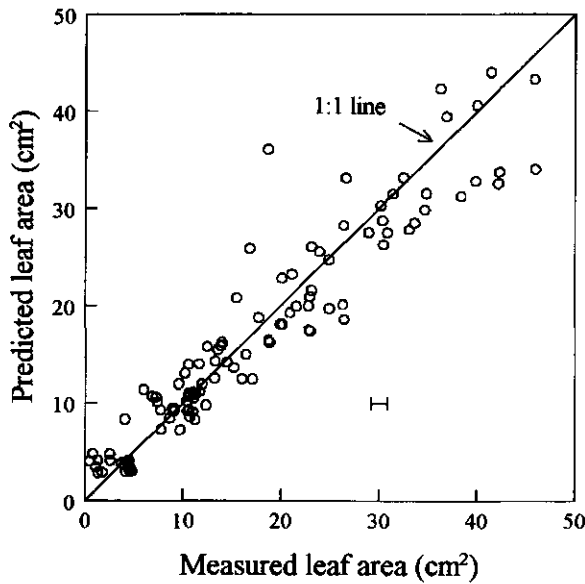


Figure 5. Predicted (using equations 4, 5, 6 and 7) vs. measured areas of individual leaves. Each data point represents the mean area for each leaf type and treatment for leaves appearing before $HS_{ms} = 4.7$. R^2_{adj} of the 1:1 line was 90%. The horizontal bar indicates twice the mean standard error.

Value of k

The leaf shape factor k (eqn. 1) was slightly dependent on temperature, but not on PPFD (values with s.e.):

$$k = 0.77 \pm 0.02 + 0.003 \pm 0.0011 \times T_d \quad (R^2_{adj} = 4\%) \quad (7)$$

where T_d is daily mean temperature ($^{\circ}\text{C}$).

Leaf area

Equations 4, 5, 6 and 7 were used to predict the fully-expanded area of leaves appearing before $\text{HS}_{ms} = 4.7$ in terms of tiller type, leaf position on the tiller, temperature and PPFD. Fig. 5 shows that this set of equations accounted for 90% of the total variation in individual leaf area.

Discussion

Calculation of LER and LED

Lengths of visible leaf blades were measured four times per phyllochron and subsequently LER and LED were calculated (Fig. 1). In this way, all elongating leaves on a plant could be measured rapidly. However, before leaf appearance, the blade elongates within the encircling sheaths and the last phase of visible elongation of the blade is caused by elongation of the sheath (Skinner and Nelson, 1995). Thus, LER as measured in this research consists of the last part of blade elongation followed by sheath elongation. This should be kept in mind when this data set is compared with real blade elongation rates, for example measured with a radial position transducer (Volencic and Nelson, 1982; Skinner and Simmons, 1993).

Usually elongation of a single leaf in time is well described using a logistic function (Kemp, 1981a; Skinner and Nelson, 1995). The exponential phase of the logistic curve occurs within the encircling sheaths and was therefore not measured in this research. The exponential decrease in the rate of blade elongation at the end of the elongation phase was probably compensated by the exponential increase in the rate of elongation of the sheath, thus obtaining a growth curve as shown in Fig. 1.

Regulation of LER

At an early stage of development, LER increased with main stem leaf position, as also found by Kirby (1973) and Robson (1973). The decrease in LER after $\text{HS}_{ms} = 4.7$, observed in all treatments, is not likely to be caused by nutrient limitation, because all treatments received the same amount of nutrients per main stem phyllochron, while biomass accumulation and tillering per main stem

phyllochron varied between treatments. Borill (1959) found strong effects of inflorescence initiation on leaf length. Inflorescence initiation was not determined here but, since stem elongation started at approximately $HS_{ms} = 5$, it is possible that reproductive development was associated with the decrease in LER.

In the new approach advanced here, not only the main stem leaves, but all leaves on a plant, were considered. Kemp (1981b) suggested that the plant is physiologically integrated and that the LER of all simultaneously-growing leaves are equal. This might be true at later stages of plant growth, but at earlier stages, this hypothesis did not account for most of the variation. Others have assumed that leaf position on a tiller determines LER (Amir and Sinclair, 1991; McMaster *et al.*, 1991; Van Loo, 1993), but this hypothesis did not account for most of the variation either. Instead, a new hypothesis proved to be the most valuable: leaf types should be quantified in terms of summed leaf position (Table 1). Using summed leaf position as an independent variable means that the LER of a leaf depends on the LER of the previous foliar leaf on the same tiller or on the parent tiller (prophylls are omitted). Thus the LER of main stem leaf 3 depends on the LER of main stem leaf 2 and the LER of leaf 1 on tiller t3.0 depends on the LER of main stem leaf 3.

A possible morphological explanation for the close relationship between summed leaf position and LER is that LER, as well as other leaf dimensions, depend on the size of the apex (Abbe *et al.*, 1941; Pieters and Van den Noort, 1988; Pieters and Van den Noort, 1990) which increases with each appearing leaf.

LER increased linearly with temperature up to 20.5 °C (Fig. 2b), while effects of PPFD were not significant. Detailed studies have revealed that LER was reduced only at very low carbohydrate concentrations (Kemp and Blacklow, 1980; Kemp, 1981a; Sambo, 1983), and that water potential (Sambo, 1983), sucrose-metabolising enzymes (Kalt-Torres and Huber, 1987), length of the elongation zone (Schnyder and Nelson, 1989) and temperature (Hay and Tunnicliffe Wilson, 1982) have much larger effects on LER. It has been reported that shading can increase the length of the elongation zone, and LER (Schnyder and Nelson, 1989; Kemp, 1981a), but this effect was not observed in this research.

Regulation of LED

LED and phyllochron, expressed in days, were closely related (Fig. 3). This supports the proposition of Tesařová *et al.* (1992) and Skinner and Nelson (1995), that consecutive leaves are synchronized in their growth and development. For main stem leaf 1, LED was shorter than the phyllochron ($D_\lambda < 1$; Fig. 3a), which means that there was a short period when main stem leaf 1 had stopped elongating but main stem leaf 2 had not yet appeared. For the other leaves on a plant, there is a period during which two leaves on one tiller are elongating at the same time ($D_\lambda > 1$; Fig. 3bcd). For these other leaves, increase in PPFD was associated with an increase in D_λ (eqn. 5). This effect of PPFD on D_λ may result from the negative effects of PPFD on sheath lengths, since a rapidly increasing sheath

length could delay leaf appearance, thereby increasing the phyllochron (eqn. 2). To test this hypothesis, instead of leaf appearance day, leaf initiation day was calculated, following Skinner and Nelson (1994):

$$\text{Initiation day leaf } \lambda = \text{Appearance day leaf } \lambda - \frac{\text{Sheath length leaf } (\lambda-2)}{\text{LER leaf } \lambda} \quad (8)$$

where the sheath length of leaf $(\lambda-2)$ is the length of sheath that leaf λ has to traverse before appearing. Using initiation day instead of appearance day in eqn. 2, the value of D_λ still increased significantly with PPF. However, since eqn. 8 assumes that the LER of the unappeared leaf is equal to the LER after appearance (which is certainly not true (Skinner and Nelson, 1995)), effects of PPF on D_λ , acting through effects on sheath length, can, therefore, not be ruled out.

Regulation of maximum leaf width

In the early stages of plant development, maximum leaf width increased with main stem leaf position as found by Friend *et al.* (1962) and Wilson and Cooper (1969a). After $HS_{ms} = 4.7$, maximum widths of the youngest leaves on a tiller were larger than predicted, whereas the first leaf on a tiller had a smaller maximum leaf width (Fig. 4a). Inflorescence initiation may have taken place around $HS_{ms} = 4.7$. After inflorescence initiation, apical dominance increases such that leaves on existing tillers might become broader, while leaves on new emerging tillers could become narrower than expected.

As found for LER, summed leaf position (Table 1) accounted for most of the variation in maximum leaf width, in contrast to previous hypotheses (Kemp, 1981b; Amir and Sinclair, 1991; McMaster *et al.*, 1991; Van Loo, 1993). A possible explanation is that leaf dimensions depend on the size of the apex (Abbe *et al.*, 1941; Pieters and Van den Noort, 1988; Pieters and Van den Noort, 1990) which increases with the appearance of each new leaf. A logistic curve accounted for most of the variation, but the part of this curve with decreasing slope could not be evaluated (Fig. 4b). However, there is other evidence that the relation between maximum leaf width and leaf position on the main stem is logistic (Borrill, 1959).

There were no statistically significant effects of temperature or PPF on maximum leaf width, confirming other results (Forde, 1966; Friend and Pomeroy, 1970; Wilson and Cooper, 1969b; Allard *et al.*, 1991). Friend *et al.* (1962) found that only in more extreme conditions (average temperature above 20 °C or PPF values below 106 $\mu\text{mol m}^{-2} \text{s}^{-1}$) was maximum leaf width reduced. These conditions are outside the ranges studied here.

Regulation of k

The value of k was only slightly influenced by temperature (eqn. 7). For maize (*Zea mays* L.) leaves, only small effects of genotype, plant density or leaf position on k were found (Van Arkel, 1978;

Sanderson *et al.*, 1981). It appears, therefore that length and maximum width are good estimators of leaf area, as they are largely independent of environmental conditions and leaf type.

Towards a dynamic mechanistic model

Models of leaf area growth of *Gramineae* species can be divided into two types: (i) leaf area is calculated from the leaf weight/shoot weight ratio and specific leaf weight (e.g. SUCROS models (Spitters *et al.*, 1989)) and (ii) leaf area is calculated from the increase in leaf and tiller numbers and area expansion of individual leaves. Results of models of the first type are not satisfactory, because they ignore that the dynamics of leaf area and leaf dry weight are controlled by different physiological processes. Models of the second type have the capability to simulate the area expansion more adequately, because variables such as leaf appearance and elongation are more directly governed by physiological and morphogenetic processes. However, existing models of the second type are descriptive. Final leaf lengths and maximum leaf widths are usually not predicted but empirical (Porter, 1984; Van Loo, 1993) or derived from a fitted descriptive function (Wilhelm *et al.*, 1993; Carberry *et al.*, 1993). Leaf length and width at certain leaf positions of different tillers are assumed to be equal (Porter, 1984; Van Loo, 1993) or slightly different (Wilhelm *et al.*, 1993). The current analysis introduces a method to calculate effects of all possible leaf types on leaf variables.

Eqns. 4, 5, 6 and 7 provide a sounder basis for a mechanistic morphological model of growth of leaf area at early plant stages. Together with the equations developed for the dynamics of leaf number (Chapter 2), leaf area per plant can be simulated in principle. These relationships can also be developed for other *Gramineae* species and effects of factors such as plant density and nitrogen supply can also be included.

Appendix I: List of abbreviations

c, f, g	fitted constants (eqn. 4)
k	leaf shape factor relating leaf length and maximum width with area
lf	leaf position on a plant counted acropetally
ms	main stem
t	tiller type
D_λ	parameter relating phyllochron and LED of leaf λ (eqn. 2)
HS	Haun Stage
L	Light treatment
LED	Leaf Elongation Duration (d)
LER	Leaf Elongation Rate (mm d^{-1})
LER_x	LER fitted with the negative exponential equation at summed leaf position = x

PPFD	Photosynthetic Photon Flux Density
R^2_{adj}	Percentage of variance accounted for (eqn. 3)
T	Temperature treatment
T_d	Daily mean temperature ($^{\circ}\text{C}$)
λ	leaf position on a tiller counted acropetally

Appendix II: Use of biologically realistic equations for data analysis

Leaf appearance day (hypothesis A), leaf position on a tiller (hypothesis B) or summed leaf position (hypothesis C) (Table 1) were used as independent variables (x) to account for variation in the dependent variables (y), maximum leaf width or LER. Biologically-realistic relations between y and x were fitted to test which hypothesis accounted for most of the variation. The following equations were evaluated: (i) the negative exponential equation, often used for the photosynthesis-light response (Goudriaan and Van Laar, 1994); three S-shaped curves (Cao *et al.*, 1988): (ii) the Gompertz function, (iii) the logistic equation and (iv) the Richards function; (v) a bell-shaped curve (Stewart and Dwyer, 1994). R^2_{adj} was determined for each of the 15 hypothesis-equation combinations. The hypothesis-equation combination with the highest R^2_{adj} was selected.

Effects of temperature and PPFD on the standard variables of the selected equation were not directly analysed, because the data range was limited and variables such as maximum asymptotic y-value are, therefore, estimated with a large standard error. For a three-parameter equation and x ranging from 1 to 5, three new parameters were calculated that: (i) fully determine the equation, (ii) have a low standard error and are not closely correlated, and (iii) cover the data range. These new parameters are y_1 (the fitted y value for $x=1$), y_3 (the fitted y value for $x=3$) and y_5 (the fitted y value for $x=5$) (y =LER or maximum leaf width; x =summed leaf position).

The negative exponential equation is:

$$y = (y_{\max} - y_1) * (1 - e^{-c x}) + y_1 \quad (a)$$

where y is LER or maximum width, x is leaf appearance day, leaf position on a tiller or summed leaf position, y_{\max} the maximum asymptotic y value, y_1 the y value at $x=1$ and c a fitted constant. Three S-shaped curves were evaluated (Cao *et al.*, 1988), (i) the Gompertz function:

$$y = y_{\max} e^{-c_1} e^{-c_2 x} \quad (b)$$

with c_1 and c_2 fitted constants; (ii) the logistic function:

$$y = \frac{y_{\max}}{1 + e^{-(c_1 + c_2 x)}} \quad (c)$$

and (iii) the Richards function:

$$y = \frac{y_{\max}}{\left(1 + e^{\frac{-(c_1 + c_2 x)}{c_3}}\right)^{c_3}} \quad (d)$$

When $c_3 = 1$, this equation equals the logistic function and when $c_3 \rightarrow \infty$ this equation equals the Gompertz function. Finally, a bell-shaped curve developed by Stewart and Dwyer (1994) was evaluated:

$$y = y_{\max} e^{c_1(x-c_2)^2 + c_3(x-c_2)^3} \quad (e)$$

All constants were estimated with non-linear regression. The equation which explained most variation (highest R^2_{adj}) was selected.

Chapter 4

Morphological analysis of leaf growth of maize: responses to temperature and photosynthetic photon flux density

with H. Tijani-Eniola and P.C. Struik

Abstract

Existing models of leaf area expansion of *Gramineae* species are empirical and species-specific. To increase understanding of the mechanisms involved in leaf area expansion, effects of environmental factors on leaf growth of the non-tillering species maize (*Zea mays* L.) were analysed quantitatively. A growth chamber experiment was carried out with the cultivar Luna including different combinations of temperature (daily average 10.5, 15.5, 20.5 or 25.5 °C) and photosynthetic photon flux density (PPFD) (104, 185 or 277 $\mu\text{mol m}^{-2} \text{s}^{-1}$); leaf appearance rate and leaf growth variables were measured. At 10.5 °C, a high proportion of the plants died due to prolonged exposure to cold stress. Both high temperatures and high PPFD values increased leaf appearance rate. Maximum leaf width was highest at intermediate temperatures and high PPFD values, and was strongly related to specific leaf weight ($R^2_{\text{adj}} = 0.88$). At higher temperatures leaf elongation rate was greater and leaf elongation duration was lower, resulting in a maximum final leaf length at 20.5 °C. At lower PPFD values leaves were slightly longer, caused by a prolonged leaf elongation. Leaf shape was described with a new function and was different for Leaves 1 and 2 than for higher-positioned leaves. The observed relationships are useful for dynamic simulation of leaf area based on plant morphology.

Introduction

In previous studies (Chapters 2 and 3), effects of temperature and photosynthetic photon flux density (PPFD) on the morphological components of leaf area dynamics of wheat were studied. It was shown that temperature and PPFD mainly affected the rate of increase in number of leaves and hardly the size of the leaves. Number of leaves was largely determined by tiller formation. When a plant lacks this tillering response to environmental conditions, growth of the main stem fully determines plant adaptation to environmental conditions. A study into the effects of environmental factors on the morphological development of such a different plant type could lead to a better understanding of mechanisms involved in the increase of leaf area. Modern maize hybrids only rarely form tillers and are therefore suitable for such a study.

In *Gramineae* species visible leaf parts are full-grown, because cell division and elongation take place within the sheath bundle (Dale, 1988). Therefore, the width of leaf parts does not change after emergence of that part. Increase in leaf area of a maize plant can thus be divided into five morphological components: (i) leaf appearance rate, (ii) leaf elongation rate (LER), (iii) leaf elongation duration (LED), (iv) maximum leaf width, and (v) leaf shape parameters. For growing leaves, the exact shape of the full-grown leaf is needed to calculate the light-exposed leaf area as a function of the fraction of the length that has appeared (Sanderson *et al.*, 1981).

In maize, especially effects of temperature on leaf appearance rate have been studied extensively (Tollenaar *et al.*, 1979; Thiagarajah and Hunt, 1982; Warrington and Kanemasu, 1983), while studies on the effects of leaf position and environmental factors on the four other components are relatively scarce. Therefore, simulation models of growth in leaf area of maize plants are descriptive (Keating and Wafila, 1992; Stewart and Dwyer, 1994). In the current research the effects of leaf position, temperature and PPFD on these five morphological components are quantified with the objective to improve future modelling efforts on leaf area expansion of maize plants and to arrive at a more general morphological model for *Gramineae* plants. To avoid changes of environmental factors in time, experiments were done in growth chambers.

Materials and methods

Maize plants (silage maize hybrid 'Luna') were grown in four growth chambers, each with a different temperature regime. Within a growth chamber, three compartments with different PPFD values were created. Treatments started one day after plant emergence. Plant density was kept low throughout the experimental period.

Plant material and growing conditions

Maize seeds were sown 3 cm deep in 5 l pots filled with a mixture of 33 % sandy soil and 67 % quartz sand. Three seeds were sown per pot. A total of 540 pots were placed on trolleys in four growth chambers (daily photoperiod 7.00-21.00 h; relative humidity 70 %; temperature 23 °C from 9.00-21.00 h and 18 °C from 21.00-9.00 h).

One day after 50 % emergence, plant number per pot and pot number were reduced to obtain a homogeneous population of plants (one plant per pot; 90 pots per growth chamber). Using white curtains, the growth chambers were divided into three compartments (3.20*1.50 m) for the PPFD treatments. Pots were distributed over the three compartments, each containing 30 plants, resulting in an initial plant density of 19 m⁻². Photoperiod and relative humidity remained the same as in the pre-emergence period.

During growth, trolleys were rotated within a compartment approximately every 0.75 ligule appearance interval (this is the period between the visible appearance of two consecutive ligules) to minimize the variation between plants. Pots were watered at least once a day. Nutrient solution was supplied every two ligule appearance intervals based on the expected growth rate and desired high nutrient concentration in the plant material (Scholte, 1987). Trolleys were lowered during growth to obtain a constant PPFD at the top of the plants. The experiment was terminated at ligule appearance of the seventh leaf.

Treatments

The different PPFD treatments were established per compartment. Every compartment ceiling contained 6 metal halide (Philips HPI 400 W) and 6 high pressure sodium (Philips AGROSON-T 400 W) lamps. At nine points per compartment, PPFD was measured just above the pots. For the highest PPFD (277 $\mu\text{mol m}^{-2} \text{s}^{-1}$) all lamps were switched on, for the middle PPFD 8 lamps (185 $\mu\text{mol m}^{-2} \text{s}^{-1}$), and for the lowest PPFD 4 lamps (104 $\mu\text{mol m}^{-2} \text{s}^{-1}$). The metal halide lamp/high pressure sodium lamp ratio was 1:1 for every treatment.

Temperature treatments (day/night: 13/8, 18/13, 23/18 or 28/23 °C) were established per growth chamber and were set for the 185 $\mu\text{mol m}^{-2} \text{s}^{-1}$ compartments. This range of temperatures assured large differences in the increase in leaf area. Day temperature started at 9.00 h, night temperature at 21.00 h. The change-over from day to night temperature and *vice versa* occurred within half an hour. On average, during the PPFD period air temperature was 0.5 °C higher at 277 $\mu\text{mol m}^{-2} \text{s}^{-1}$ and 0.5 °C lower at 104 $\mu\text{mol m}^{-2} \text{s}^{-1}$ than at 185 $\mu\text{mol m}^{-2} \text{s}^{-1}$.

Measurements

Six plants per treatment were harvested every ligule appearance interval, starting from ligule appearance of Leaf 3 up to ligule appearance of Leaf 7 (5 harvests). After every harvest, the remaining pots were rearranged to minimize inter-plant competition (plant density at last harvest 3.9

m²). At each harvest, length and maximum width of all leaves were measured with a ruler. On one plant, leaf width of full-grown leaves was measured at six or seven equidistant places covering the whole leaf length to determine leaf shape parameters. After this, plants were dissected into roots and shoots, and the shoot into separate visible leaves and internodes/sheaths. Dry weight was measured after drying the material at 70 °C until constant weight.

To determine LER and LED, throughout the experimental period the length (i.e. from the leaf tip to the last visible ligule) of growing leaves (except Leaf 1) was measured with a ruler until the leaf was full-grown. These measurements were done approximately four times per ligule appearance interval at a fixed time on a day on six plants which were used for the last harvest.

Definitions and calculations

Leaf positions were counted acropetally. Leaf appearance was defined as the moment the tip of a leaf blade reached above the uppermost visible ligule. Number of growing leaves was defined as the number of leaves that had appeared with their ligule not yet visible.

Leaf elongation rate (LER) was assumed to be constant until the leaf was full-grown. Leaf elongation rate and LED were estimated with a two-step regression as was done in Chapter 3. Data of recently full-grown leaves in the destructive harvests were used to analyse full-grown leaf length, maximum leaf width, dry weight and specific leaf weight (SLW). Shape of full-grown leaves was evaluated with the Sanderson model (Sanderson *et al.*, 1981):

$$\frac{w}{W} = \sin^{\alpha} \left(\frac{\pi}{2} \frac{x}{X} \right) \quad (1)$$

where w is the leaf width at distance x from the leaf tip, W the maximum leaf width, X the full-grown leaf length, a the ratio of x/X at the position of maximum leaf width and α a constant that allows for differences in leaf shape. Values for a and α are limited:

$$\begin{aligned} 0.5 < a \leq 1 \\ \alpha > 0 \end{aligned}$$

because $w/W \geq 0$ and maximum width does not occur at the leaf base for maize leaves. For full-grown leaves, leaf area can be directly derived from leaf length and maximum leaf width:

$$\text{Full-grown leaf area} = k * \text{Maximum leaf width} * \text{Full-grown leaf length} \quad (2)$$

The variable k was calculated by numerical integration of Eq. 1.

Statistical analysis

It was assumed that effects on plants due to differences in growth chambers could be attributed to temperature, because the growth chambers were of the same type, the conditions could be controlled very well and the difference in temperatures between growth chambers were large. Although we realize that replicates are actually subsamples, we feel that it is justified to use each plant as a replicate. An analysis of variance was carried out for significance of treatment effects and to calculate the least significant difference (LSD) ($P=0.05$). Effects on leaf area per plant were analysed with a stepwise-regression method (Montgomery and Peck, 1982). Linear, quadratic and interaction terms of the quantitative variables number of appeared leaves (N_{LF}), temperature (T) and PPFD (L) were used as independent variables. The analysis started with the fit of an empty model. One by one terms were added that gave the greatest improvement of R^2_{adj} , until six terms were added.

Results

Due to continuous exposure to cold stress, a large portion of the plants grown at 13/8 °C died in an early stage, especially at 104 $\mu\text{mol m}^{-2} \text{s}^{-1}$. We therefore decided to stop the 13/8 °C treatment before 7 leaves were full-grown. The remaining data are shown in the graphs, but were not part of the statistical analyses and calculation of main effects of PPFD. Death of leaves was negligible in the other growth chambers with higher temperatures.

Leaf area and number of leaves per plant

The leaf area per plant increased almost exponentially in time (Fig. 1, Quadrant I). Relative growth rate of leaf area (RGR_{LA} = the slope of $\ln(\text{leaf area})$ vs. days after emergence (DAE)) was greater at higher temperatures but similar at 23/18 and 28/23 °C (Table 1). Photosynthetic photon flux density affected RGR_{LA} less; RGR_{LA} was highest at 185 $\mu\text{mol m}^{-2} \text{s}^{-1}$. The lower RGR_{LA} at 277 $\mu\text{mol m}^{-2} \text{s}^{-1}$ was caused by a lower RGR_{LA} in the last harvest interval.

Number of leaves increased linearly in time up to Harvest 4 (Fig. 1, Quadrant III). In Harvest 5, tassels had appeared for most treatments and this harvest was therefore excluded from calculations of leaf appearance rate. Leaf appearance rate (i.e. slope of number of leaves vs. DAE) was greater at higher temperatures, although less pronounced above 23/18 °C (Table 2). To a lesser extent also PPFD increased leaf appearance rate.

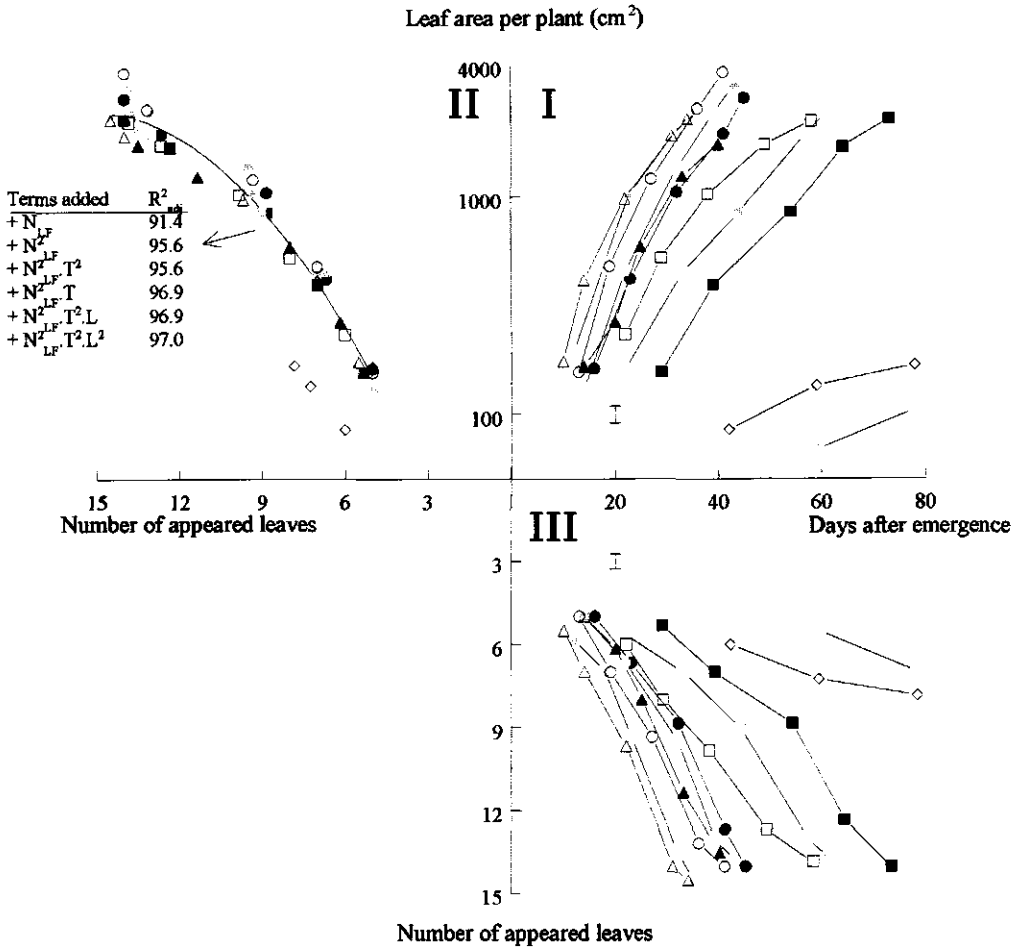


Figure 1. Leaf area per plant in relation to days after emergence and number of appeared leaves. Quadrant I: increase of leaf area per plant (log scale) with days after emergence. The bar indicates average LSD ($P=0.05$). Quadrant II: relation between leaf area per plant (log scale) and number of appeared leaves. The result of the stepwise regression (see text) with independent variables number of appeared leaves (N_{LF}), temperature (T) and PPFD (L) is given (13/8 °C treatments excluded). The fitted line represents the regression model with only the first two terms (N_{LF} and N_{LF}^2) included. Quadrant III: increase of number of appeared leaves with days after emergence. The bar indicates average LSD ($P=0.05$). Open symbols: PPFD=277 $\mu\text{mol m}^{-2} \text{s}^{-1}$; Symbols in grey: PPFD=185 $\mu\text{mol m}^{-2} \text{s}^{-1}$; Black symbols: PPFD=104 $\mu\text{mol m}^{-2} \text{s}^{-1}$. The shape of the symbols indicates the temperature treatment: 13/8 °C: \diamond ; 18/13 °C: \square ; 23/18 °C: \circ ; 28/23 °C: \triangle .

Table 1. RGR_{LA} (d^{-1}) calculated from Figure 1, Quadrant I by linear regression.

PPFD ($\mu\text{mol m}^{-2} \text{s}^{-1}$)	Temperature ($^{\circ}\text{C}$)			
	13/8	18/13	23/18	28/23
104	-	0.060	0.096	0.095
185	0.022	0.068	0.110	0.108
277	0.019	0.061	0.109	0.101
LSD (P=0.05) = 0.007				

Table 2. Leaf appearance rate (d^{-1}) calculated from Figure 1, Quadrant III by linear regression (last harvest excluded).

PPFD ($\mu\text{mol m}^{-2} \text{s}^{-1}$)	Temperature ($^{\circ}\text{C}$)			
	13/8	18/13	23/18	28/23
104	-	0.19	0.30	0.34
185	0.08	0.21	0.31	0.39
277	0.05	0.24	0.35	0.40
LSD (P=0.05) = 0.03				

The number of appeared leaves was strongly related to $\ln(\text{leaf area per plant})$ (Fig. 1, Quadrant II). The stepwise regression showed that for temperatures above 13/8 $^{\circ}\text{C}$ a second order polynomial of number of appeared leaves accounted for 95.6 % of the variation in $\ln(\text{leaf area per plant})$ (N_{LF} and N_{LF}^2 terms, Fig. 1, Quadrant II). Effects of temperature and PPFD were larger at higher leaf number per plant (T and L interacted with N_{LF}). At comparable numbers of appeared leaves, leaf area per plant was greater at 23/18 than at 18/13 or 28/23 $^{\circ}\text{C}$ ($N_{LF}^2 \cdot T$ and $N_{LF}^2 \cdot T^2$ terms) and plants grown at 104 $\mu\text{mol m}^{-2} \text{s}^{-1}$ had a lower leaf area than at 185 or 277 $\mu\text{mol m}^{-2} \text{s}^{-1}$, an effect that increased slightly with an increase in temperature ($N_{LF}^2 \cdot T^2 \cdot L$ and $N_{LF}^2 \cdot T^2 \cdot L^2$ terms). Using predictions of the full 6-term regression model with $N_{LF}=14$, leaf area per plant ranged between 17.5 dm^2 for the [28/23 $^{\circ}\text{C}$, 104 $\mu\text{mol m}^{-2} \text{s}^{-1}$] treatment and 32.7 dm^2 for the [23/18 $^{\circ}\text{C}$, 185 $\mu\text{mol m}^{-2} \text{s}^{-1}$] treatment. This shows that treatments had large effects on leaf sizes at later stages of development.

Area, length and maximum width of full-grown leaves

Figure 2 shows the separate effects of temperature and PPFD on full-grown area, length and maximum width of Leaves 1 to 7. For all treatments, the increase of length with leaf position was sigmoidal, while the maximum width was almost constant for Leaf positions 1 to 3 and increased linearly for higher leaf positions. As a result, the increase of area with leaf position was exponential-linear.

Interactions between effects of temperature and PPFD were not significant for most leaves and are not shown. Leaf area was smaller at 18/13 °C than at 23/18 °C, mainly because leaves were shorter (Fig. 2). Area of leaves grown at 28/23 °C were smaller than at 23/18 °C mainly caused by a lower maximum leaf width. The effect of PPFD on leaf area depended on leaf position. Leaf area was slightly larger for low PPFD values at Leaf position 2 caused by longer leaves. However, for Leaf positions 4 to 7 the effect reversed, because the negative effect of low PPFD on maximum leaf width became more important than its positive effect on leaf length.

Dry weight of leaves and SLW

Comparable to leaf area (Fig. 2), dry weight per leaf increased exponentially with leaf position (Fig. 3). Since the linear increase of dry weight was faster than that of leaf area, SLW increased from Leaf 4 onwards (Fig. 3).

Interactions between temperature and PPFD effects are not shown in the graphs. Effects of temperature on dry weight were qualitatively equal to effects on area (23/18 > 18/13 > 28/23 > 13/8 °C). The resultant SLW decreased with temperature above 18/13 °C. More pronounced than leaf area (Fig. 2), dry weight of leaves at 104 $\mu\text{mol m}^{-2} \text{s}^{-1}$ was less than at 185 or 277 $\mu\text{mol m}^{-2} \text{s}^{-1}$ (Fig. 3). The resultant SLW was significantly greater for higher PPFD values on all leaf positions. For Leaves 4, 6 and 7, interactions between effects of temperature and PPFD on SLW were significant, because temperature effects were stronger at low PPFD values.

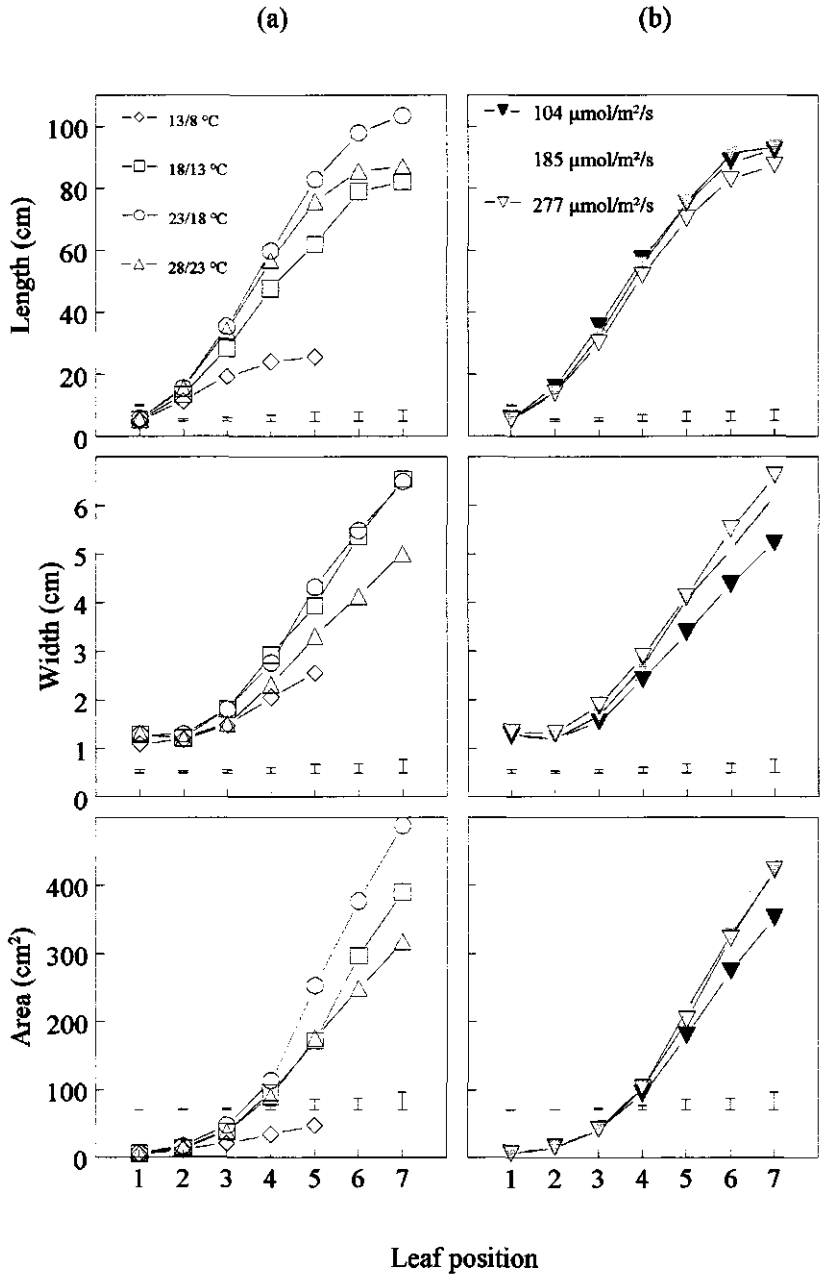


Figure 2. Full-grown length, maximum width and area of Leaves 1-7, (a) averaged per temperature treatment (°C) and (b) averaged per PPFD treatment. Bars indicate the LSD (P=0.05).

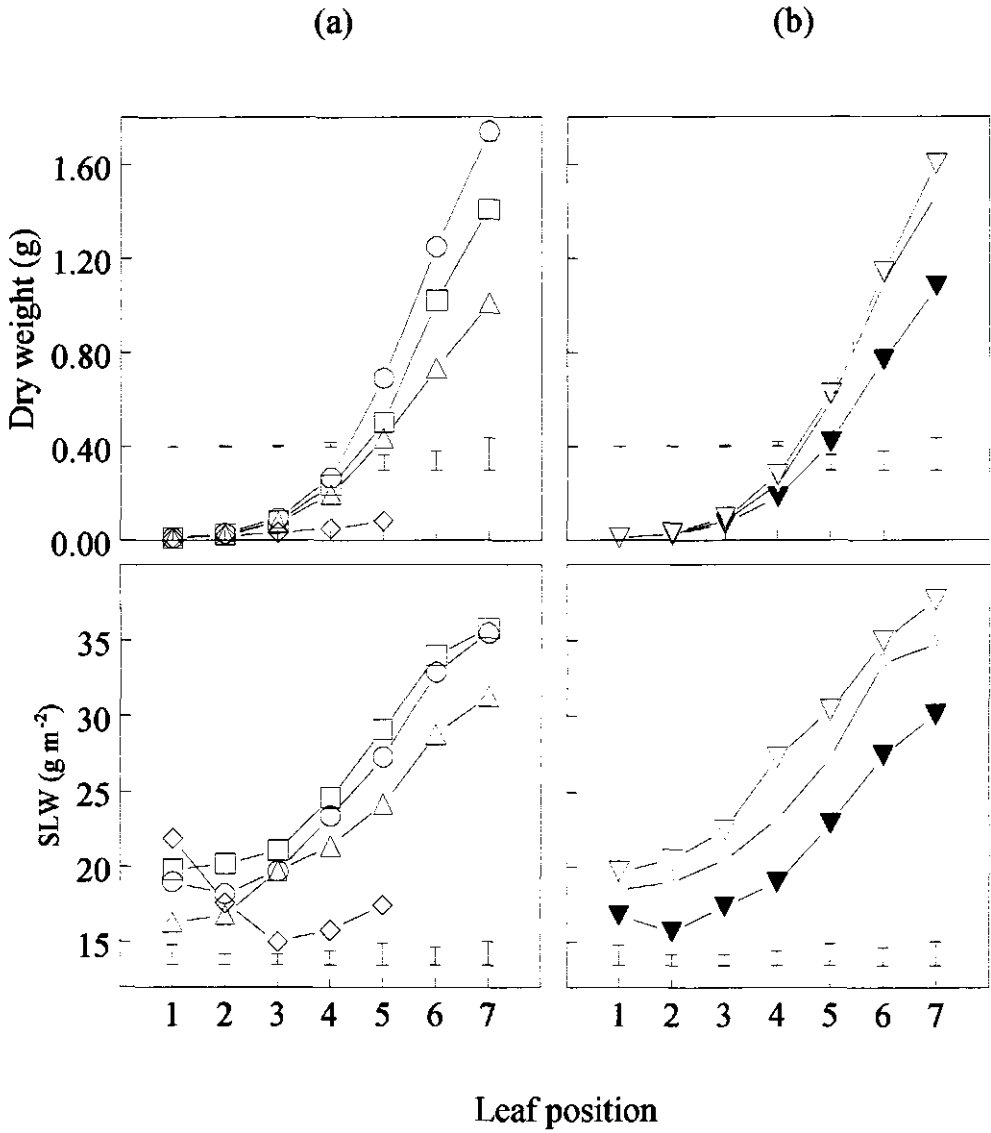


Figure 3. Dry weight and SLW of Leaves 1-7, (a) averaged per temperature treatment and (b) averaged per PPFd treatment. Markers as in Fig. 2. Bars indicate the LSD (P=0.05).

Leaf elongation

Rate of leaf elongation increased with leaf position up to Leaf 5 and then decreased, an effect that was more pronounced for high temperatures (Fig. 4). Leaf elongation rate increased linearly with leaf position.

Interactions between effects of temperature and PPFD were not significant for most leaves and are not shown. Leaf elongation rate was significantly greater and LED was significantly shorter for higher temperatures. The shorter Leaves 5 and 6 at 28/23 °C compared with 23/18 °C (Fig. 2) were related to the sharp decrease of LER with leaf position at 28/23 °C (Fig. 4a). Leaves grown under high PPFD values showed a significantly higher LER compared with leaves grown in low PPFD values for Leaf positions 2 to 5, but differences were small. Duration of leaf elongation was significantly longer at low PPFD values than at high PPFD values for all leaves, and differences were slightly larger than for LER. Therefore, longer leaves in lower PPFD values (Fig. 2) were related to a longer LED.

Leaf shape

The Sanderson model (Eq. 1) did not fit Leaf positions 1 and 2 well, because the maximum width occurred close to the leaf tip. Therefore, another two-parameter model was developed, which accounted for a maximum width that can occur from leaf base to leaf tip and was very similar to the Sanderson model:

$$\frac{w}{W} = \sin \left(\frac{\pi}{2} b^\beta \left(\frac{x}{X} \right)^\beta \right) \quad (3)$$

where b is the value of x/X where the maximum width occurs and β a constant which allows for differences in leaf shape. For low values of β the leaves tend to be wider towards the leaf tip relative to the maximum leaf width. Also for this new model, the values of b and β are limited:

$$\begin{aligned} 0 < b &\leq 1 \\ 0 < \beta &\leq \frac{\ln 0.5}{\ln b} \end{aligned}$$

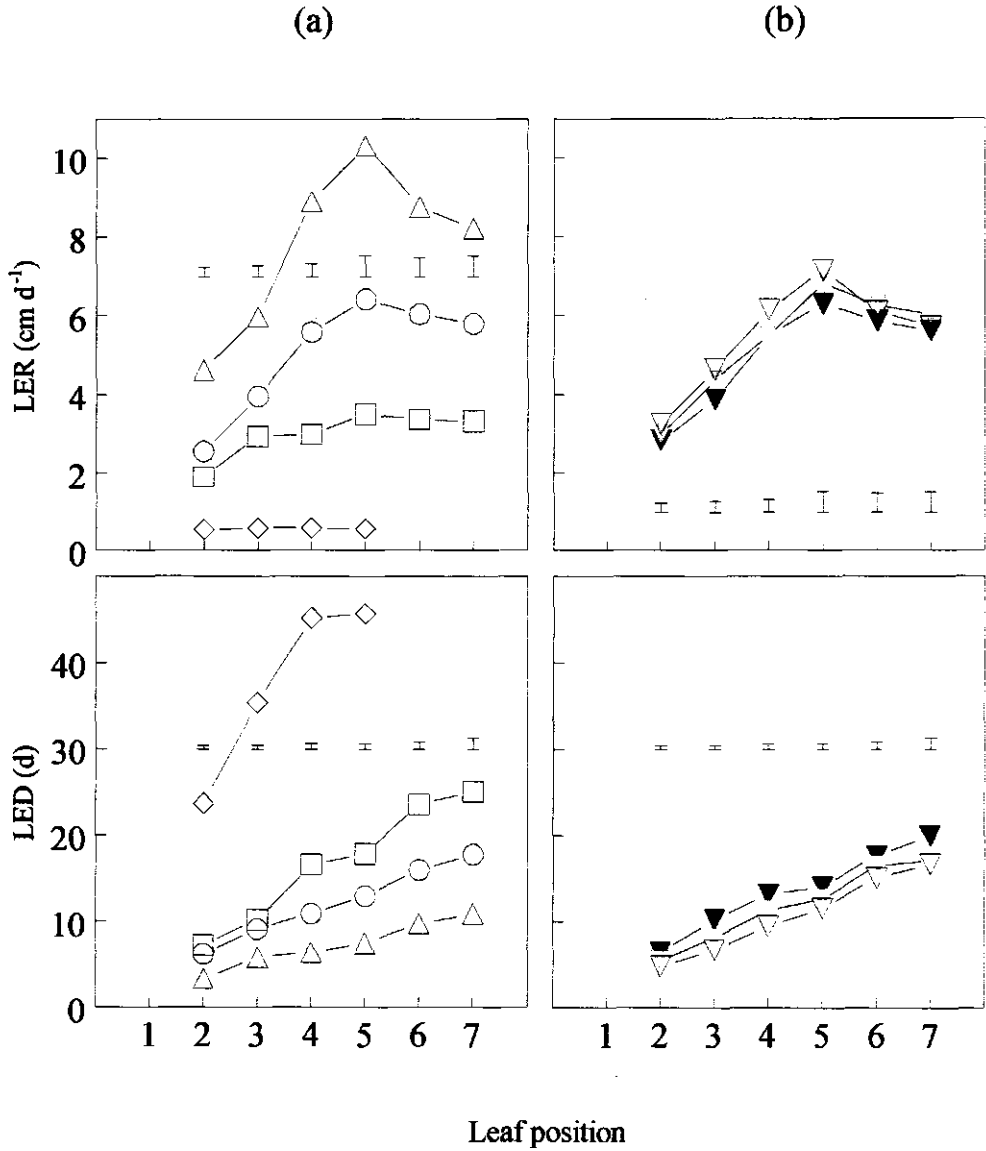


Figure 4. LER and LED of Leaves 2-7, (a) averaged per temperature treatment and (b) averaged per PPFD treatment. Markers as in Fig. 3. Bars indicate the LSD (P=0.05).

Figure 5 shows an example of a fit of the Sanderson model and the new model on a representative Leaf 2 and 6. The Sanderson model assumes that leaves have an axis of symmetry through the point where maximum leaf width occurs, which is unrealistic especially for lower leaves. The maximum leaf width for Leaf 2 in Fig. 5a occurred clearly below $x/X = 0.5$, which was outside the range of the Sanderson model. The maximum width for Leaf 6 occurred above $x/X = 0.5$, and both models gave a similar fit (Fig. 5b). Both models were fitted through leaf length and width data of recently full-grown Leaves 1-7 (13/8 °C treatments excluded). The new model accounted for a greater proportion of the variation for Leaves 1 and 2, while for Leaves 3 to 7 the models performed similarly (Fig. 6). The parameters of the new model b and β increased with leaf position for lower leaves, but remained fairly stable from Leaf 4 to 7 (Fig. 6), and were not influenced by temperature or PPFD. The variable k (Eq. 2) decreased from 0.80 for Leaf 1 and 2 to 0.70 for Leaf 4 to 7.

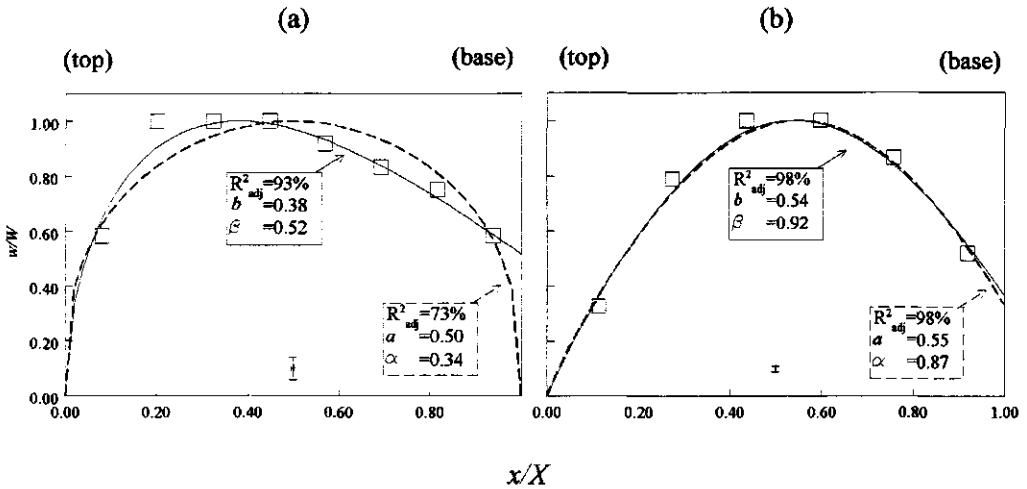


Figure 5. w/W as a function of x/X for a representative Leaf 2 (a) and 6 (b). The dashed line represents the non-linear fit of the Sanderson model (Eq. 1), the solid line the fit of the new model (Eq. 3). R^2_{adj} and parameter estimates are shown in the rectangles. The bars indicate the measuring error of the ruler that was used (± 0.5 mm).

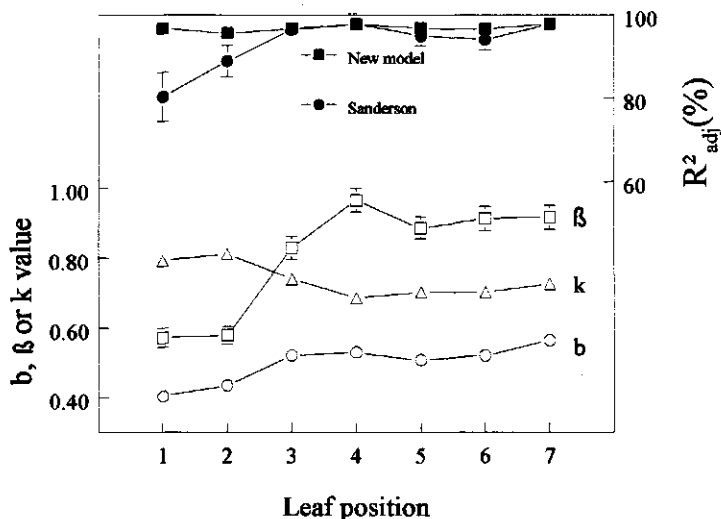


Figure 6. Estimated parameter values of the new model and R^2_{adj} of the two models for Leaf positions 1 to 7. Data points are averages of the 9 treatment combinations (13/8 °C was excluded), with 1 plant per treatment. Bars indicate twice the standard error of the mean. Bars smaller than the marker size do not appear.

Discussion

Limitations of the current experiment

The current experiment was carried out in growth chambers. The PPFD level is therefore low. However, the data on rate of leaf appearance, leaf growth and dry weight are comparable with those found under field conditions, at least at lower temperatures. We are therefore confident that the results obtained are meaningful. The inter-plant competition was kept low due to frequent sampling and even possible changes in the ratio of red/far-red of the photon flux caused by the continuous adaptation of the plant density during the experiment will not have affected the outcome of the experiment.

Dynamics of leaf number

Leaf appearance rate was faster at higher temperatures and to a lesser extent at higher PPFD values. The current data set is compared with growth chamber data from Tollenaar *et al.* (1979) (PPFD = 500 $\mu\text{mol m}^{-2} \text{s}^{-1}$; daylength = 15 h d^{-1}) and Thiagarajah and Hunt (1982) (PPFD = 620 $\mu\text{mol m}^{-2} \text{s}^{-1}$; daylength = 15 h d^{-1}) (Fig. 7). Generally leaf appearance rates were very similar, but at 25.5 °C somewhat lower for the current data set. This difference could be due to the lower PPFD values of

the current experiment compared to the other experiments, or to cultivar effects, which can be strong, especially at higher temperatures (Ellis *et al.*, 1992).

Positive effects of PPFD on leaf appearance rate of maize have also been found by Gmelig Meyling (1973) and Struik (1983) and could be due to the slight increase of temperature of the growing point with PPFD.

Individual leaf growth

In the current research, area growth of individual leaves has been separated into maximum leaf width, LER and LED. Temperature and PPFD affected these three components in different ways, which confirms earlier findings with small cereals and grasses (Friend *et al.*, 1962; Allard *et al.*, 1991) and maize (Hesketh and Warrington, 1989).

The width of leaves has received little attention in literature and it is unknown how the width is related to other plant variables. However, for a mechanistic model it is necessary to find simple relationships with physiological background. In the current research, effects of leaf position, temperature and PPFD on leaf width (Fig. 2) were similar to effects on SLW (Fig. 3) and a good correlation between the two existed (Fig. 8). A possible physiological explanation for this relation is that not only SLW is determined by carbohydrate availability (Thiagarajah and Hunt, 1982; Van Loo, 1993; Grant and Hesketh, 1992), but also maximum leaf width. Leaf width is well related to the number of cell rows across the width (Borrill, 1961; Forde, 1966; Jewiss, 1966) and accordingly to the basal circumference of the shoot apex when the primordium is initiated (Abbe *et al.*, 1941; Robson *et al.*, 1988). The size of the shoot apex is related with the growth rate of the shoot (Pieters,

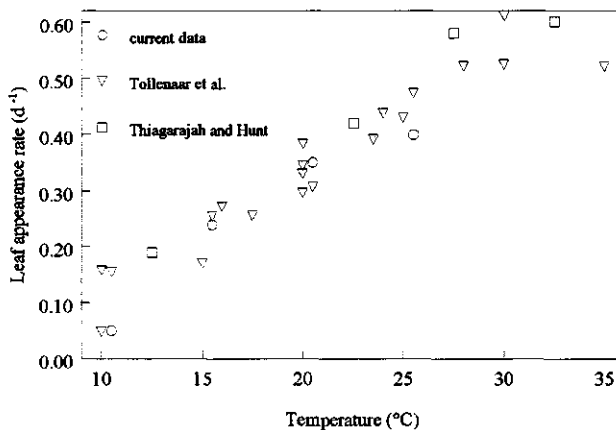


Figure 7. Comparison of leaf appearance rate at different temperatures from the current data set at $277 \mu\text{mol m}^{-2} \text{s}^{-1}$ with data from Tollenaar *et al.* (1979) and Thiagarajah and Hunt (1982).

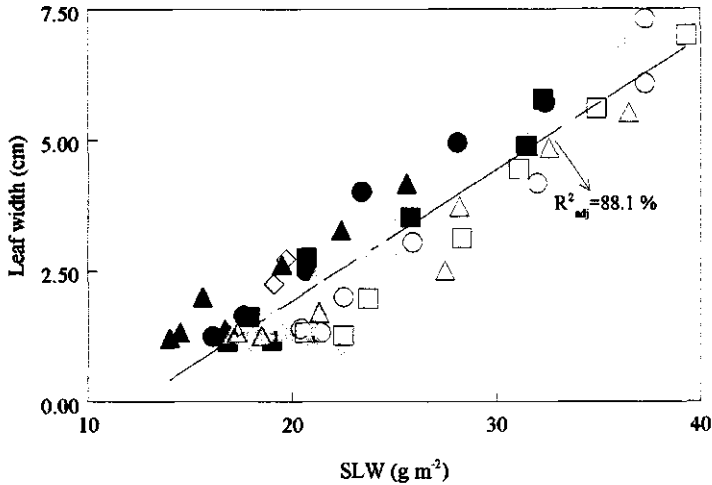


Figure 8. Relation between maximum width and SLW of Leaves 1 to 7. Every data point represents the average value per leaf position per treatment. Markers as in Fig. 1.

1986), and thus with carbohydrate availability.

Leaf elongation rate increased with leaf position up to a maximum, after which it remained stable or declined (Fig. 3). This was also found for reproductive barley plants (Kirby, 1973), vegetative perennial ryegrass (Robson, 1973), tall fescue (Skinner and Nelson, 1994) and maize (Grant and Hesketh, 1992) plants. As for wheat plants (Chapter 3), effects of PPF_D on LER were small. This confirms studies on temperate species by Kemp and Blacklow (1980), Kemp (1981a) and Sambo (1983), who showed that LER only depends on carbohydrate supply at very low levels. The longer leaves formed at lower PPF_D values were related to a longer LED, which was also found for wheat (Chapter 3) and tall fescue (Allard *et al.*, 1991).

For grasses and small cereals the development of successive leaves is related (Skinner and Nelson, 1995; Tesařová *et al.*, 1992) and in all these species the number of growing leaves on one stem remains constant. However, in the current study with maize, leaf appearance rate remained rather constant (Fig. 1), while the LED increased with leaf position (Fig. 3). Figure 9 shows that as a result of both, the number of growing leaves increased with number of full-grown leaves, especially between 5 and 6 full-grown leaves. Temperature did not significantly change this relation, which confirms earlier findings of Thiagarajah and Hunt (1982) and Hesketh and Warrington (1989). Low PPF_D values significantly decreased the number of growing leaves as a function of number of full-grown leaves (Fig. 9). Apparently, as maize plants develop, the number of growing leaves on one stem increases, while for grasses and small cereals the number of growing leaves increases by the formation of tillers.

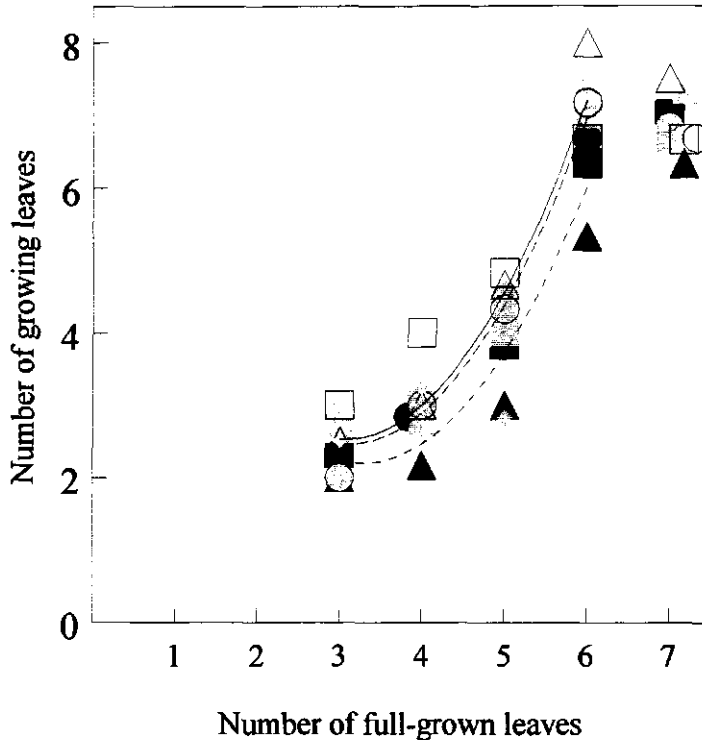


Figure 9. Number of growing leaves in relation to number of full-grown leaves. Every data point represents the average value per harvest per treatment. Markers as in Fig. 1. The lines are the results of a forward stepwise regression for the first four harvests using the interactive linear and quadratic terms of number of full-grown leaves, temperature and PPFD as independent variables. The stepwise regression was halted after no significant ($P < 0.05$) term could be added. Short dashed line: $104 \mu\text{mol m}^{-2} \text{s}^{-1}$; long dashed line: $185 \mu\text{mol m}^{-2} \text{s}^{-1}$; solid line: $277 \mu\text{mol m}^{-2} \text{s}^{-1}$.

Leaf shape

The new two parameter model (Eq. 3) described leaf shape of Leaf positions 1 and 2 much better than the Sanderson model (Eq. 1), because in the new model the maximum width can occur at any point along the whole length of the leaf. Data for higher leaf positions fitted equally well to both models. Sanderson *et al.* (1981) validated their model on higher Leaf positions 6 to 14. The new model appeared to be more flexible in describing the shape of lower positioned leaves and is therefore wider applicable than the Sanderson model.

Leaf positions 1 and 2 showed clearly different values for b and B than higher leaf positions. It is a common finding that the first leaves of a seedling plant have a different shape and internal structure than higher positioned leaves (Eames, 1961).

Towards a dynamic mechanistic model

Both the range of temperatures (13/8-28/23 °C) and PPFD values (104-277 $\mu\text{mol m}^{-2} \text{s}^{-1}$) changed the increase of leaf area per plant in time profoundly, as a result of differences in leaf appearance rate and, especially for higher leaf positions, leaf size (Fig. 1). This is at variance with the proposition of Dwyer and Stewart (1986), that under non-drought conditions the full-grown leaf area of maize is only a function of leaf position. In dynamic mechanistic models, leaf appearance rate, LER, LED and maximum leaf width should be incorporated separately, because temperature and PPFD affect these variables in a different way. Such models will be more accurate and wider applicable than current models for *Gramineae* species. At our Department we are in the process of developing such a model.

Part II

Analysis of plant density effects

Chapter 5

Morphological analysis of plant density effects on leaf area growth in wheat

with J. Vos

Abstract

Effects of temperature and photosynthetic photon flux density (PPFD) on leaf area growth of *Gramineae* species were separated into effects on seven morphological variables (Chapters 2 and 3): (i) specific site usage (SSU), i.e. fraction of existing leaf-axil buds that grow out into a visible tiller, (ii) leaf appearance rate per tiller, (iii) relative time of tiller emergence, (iv) leaf elongation rate, (v) leaf elongation duration, (vi) maximum leaf width, and (vii) a leaf shape factor. In this paper we analyse for wheat (a) the effects of plant density on these seven variables and (b) the mechanisms explaining plant density effects (through effects on temperature, plant growth rate and/or red/far-red ratio (R/FR)). Spring wheat plants were grown in different plant densities (0 - 494 m⁻²) in the field and in growth chambers. Ratios of R/FR were manipulated by using different combinations of lamps (growth chamber) or adding red light to the base of the plant with diodes (experiments outdoors).

Initially, leaf properties and tillering were not affected by plant density. However, SSU of later-appearing tillers was reduced at higher plant densities. For late tillers, leaf appearance rate was slower and relative time of tiller appearance was longer at higher plant densities. Furthermore, maximum leaf width and full-grown leaf length of high-positioned leaves on the main stem were significantly smaller. Plant density effects occurred at lower leaf and tiller number the higher the plant density. A dynamic model was used to evaluate the relative importance of effects of plant density on the seven variables with respect to leaf area per plant. The model analysis showed that the effect of plant density on SSU was by far the strongest determinant of density-dependent changes in leaf area per plant during early growth of wheat.

The effects of plant density on SSU could not be fully explained by temperature differences, plant growth rate or R/FR effects. The parameter SSU appeared to be well related to the specific leaf weight (SLW) of the parent leaf (i.e. the leaf from which the tiller is appearing) at the time of tiller appearance, independent of R/FR ratio. While SLW of a single leaf depends on local assimilate supply, we surmise that SSU is regulated by local assimilate supply.

Introduction

After crop emergence, the rate of increase in soil cover and radiation interception are strong determinants of crop production (Goudriaan and Van Laar, 1994). However, present simulation models of leaf area development are descriptive and do not predict leaf area increase well (Lotz *et al.*, 1996). In Chapters 2 and 3 the following distinctions were made between several developmental and growth processes that determine leaf area increase of *Gramineae* species. The dynamics of leaf number, i.e. development, is completely defined by: (i) specific site usage (SSU; list of abbreviations in Appendix 1), i.e. fraction of existing leaf-axil buds that grows out into a visible tiller, (ii) leaf appearance rate (L_A) of individual tillers, (iii) relative time of tiller appearance, expressed as Haun Stage-delay (HS-delay). Growth of individual leaves can be calculated from (iv) leaf elongation rate (LER), (v) leaf elongation duration (LED), (vi) maximum leaf width and (vii) shape factor: k , a variable that relates full-grown length and maximum width to individual leaf area.

Mechanistic modelling of foliar development becomes possible if effects of environmental conditions on these seven variables are quantified. For spaced wheat plants, in Chapters 2 and 3 it was found that the effects of photosynthetic photon flux density (PPFD) and temperature on leaf area were mainly due to effects on SSU, L_A , LER and LED. These effects depended on the position of leaves and tillers on the plant. Plant density is also an important factor affecting the increase in leaf area in the initial stages of crop growth. The objectives of this paper are to (i) analyse the effects of plant density on the seven component variables of leaf area growth mentioned, (ii) determine the quantitative significance of effects of plant density on these variables with respect to leaf area per plant and (iii) discuss which mechanisms cause the changes in these variables with higher plant densities. Three of such possible mechanisms will be examined: (i) decrease in temperature due to increased leaf shading (Peacock, 1975), (ii) source limitation, i.e. decrease in radiation interception and in carbohydrate production per plant per day; this mechanism is used in most simulation models, e.g. SUCROS (Goudriaan and Van Laar, 1994), and (iii) a photomorphogenic effect induced by a decrease of red/far-red (R/FR) ratio with increase in plant density (Smith, 1982).

Plant density effects were studied in a series of experiments, under controlled conditions (growth chamber) and in outdoor conditions. A dynamic model of foliar growth and development was used to evaluate the quantitative effects of plant density on the seven component processes. Effects of R/FR ratio were examined by selecting suitable combinations of lamps (controlled conditions) or using diodes (outdoor conditions).

Materials and methods

General

Four experiments were conducted under different natural and controlled conditions. In all trials, spring wheat cv. Minaret was sown by hand at equal distances to create the desired plant density (designated as Dx, with x the number of plants per m²). Water and nutrients were sufficiently supplied throughout the experimental periods. The plots were regularly sampled. Leaves and tillers were identified with the system of Klepper *et al.* (1982). In this system, a daughter tiller (e.g. t1) is the outgrowth of the axillary bud of its parent leaf (e.g. Leaf 1 on the main stem). Haun stage (HS; Haun, 1973) was taken as a measure of leaf stage. The seven component variables (L_A, HS-delay (a measure for relative time of tiller appearance), SSU, LER, LED, maximum leaf width and k) were measured as described in Chapters 2 and 3. Dissected material was oven-dried at 70 °C to constant weight. Spectral light measurements were performed with a LiCor-1800 spectroradiometer every 2 nm from 400 to 800 nm. An outline of treatments and special measurements of the different experiments is given in Table 1. Figure 1 shows that accumulation of temperature and PPFD with time varied little between experiments, except for the slow rate of increase in accumulated PPFD in the growth chamber.

Table 1. Specifications of the four experiments mentioned in the text. Abbreviations are explained in Appendix 1.

	GC	F93	F94	C95
Treatments	D: 31, 123, 278, 494 R/FR: 1.2, 3.6	D: 0, 31, 123, 494	D: 123, 494	D: 123 R: 0, 1
Number of harvests	6	4	3	2
Special measurements	LER and LED	Temperatures in crop and soil	-	-

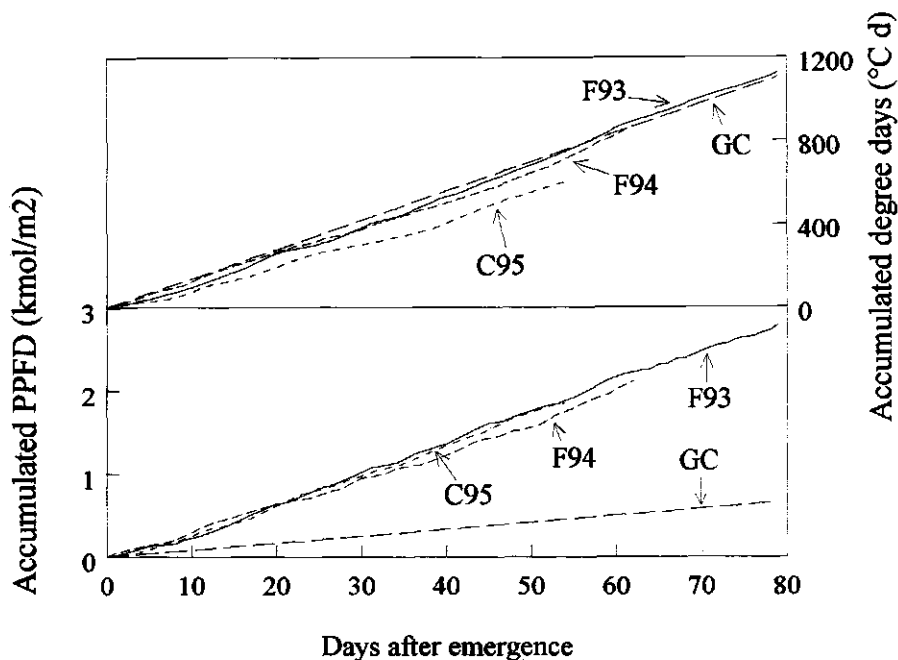


Figure 1. Accumulated PPFD and accumulated degree days (base temperature 0 °C) after crop emergence.

Growth chamber experiment (GC)

This experiment was performed in two growth chambers which were set to a temperature of 17 °C from 9.00-21.00 h and 11 °C from 21.00-9.00 h and a relative humidity of 75%. Daily light period lasted from 7.00-21.00 h with a PPFD of 166 $\mu\text{mol m}^{-2} \text{s}^{-1}$ at the top of the crop canopy for both chambers. The R/FR ratio (measured as the ratio of photons in 10 nm bandwidths centred on 660 nm and 730 nm) was 1.2 (R0 treatment; natural value) or 3.6 (R1 treatment) by the use of a different combination of metal halide and high pressure sodium lamps, fluorescent tubes and incandescent bulbs per growth chamber. Incoming radiation with a R/FR = 3.6 results in a higher phytochrome photoequilibrium at soil level than natural incoming radiation (R/FR = 1.2) at the top of a crop canopy, even at high LAI values (Smith, 1982). Within the two chambers minicrops of spring wheat were grown from sowing to the soft dough stage by placing 48 square (18 by 18 cm) 4.5 l pots filled with quartz sand on a moveable cart. Four such minicrops were placed in one growth chamber, with one (D31), four (D123), nine (D278) or 16 (D494) plants per pot. The inner 24 pots were used as net pots. During growth carts were lowered to obtain a constant PPFD at the top of the plants and rotated within a growth chamber twice a week to minimise effects of small but persistent gradients in environmental variables within a growth chamber. Five times three pots were harvested up to

anthesis (H1-5: 11, 24, 34, 46 and 81 DAE). After every harvest pots were readjusted to retain the desired plant density. At the last harvest (H6: 127 DAE) eight pots were taken. To determine LER and LED (Chapter 3), the length of growing leaves was carefully measured with a ruler during the whole growth period on eight plants per treatment three times a week.

Field experiment 1993 (F93)

Seeds were sown on 25 and 26 March 1993 in a heavy clay soil in Wageningen (52 °N, 6 °E) and plants emerged on 12 April. Plants were grown in four densities (D0 (= spaced), D31, D123, D494) in two blocks. Temperatures at -1, 0 and 40 cm above soil level were recorded in the D0 and D494 treatments from 34 DAE onwards. Individual plots were 3*3 m and the inner 2*2 m was regarded as net plot. Four times (23, 50, 64 and 79 DAE) plots were sampled by harvesting two spaced plants (D0 treatments) or a square area of 3*3 plants (other D treatments).

Field experiment 1994 (F94)

Seeds were sown on 25 and 26 April 1994 in a field located within 1 kilometre from the F93 experiment and the same soil type. Plants emerged on 3 May. The layout of this experiment was equal to F93, but most of the plots were discarded because of a high variability between plants. The remaining plots were D123 and D494 in two blocks. Temperatures were not recorded at the site and three harvests (29, 50 and 62 DAE) of a square area of 3*3 plants each were done.

Container experiment 1995 (C95)

Outside and within one kilometre from the locations of the field experiments, eight containers (l*w*h: 1.56*1.25*0.35 m) were filled with potting medium above a small layer of gravel at the bottom. Seeds were sown on 3 April 1995 and plants emerged on 15 April. Plant density was 123 m⁻² in all containers. In half of the containers (R1 treatments), on 14 DAE red light was added to a central square area of 5*5 plants by placing two light emitting diodes on the soil on both sides of a plant shining towards the plant base. Each diode emission was 170 μmol m⁻² s⁻¹ measured at a distance of 1 cm (λ_{max} =664 nm; 95% of photons between 638-690 nm). Diodes were switched on daily from 15 minutes before dawn until 15 minutes after dusk. The central 3*3 plants were considered as net plot. Also in the other four containers (R0 treatments) the net plot consisted of a central square area of 3*3 plants. Two harvests (H1-2: 37 and 54 DAE) were done of two net plots per R treatment.

Evaluation of quantitative significance of effects of plant density on the seven variables defining leaf area growth

The seven variables of leaf growth completely define the change with time in leaf area expansion per plant. With these variables, a model was built which simulates the dynamics of leaf area per plant (Appendix 2). This model was run for treatments R/FR1.2,D31 and R/FR1.2,D494 of the GC experiment, inserting the experimental data on LER, LED, maximum width, k and L_A of individual leaves and HS-delay and SSU of individual tillers. To investigate the importance of the model components on the difference in leaf area per plant between D31 and D494, parameter values of D494 were successively changed into the values observed in D31.

Results and discussion

Effects of plant density on the seven variables defining leaf area growth

Plant density generally did not affect L_A of the main stem (ms) (expressed as the increment in HS per unit of thermal time with a base temperature of 0 °C); in Experiment F93 effects were significant ($P < 0.05$) but numerically the differences were only small (Fig. 2). The leaf appearance rate of the ms was faster in the field experiments than in the GC experiment. This is probably related to the lower accumulated PPFD per day in the GC experiment (Fig. 1), which can reduce L_A (Chapter 2).

The leaf appearance rate of primary tillers (t_1 , t_2 , t_3) in the GC experiment decreased significantly with increase in plant density (Table 2) and L_A of t_2 in D494 was almost half the one in D31. While L_A of the ms was not affected by plant density, L_A of primary tillers was significantly lower than the ms in treatments D123, D278 and D494, and differences increased with plant density. Primary tillers grow lower in the crop canopy than the ms (Masle, 1985). Therefore, the reductions in L_A are probably related to a reduced PPFD for primary tillers by increased shading at higher plant densities and higher tiller positions.

Haun Stage-delays for tiller appearance declined with position of the primary tiller ($t_1 > t_2 > t_3$) in the GC experiment (Table 2). This is generally found for wheat and other *Gramineae* species (Chapter 2). Haun Stage-delay significantly increased with plant density for t_2 and t_3 , indicating a delay in tiller appearance. In Chapter 2 it was found that HS-delay only increased when conditions were unfavourable for tiller appearance (SSU between 0 and 1). This is probably also the case for tiller t_2 in D278 and D494 and for tiller t_3 in D123, because these tillers appeared when LAI was already higher than 3.

Effects of plant density on SSU were complicated and differed between the GC and F94 experiments (Fig 3a,b). For spaced plants, in Chapter 3 it was suggested that SSU depended on the growth rate of the parent tiller. The absence of t_0 and the low SSU of t_1 for treatments D278 and D494 in the GC experiment (Fig. 3a) were probably related to a low growth rate of parent tillers ms

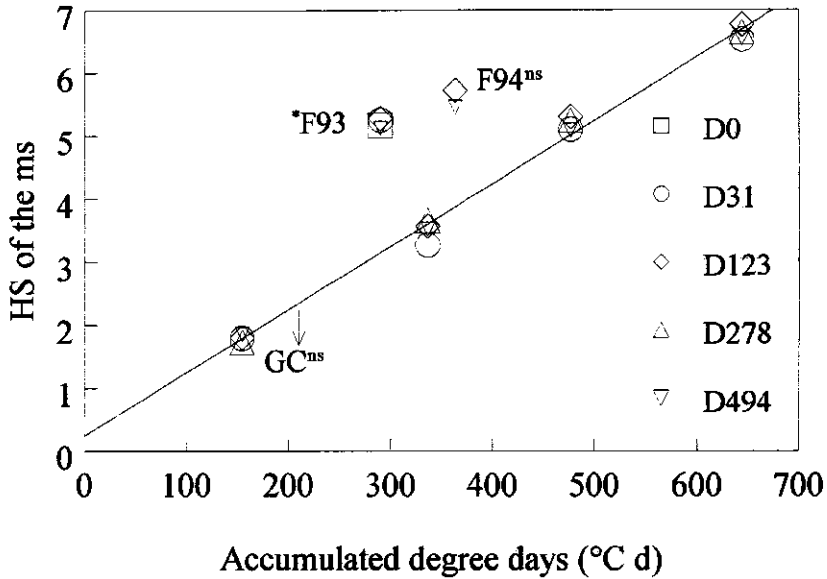


Figure 2. Effects of plant density (D) on HS of the ms as a function of accumulated degree days (base temperature 0°C) for three experiments mentioned in the text. Significance of the effect of plant density ($P < 0.05$): * significant; ns=not significant. For the F93 and F94 experiment, statistical analysis was based on one harvest; for the GC experiment, four harvests were used and a statistical analysis was done on the linear regression parameters per plant density.

Table 2. L_A ($^{\circ}\text{C d}$)¹ and HS-delay of specific tiller types at different plant densities in the GC experiment. Different letters indicate significant differences between plant densities and tiller types based on LSD values ($P < 0.05$). In case no or few tillers appeared and no reliable data could be derived, no numbers are given.

	L_A				HS-delay		
	ms	t1	t2	t3	t1	t2	t3
D31	0.0104 ^{def}	0.0112 ^g	0.0106 ^{efg}	0.0109 ^{fg}	2.01 ^f	1.61 ^{bc}	1.37 ^a
D123	0.0108 ^{fg}	0.0099 ^{cd}	0.0100 ^{cdc}	0.0096 ^c	2.01 ^f	1.69 ^{cd}	1.58 ^b
D278	0.0107 ^{fg}	0.0085 ^b	0.0083 ^b	-	2.04 ^f	1.80 ^e	-
D494	0.0105 ^{def}	-	0.0058 ^a	-	-	1.83 ^{def}	-

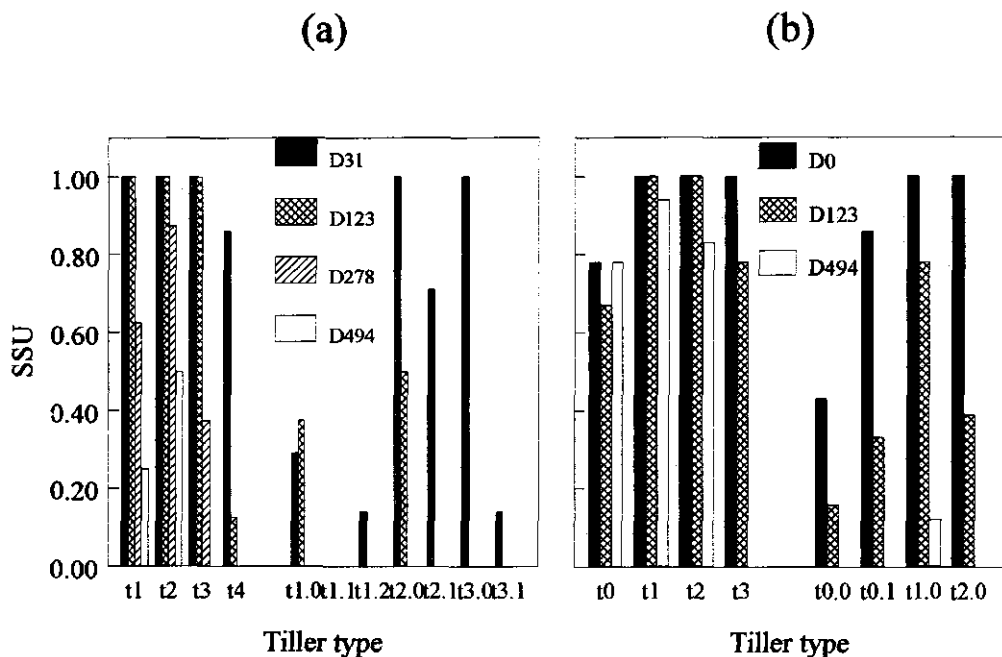


Figure 3. Effects of plant density on SSU of different tiller types. (a) GC experiment; (b) F94 experiment.

and t1 respectively at the time of daughter tiller appearance. While plant growth rates for comparable treatments were higher in the F94 than in the GC experiment (above-ground dry weight per plant at appearance of Leaf 6 on the ms was 0.51 and 0.39 g in the F94 and GC experiment, respectively), the effect of plant density on SSU was stronger in the GC experiment. Effects of plant density on SSU were larger if the tiller appeared later and consequently LAI was higher (magnitude of effects in order of $t4 > t3 > t2 > t1$, $t2.1 > t2.0 > t2$, $t3.0 > t2.0 > t1.0$ (Fig 3a,b)).

Full-grown leaf areas of the first five leaves on the ms were hardly different between density treatments in each of the GC, F93 and F94 experiments. Leaf area increased continuously with leaf position in low density treatments. However, the trend of increase of leaf area with leaf position reversed in a decline at higher leaf positions in higher plant density treatments (illustrated with data from the F93 experiment: Fig 4a). At higher plant densities maximum leaf width was lower for leaf positions larger than 5 (Fig. 4b), and leaf length was smaller for leaf positions higher than 7 (Fig. 4c). Measurements of LER and LED in the GC experiment showed that the shorter leaves at higher plant densities were related to a slower LER, while LED was hardly changed by plant density (data not shown). Variable k was never significantly affected by plant density (data not shown).

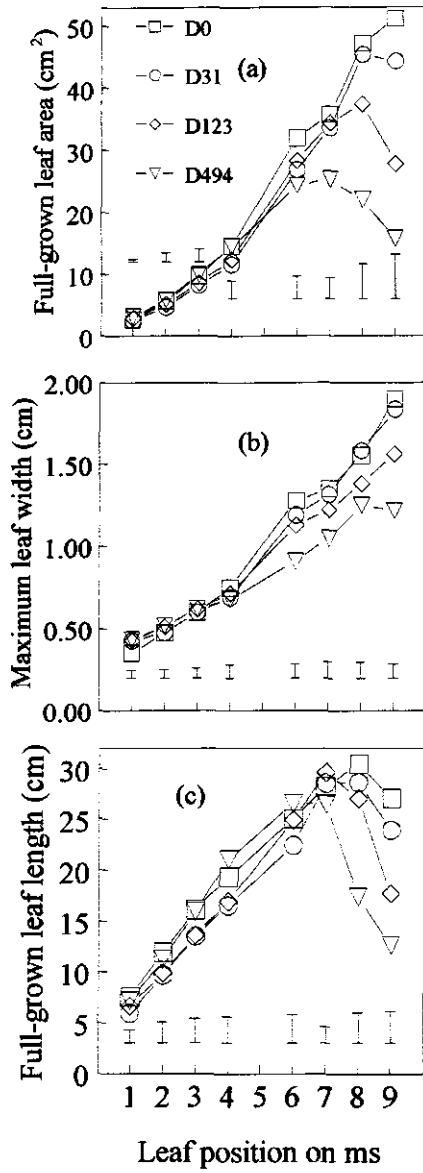


Figure 4. Effect of plant density on full-grown leaf dimensions at different positions on the ms in the F93 experiment. (a) area; (b) maximum width; (c) length. Bars indicate LSD (P=0.05).

Significance of plant density effects on the seven variables defining leaf area growth

To assess the significance in absolute contributions of density effects to the seven variables, the model on leaf area (Appendix 2) was run for treatment R/FR1.2,D494 of the GC experiment, inserting the experimental data on k , LER, LED, maximum width and L_A of individual leaves and HS-delay and SSU of individual tillers. To investigate the importance of the seven variables on the difference in leaf area per plant between densities, D31 and D494 parameters were used as a test criterion. The parameter values observed in treatment R/FR1.2,D494 were successively changed into the values observed in the R/FR1.2,D31 treatment. In this way, a plant growing at 494 plants m^{-2} was changed in seven steps into a plant with the leaf properties of a plant growing at 31 plants per m^2 . Fig. 5 shows the results for three durations of simulation resulting in different LAI values for the D494 treatment. Difference in leaf area per plant between the D494 and D31 treatment increased from 1 cm^2 at LAI = 2.9 (in treatment D494) to 75 cm^2 at LAI = 5.1 (in treatment D494).

First k (≈ 0.76), LER (1.5 - 6 $cm d^{-1}$), LED ($\approx 8 d$) and maximum width observed in D494 were successively changed into values observed in D31, thus obtaining a plant with the leaf and tiller types

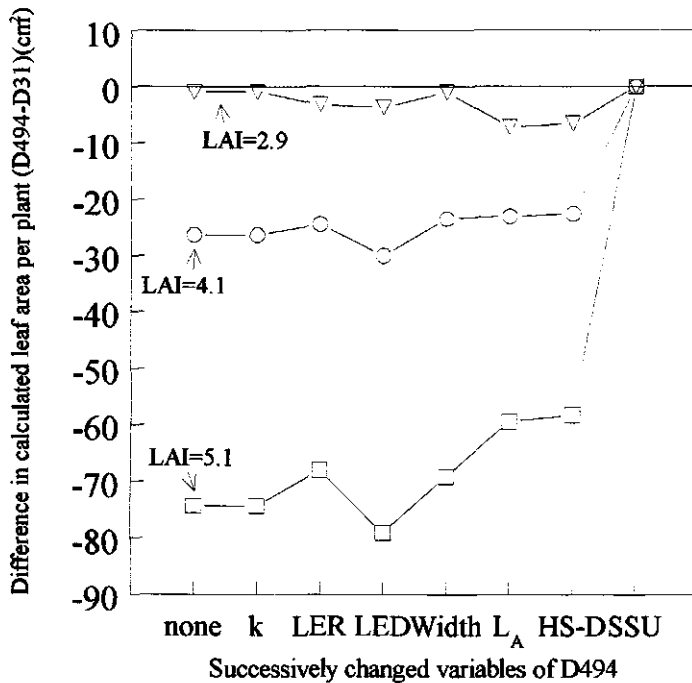


Figure 5. Effects of successively changed variables observed in treatment D494 into values observed in treatment D31 in the GC experiment on the difference in leaf area between the two treatments. This was done for three different LAI values in D494, as calculated with the leaf area model (Appendix 2). HS-Delay is abbreviated to HS-D.

of D494, but with individual leaf dimensions of D31. Because the difference in leaf area did not decrease (Fig. 5), individual leaf dimension variables did not explain differences in leaf area per plant between D31 and D494, irrespective of LAI. Changing the L_A into values observed in D31 decreased the difference in leaf area slightly and only at LAI = 5.1. This was due to the lower L_A in D494 for late emerging tillers (Table 2). Changing HS-delay values of D494 into values observed in D31 did not have any effect. The quantitative significance of plant density effects were primarily mediated by effects on SSU, which means that the leaf area per plant growing at 494 m² was lower than for plants growing at 121 m² mainly because some specific tillers did not appear (Fig. 3b). Therefore, the mechanism of plant density effects will only be studied on SSU, after analysing effects of plant density on some other plant variables.

Early effects of plant density on other variables

Other plant variables were also influenced by plant density, and some of them even in an earlier phase than leaf area variables. In F93, at HS of the ms = 5.2, plant density had no significant effect on leaf area or dry weight of the ms, but the distribution of dry weight was significantly changed. The leaf-blade fraction in the dry weight of the ms was significantly lower for D494 (0.81) than for the other densities (0.84). More pronounced, specific leaf weight (SLW) of low-positioned leaves was significantly lower at higher plant densities (Fig. 6). The same phenomena were visible in the F94 and GC experiment (data not shown).

In the GC experiment, regular harvests were done in early growth phases and the dynamics of SLW of individual leaves could be analysed. For Leaf 3 on the ms, Fig. 7 illustrates a trend that occurred for ms Leaves 1-4: when the leaf was just full-grown, SLW was hardly affected by plant density, but during ageing SLW decreased faster at higher plant densities. As a 'shade avoider', the wheat plant responds to competition for light by investing more dry matter in longer sheaths at the expense of leaf dry matter, thereby allowing the young leaves to be kept out of shade (Smith, 1982). This study showed that only dry weight of lower-positioned leaves was reduced, before reductions in total plant dry weight occurred. This reduction in SLW could be due to a reduced photosynthesis at a low position in the crop canopy or to a larger fraction of the dry matter in the lower leaves being remobilized at a higher plant density.

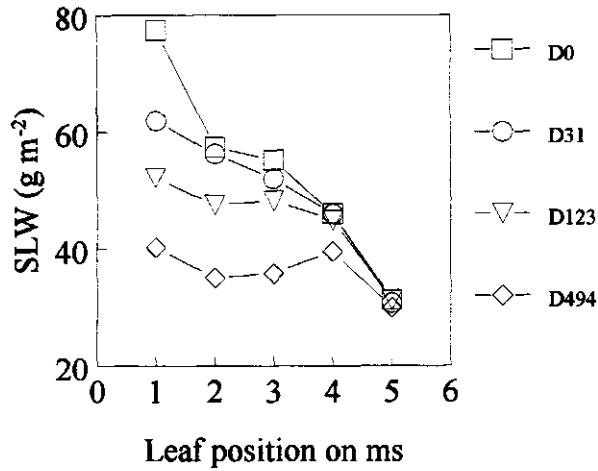


Figure 6. Effects of plant density on SLW of Leaf positions 1-5 on the ms measured at HS of the ms = 5.2 in the F93 experiment. Bars indicate LSD ($P=0.05$).

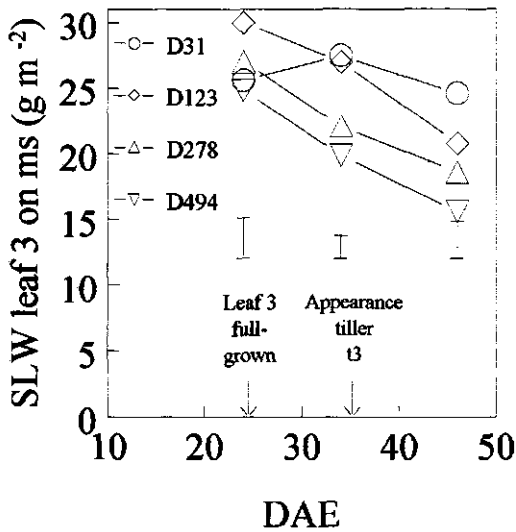


Fig. 7. Effects of plant density on SLW of Leaf 3 on the ms during ageing of the leaf in the GC experiment. Average time that leaf 3 was full-grown and appearance of daughter tiller t3 are indicated. Bars indicate LSD ($P=0.05$).

Possible role of temperature in effects of plant density on SSU

Temperatures measured between 35 and 64 DAE were analysed in the F93 experiment for treatments D0 (LAI=0) and D494 (LAI>4). On average, mean daily temperatures at -1, 0 and 40 cm were 3.5, 3.8 and 0.7 °C lower in D494 than in D0, respectively. Differences in temperature between D0 and D494 were larger when daily accumulated PPFD was higher. The decreased SSU at higher plant densities can not be explained by these temperature differences, because lower temperatures result in an increase rather than a decrease in SSU (Chapter 2).

Source and R/FR effects on SSU

The largest effect of plant density on leaf area per plant was due to effects on SSU (Fig. 5). A decline in SSU with an increase in plant density could be related to source limitation: when plants compete for light, daily assimilate or dry matter production per plant will decline with an increase in plant density. Such a mechanism has been proposed to explain density effects in wheat (Van Keulen and Seligman, 1987), guar (Charles-Edwards and Beech, 1984) and lupin (Munier-Jolain *et al.*, 1996). We tried to relate SSU of tillers t1 and t3 to the growth rate of the plant at the time of appearance of these tillers (Fig. 8). For t3, there was indeed a positive relation between SSU and plant growth rate. For t1, no relation was found. Therefore, the current results are inconclusive to show a role for plant growth rate in explaining differences in SSU.

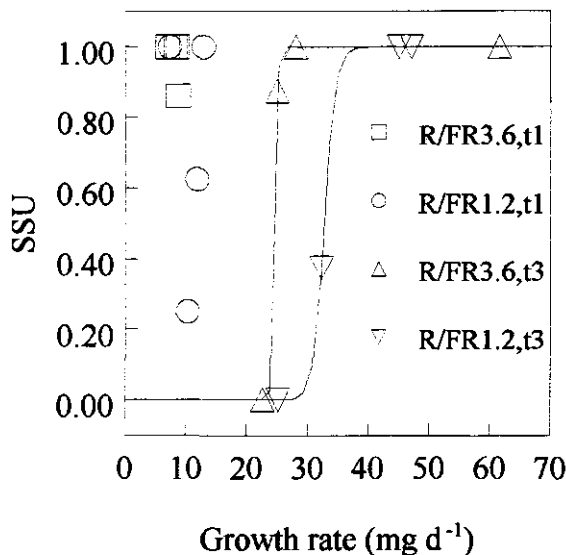


Figure 8. SSU of tiller t1 and t3 at two levels of R/FR in the GC experiment, as a function of total plant growth rate measured at the time of tiller appearance. Statistically significant logistic functions ($P < 0.05$) are drawn.

The decline in SSU with increase in plant density could also be induced by declining R/FR ratio at the base of the plant (Kasperbauer and Karlen, 1986; Casal *et al.*, 1990; Barnes and Bugbee, 1991). In the current study the enhanced red radiation was imposed to create in the plant stands the R/FR ratio that free standing plants experience in nature. Under natural weather conditions in the C95 experiment, the addition of red light at the plant base did not significantly change SSU of any tiller position and total number of tillers formed was also not significantly different (15.2 and 15.6 tillers per plant for R0 and R1 treatments, respectively; $P=0.7$). In the GC experiment, there was a significant R/FR effect on the relation between plant density and SSU for tiller types t1 and t3 (Fig. 9). As expected, SSU of t3 is reduced at a lower plant density than the SSU of t1 is, because plants are larger at appearance of t3 and (self-)shading is more intense. At R/FR = 3.6, the SSU of t1 declined at a higher plant density than at R/FR = 1.2. These results imply that R/FR ratio can partly explain effects of plant density on SSU in the GC experiment.

The difference in R/FR effects in the field and growth chamber experiments could be due to the methodology of applying extra red light. The addition of red light only to the plant base could underestimate photomorphogenic effects, because elongating leaves are also a site of R/FR perception. However, Deregisus *et al.* (1985), Casal *et al.* (1986) and Casal *et al.* (1987) found tillering responses to addition of red light to the plant base, even with one diode per plant. Another explanation could be that the R/FR ratio has larger effects under more 'adverse' conditions for SSU

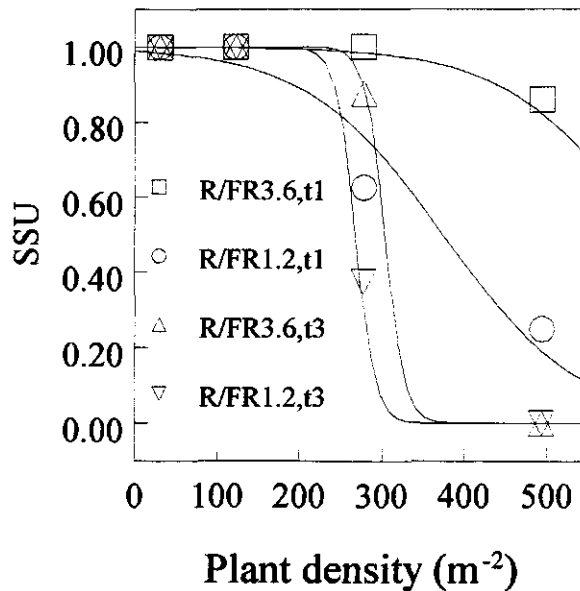


Figure 9. SSU of tiller t1 and t3 at two levels of R/FR in the GC experiment, as a function of plant density. Statistically significant logistic functions ($P<0.05$) are drawn.

(low PPFD in the GC experiment). Indeed, most of the evidence for photomorphogenic tillering responses have come from growth chamber experiments with relatively low PPFD (Barnes and Bugbee, 1991; Kasperbauer and Karlen, 1986; Casal *et al.*, 1985; Casal *et al.*, 1987). Under natural weather conditions, addition of red light only increased SSU at low plant densities (*Paspalum dilatatum*: 6.7 plants m⁻²; *Lolium multiflorum*: < 56 plants per m⁻²) in an advanced plant stage (Casal *et al.*, 1986).

A new hypothesis

It appears that neither plant growth rate nor R/FR ratio can fully explain effects of plant density on SSU. A new hypothesis is therefore proposed here. Specific leaf weight of lower positioned leaves was the first plant property measured that was affected by plant density (Fig. 6). Specific site usage of t1 and t3 and SLW of Leaves 1 and 3 on the ms at the time of daughter tiller appearance were strongly related, independent of R/FR treatment in the GC experiment (Fig. 10). While both SLW and SSU depend on assimilate supply, a local reserve pool which is determined by local assimilate supply and translocation could regulate SLW and SSU (Fig. 11). Low R/FR ratios have been shown to accelerate senescence and translocation of structures out of old leaves (Guamet *et al.*, 1989), while lower PPFD values reduce photosynthesis (Lawlor, 1987).

This hypothesis is an elaboration of the hypothesis discussed in Chapter 2, where it was stated that SSU depends on the growth rate of the parent tiller, based on observations on spaced plants. In the current plant density experiments it appears that assimilation supply of the parent leaf (assumed

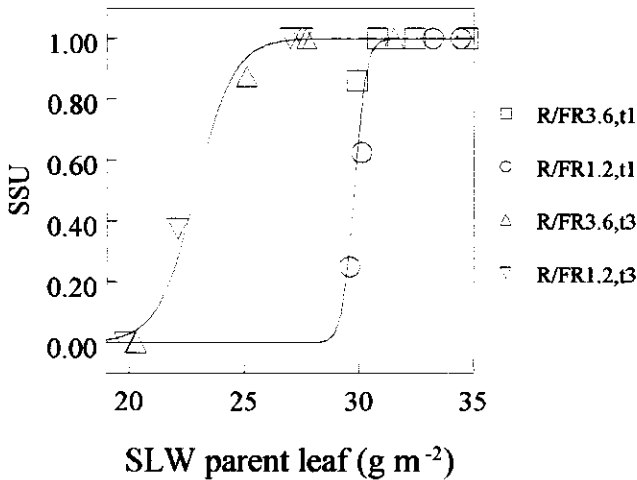


Figure 10. SSU of tiller t1 and t3 at two levels of R/FR in the GC experiment, as a function of SLW of their parent leaves at the time the daughter tiller appeared. Statistically significant logistic functions (P<0.05) are drawn.

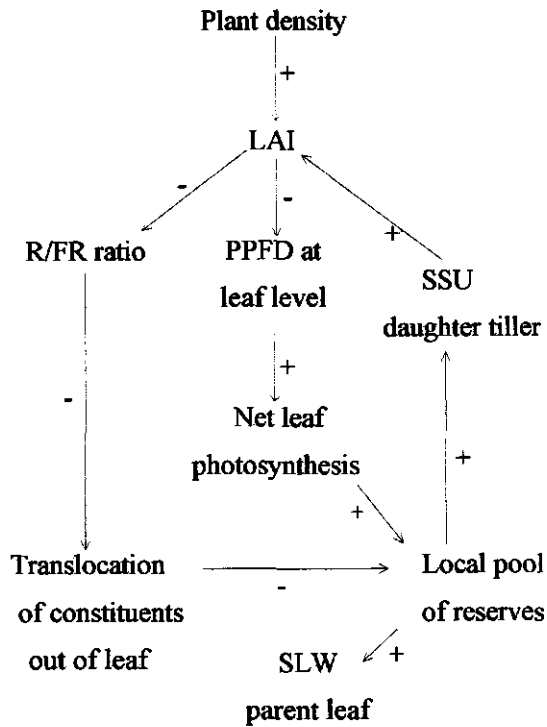


Figure 11. Hypothetical relationships for effects of plant density on leaf area development via changes in R/FR ratio and PPFD.

to be represented by SLW) gives a better explanation of SSU differences than the assimilate supply of the parent tiller.

Conclusions

- i) Effects of plant density on leaf area per wheat plant were mainly caused by effects on Specific Site Usage (SSU).
- ii) These effects on SSU were associated with effects on SLW of the parent leaf.
- iii) R/FR ratio and PPFD can determine both SLW of individual leaves and SSU of daughter tillers, probably by changing the local assimilate supply.

Appendix 1. List of abbreviations used

C95	Container experiment 1995
D	Plant density (m^{-2})
DAE	Days After Emergence (d)
F93	Field experiment 1993
F94	Field experiment 1994
GC	Growth Chamber experiment
H	Harvest number
HS	Haun Stage
k	parameter relating maximum width and full-grown length with individual leaf area
LAI	Leaf Area Index
L_A	Leaf Appearance Rate ($^{\circ}\text{C}^{-1} \text{d}^{-1}$)
LED	Leaf Elongation Duration (d)
LER	Leaf Elongation Rate (cm d^{-1})
LSD	Least Significant Difference
ms	main stem
PPFD	Photosynthetic Photon Flux Density ($\mu\text{mol m}^{-2} \text{s}^{-1}$)
R	Red diode treatment; R0: no diodes, R1 diodes at base of plant
R/FR	Red/far-red ratio
SLW	Specific Leaf Weight (g m^{-2})
SSU	Specific Site Usage
t	tiller type as classified by Klepper <i>et al.</i> (1982)

Introduction

At higher plant densities, leaf area per plant is reduced in later phases of growth (Hay and Walker, 1989). As an example of a tillering *Gramineae* species, in Chapter 5 it was analysed for wheat which morphological leaf components were affected by plant density and which mechanisms were involved. It was found that the most significant effect of higher plant densities on leaf area per plant was the absence of later-formed tillers. The lack of tiller formation was related to low local assimilate availability, induced by low photosynthetic photon flux densities (PPFD) or low red/far-red ratios at the site of the incipient tiller. When a species does not form tillers, plant density can only affect the growth of leaves on the main stem. A study into the effects of environmental factors on the morphological development of such a plant type could lead to a better understanding of mechanisms involved in the effects of plant density on leaf area development.

Modern maize (*Zea mays* L.) hybrids only rarely form tillers. Leaf area development on one (main) stem fully determines the leaf area development per plant, and effects of plant density must be related to effects on leaf area growth of this main stem. Several authors (e.g. Williams *et al.*, 1965) found a decrease in leaf area per plant with an increase in plant density for maize. Grant and Hesketh (1992) assumed that leaf area growth on a maize plant is a function of leaf dry weight and the increase in leaf dry weight. However, they tested this hypothesis on plants grown in a range of rather low plant densities (1.5 - 10.3 m⁻²), resulting in only small differences in leaf area per plant, even between the extreme plant densities. How leaf area is reduced at higher plant densities (is the appearance of leaves reduced or are individual leaves smaller?) and by what mechanisms is still unknown.

The objectives of the current paper are: (i) to determine which leaf area variables in maize are affected by plant density, and (ii) to analyse which mechanisms could be involved. The effects of a wide range of plant densities and of 50% shade on leaf area variables were tested in a field experiment repeated for two years.

Materials and methods

Field experiment 1993 (F93)

Maize seeds (hybrid 'Luna') were sown by hand at equal distances per plot in a heavy clay soil in Wageningen (52 °N, 6 °E) on 25 and 26 May 1993; plants emerged on 6 June. Treatments included all combinations of four densities (D0 (= spaced), D7.7, D31, D123) and two shading levels (S0: not shaded; S1: shaded) in two blocks. D0 plots were sown in a plant density of 4.5 m⁻², and this density decreased in time by periodic harvesting. In early growth stages plots were irrigated and abundantly fertilised. Twelve days after emergence (DAE) (appearance Leaf 5) shading treatments were started

by placing white nets above the S1 plots. Transmission of the nets was 50% in the wavelength range 400-800 nm, with no effects of the nets on the red/far-red ratio. Nets were lifted during growth to assure a distance of 30 cm between the top of the crop canopy and the net. Individual plots were 5.40*4.32 m and the inner 3.24*2.16 m was regarded as net plot. Every full-grown 5th leaf on a plant was marked to facilitate leaf identification.

Field experiment 1994 (F94)

Seeds were sown in a heavy clay soil in Wageningen on 20 May 1994; plants emerged on 31 May. Experimental layout was as in the F93 experiment. Fifteen DAE (appearance Leaf 4) shading treatments were started.

Measurements and calculations

Harvesting procedure. Plots were sampled 16, 30, 43 and 56 DAE (F93 experiment) or 24, 35 and 55 DAE (F94 experiment) by harvesting above-ground parts of eight plants. Due to severe lodging, the D123S0 plots in both blocks in the F94 experiment were discarded in Harvests 2 and 3. Plant material was dissected into individual leaf blades ("leaves"). The remaining plant was divided into three fractions: sheaths, stems and tassels. Leaves were counted acropetally. If more than 50% of a leaf was yellow or the leaf was broken off from the plant, it was considered dead and discarded. Full-grown leaves were cut off at their ligule, growing leaves were cut off at the uppermost visible ligule on the plant. In this way, a leaf was supposed to have appeared when its tip reached above the uppermost visible ligule. Dissected material was oven-dried at 70 °C to constant weight.

Temperature and light measurements. Daily values of maximum and minimum air temperatures and global radiation were recorded within 1 km from the experimental sites. Figure 1 shows that the first 25 DAE were colder and darker in F94 than in F93 and that between 25 DAE up to 55 DAE temperature and PPFD were lower in the F93 than in the F94 experiment. Crop temperatures at -1, 0 and 40 cm above soil level were recorded every two hours in all plots in one block in the F93 experiment from 19 DAE onwards.

Leaf appearance. The base temperature for leaf appearance was calculated as a linear function of growing degree days (gdd). Growing degree days were calculated with two methods: in Method 1 daily average air temperatures were used; in Method 2 the suggestion of Grant (1989) and Yin *et al.* (1996) that diurnally fluctuating temperatures should be used, was taken into account for calculation of gdd. To do so, from the daily maximum and minimum measured air temperatures, hourly values were calculated with equations given by Goudriaan and Van Laar (1994). Leaf appearance rate (LAR) was calculated with linear regression as the slope of the number of appeared leaves (a leaf is here defined to be appeared when its tip is visible) vs. gdd.

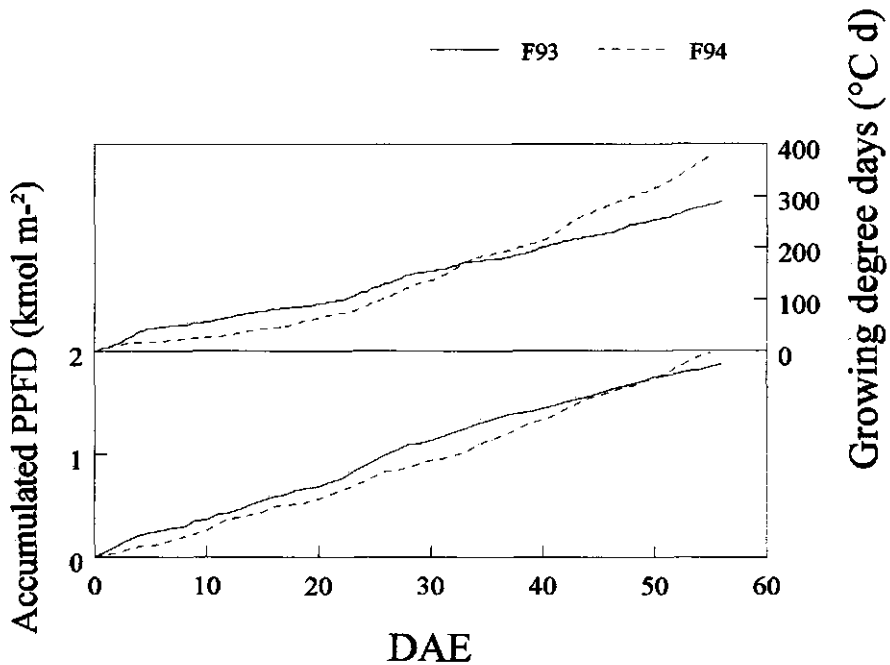


Figure 1. Accumulated photosynthetic photon flux density (PPFD) and growing degree days (base temperature 11.1 °C based on hourly values) after crop emergence. Solid lines: F93 experiment; dashed lines: F94 experiment.

Leaf appearance rate (LAR) was fitted as a function of plant density using a hyperbolic spacing formula (De Wit, 1960):

$$LAR = \frac{LAR_0}{\frac{\beta}{LAR_0} D + 1} \quad (1)$$

where LAR_0 ($^{\circ}\text{C}^{-1} \text{d}^{-1}$) is the fitted LAR for plant density (D) = 0 m^{-2} and β ($^{\circ}\text{C}^{-1} \text{d}^{-1} \text{m}^2$) the fitted slope of the curve for $D=0 \text{ m}^{-2}$.

Individual leaf area variables. Length and maximum width were measured on all appeared leaves. On one plant per plot, length, maximum width and width of full-grown leaves were measured at six or seven equidistant places covering the whole leaf length. With numerical rectangular integration, leaf area was calculated from leaf length and the leaf widths. After this, the leaf shape factor k was calculated:

$$k = \frac{\text{Leaf area}}{\text{Leaf length} * \text{Maximum leaf width}} \quad (2)$$

For analysis of maximum leaf width and full-grown leaf length, data were used from leaves that were recently full-grown.

Leaf elongation rate (LER) and leaf elongation duration (LED) were not directly determined but were calculated for Leaf 7. Leaf 7 was chosen because it elongated in the period during which observations were done. The calculation is as follows:

- i) the number of appeared leaves was plotted against the number of full-grown leaves (two example treatments shown in Fig. 2). Linear regression was used to estimate the number of appeared leaves at the time Leaf 7 was full-grown;
- ii) the LED of Leaf 7 can now be calculated in units of 'appeared leaves between emergence and cessation of elongation of Leaf 7' (Fig. 2);
- iii) using the estimated LAR, LED can be expressed in gdd ($^{\circ}\text{C d}$);
- iv) average LER ($\text{cm } ^{\circ}\text{C}^{-1} \text{ d}^{-1}$) was calculated by dividing full-grown leaf length (cm) by LED.

Dry weight. Above-ground dry matter production per plant (W (g)) in time (t (d)) was fitted with the exponential equation (Goudriaan and Van Laar, 1994):

$$W = \frac{c_m}{r_m} \ln(1 + e^{r_m(t-t_b)}) \quad (3)$$

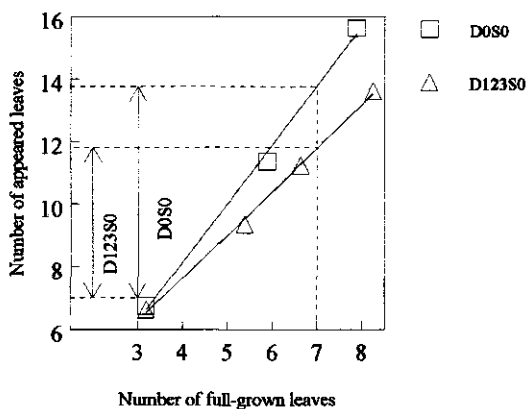


Figure 2. Illustration of the calculation of the number of appeared leaves during elongation of Leaf 7. Lines are fitted linear regressions and the length of the arrows represent the number of appeared leaves during elongation of Leaf 7 for treatments D0S0 and D123S0 in the F93 experiment.

where c_m is the maximum growth rate for $t \rightarrow \infty$ ($g\ d^{-1}$), r_m the initial relative growth rate ($g\ g^{-1}\ d^{-1}$) and t_b the moment at which the linear phase effectively starts (d). While shading treatments commenced some time after emergence, Equation 3 was rewritten to obtain Equation 4 and one common W value (W_{sh}) was estimated at the day when the shading treatments started (t_{sh}) for the two shading treatments per plant density per year.

$$W = W_{sh} \frac{\ln(1 + e^{r_m(t-t_b)})}{\ln(1 + e^{r_m(t_{sh}-t_b)})} \quad (4)$$

Variable W was log transformed and W_{sh} , r_m and t_b were estimated with nonlinear regression. The coefficient c_m was calculated with Equation 5:

$$c_m = \frac{W_{sh} r_m}{\ln(1 + e^{r_m(t_{sh}-t_b)})} \quad (5)$$

To examine whether plant growth rates (expressed in $g\ ^\circ C^{-1}\ d^{-1}$) could explain effects of plant density on LAR, plant growth rate was calculated for the period LAR was determined:

$$\text{Plant growth rate (g } ^\circ C^{-1} d^{-1}) = \frac{(W(g) \text{ at } gdd = 210\ ^\circ C d) - (W(g) \text{ at } gdd = 90\ ^\circ C d)}{(210 - 90)\ ^\circ C d} \quad (6)$$

Variable W was estimated with Equation 3 with the estimated values of c_m , r_m and t_b .

Results and discussion

Temperatures in the crop

Between 19 and 56 DAE in the F93 experiment, mean daily temperatures in the crop were lower in shaded treatments and at higher plant densities. The maximum difference in temperature was observed between D0S0 and D123S1 plots. The average temperatures during the measuring period in the D0S0 plot were 2.7 (at -1 cm), 2.8 (at 0 cm) or 0.5 (at 40 cm height) $^\circ C$ higher than in the D123S1 plot.

Dry matter accumulation

Fitted values for r_m (Eq. 4) were not significantly ($P < 0.05$) different between plant densities. Therefore, the analysis was redone with one common estimate for r_m for the four plant density treatments per shading level per year and one common estimate for W_{sh} for the two shading

treatments per plant density per year. Parameter t_b was estimated for every individual treatment. Table 1 shows the estimates of W_{sh} , c_m (recalculated using Equation 4), r_m and t_b . Parameter r_m was higher in F94 than in F93, probably related to the higher temperatures in F94 from 25 DAE onwards (Fig. 1). Shading decreased r_m and especially c_m . These effects are probably related to a reduced photosynthesis for shaded plants (Lawlor, 1987). At higher plant densities, t_b was lower, indicating that competition between plants for resources started earlier at higher plant densities. Also c_m (expressed per plant) was lower at higher plant densities, indicating that at later stages there was competition for resources between plants.

Leaf area per plant

Leaf area per plant was clearly lower at higher plant densities: e.g. for the F93 experiment 30 days after emergence leaf area per plant of treatment D0S0 was 1.7 times as high as treatment D0S123 and even 3.2 times as high 56 days after emergence (data not shown).

Leaf appearance rate (LAR)

When daily average air temperatures (Method 1) were used to calculate the number of appeared leaves as a linear function of growing degree days (gdd) for unshaded free standing plants (D0S0 treatments in F93 and F94), a very low base temperature of $-8\text{ }^{\circ}\text{C}$ fitted the data best ($R^2_{adj} = 95.6\%$). This is a very unrealistic value for maize. Using estimated hourly temperature values (Method 2), a base temperature of $11.1\text{ }^{\circ}\text{C}$ fitted the data best ($R^2_{adj} = 99.3\%$). Although this value is higher than commonly found in literature, the hourly method with a base temperature of $11.1\text{ }^{\circ}\text{C}$ was used to calculate gdd (Fig. 1), because more variance was accounted for by the use of hourly instead of daily values while a realistic base temperature was obtained (Ellis *et al.*, 1992).

The LAR per treatment was plotted against plant density in Fig. 3. The data are fitted to Equation 1. Figure 3 shows that LAR was lower at higher plant densities and for shaded plots compared to unshaded plots over the entire range of plant densities.

Temperatures in the crop were lower for shaded treatments and at higher plant densities. Crop temperature differences between plots were up to $2.8\text{ }^{\circ}\text{C}$, which will reduce LAR for this hybrid by 20 % (Chapter 4). Differences in LAR were much larger and temperature can therefore only partly explain the effects of plant density on LAR.

Figure 4 shows a very close relationship between plant growth rate and LAR independent of year, plant density or shading level. While the effects of growth rate on LAR were independent of shading level, it seems likely that the amount of assimilates determines LAR in the wide range of plant densities studied here. Effects of other factors such as red/far-red ratio can not be ruled out, but are probably less important.

Table 1. W_m (estimated per density*year combination), r_m (estimated per shading*year combination) and t_b (estimated per individual treatment) in Equation 3 (exponential growth equation), and calculated c_m (Equation 4; expressed per plant and per area) for different plant densities and shading levels in the F93 ($R^2_{adj} = 99.3\%$) and F94 ($R^2_{adj} = 99.8\%$) experiments. Standard errors are indicated between brackets.

	W_m (g)	r_m (g g ⁻¹ d ⁻¹)	t_b (d)	c_m (g pl ⁻¹ d ⁻¹)	c_m (g m ⁻² d ⁻¹)
F93:					
D0S0	0.24 (0.02)	0.170 (0.008)	36 (2)	2.6	-
D7.7S0	0.26 (0.02)	0.170 (0.008)	34 (2)	1.9	15
D31S0	0.26 (0.02)	0.170 (0.008)	30 (2)	0.94	29
D123S0	0.26 (0.02)	0.170 (0.008)	20 (1)	0.20	25
D0S1	0.24 (0.02)	0.161 (0.009)	35 (2)	1.4	-
D7.7S1	0.26 (0.02)	0.161 (0.009)	32 (2)	1.2	8.9
D31S1	0.26 (0.02)	0.161 (0.009)	27 (2)	0.48	15
D123S1	0.26 (0.02)	0.161 (0.009)	21 (2)	0.19	23
F94:					
D0S0	0.032 (0.003)	0.285 (0.008)	37 (1)	4.7	-
D7.7S0	0.028 (0.003)	0.285 (0.008)	36 (1)	2.8	22
D31S0	0.034 (0.003)	0.285 (0.008)	31 (1)	0.96	29
D123S0	-	-	-	-	-
D0S1	0.032 (0.003)	0.246 (0.007)	40 (1)	3.4	-
D7.7S1	0.028 (0.003)	0.246 (0.007)	38 (1)	1.9	14
D31S1	0.034 (0.003)	0.246 (0.007)	32 (1)	0.58	18
D123S1	0.032 (0.004)	0.246 (0.007)	27 (1)	0.16	19

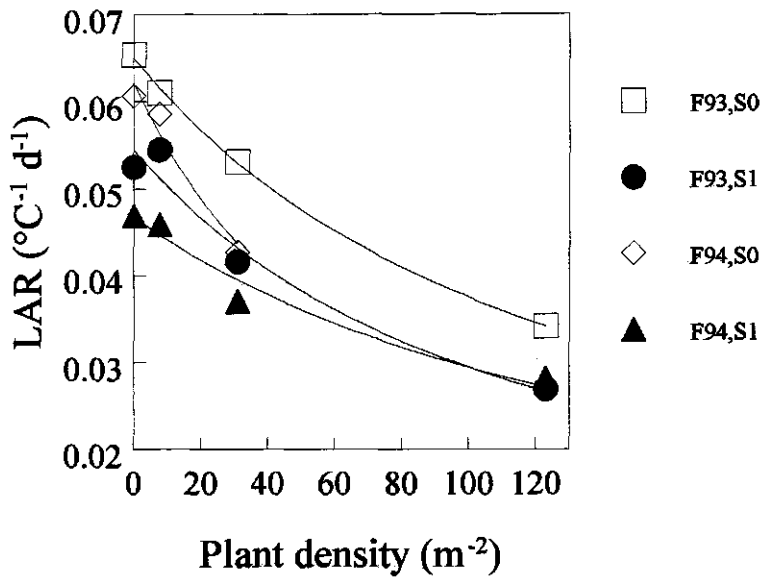


Figure 3. Effect of plant density on LAR for the two field experiments and shading levels. Lines are fitted curves using Equation 4.

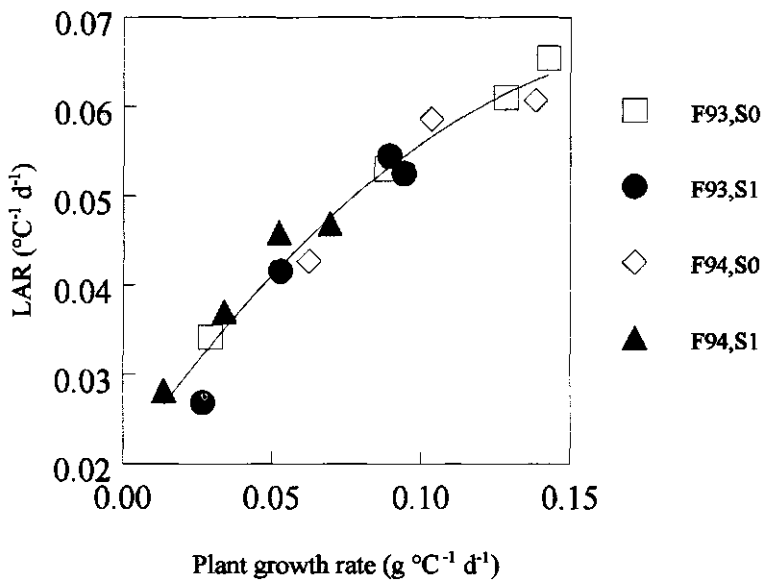


Figure 4. Relation between LAR and plant growth rate, calculated with Equation 5. A second order polynomial equation was fitted.

Leaf length, LER and LED

Shading significantly increased the length of full-grown leaves that appeared after the shading treatments commenced in both experimental years (data not shown). The effect of plant density on full-grown leaf length differed between the experimental years: in F93 full-grown leaves in both unshaded and shaded treatments were longer at higher plant densities at leaf positions higher than 5 (shown for unshaded treatments in Fig. 5a), while in F94 there was no significant effect of plant density on full-grown leaf length, neither for unshaded nor for shaded treatments (shown for unshaded treatments in Fig. 5b).

The calculated LER and LED of Leaf 7 relative to the value for spaced unshaded plants (treatment D0S0) are shown in Table 2. For both years, length and LED of Leaf 7 of shaded plants were longer. In the F93 experiment, at higher plant densities LED was longer and LER was unaffected resulting in longer leaves. In the F94 experiment, at higher plant densities LED was longer but LER was slower, resulting in no or a small effect of plant density on full-grown leaf length.

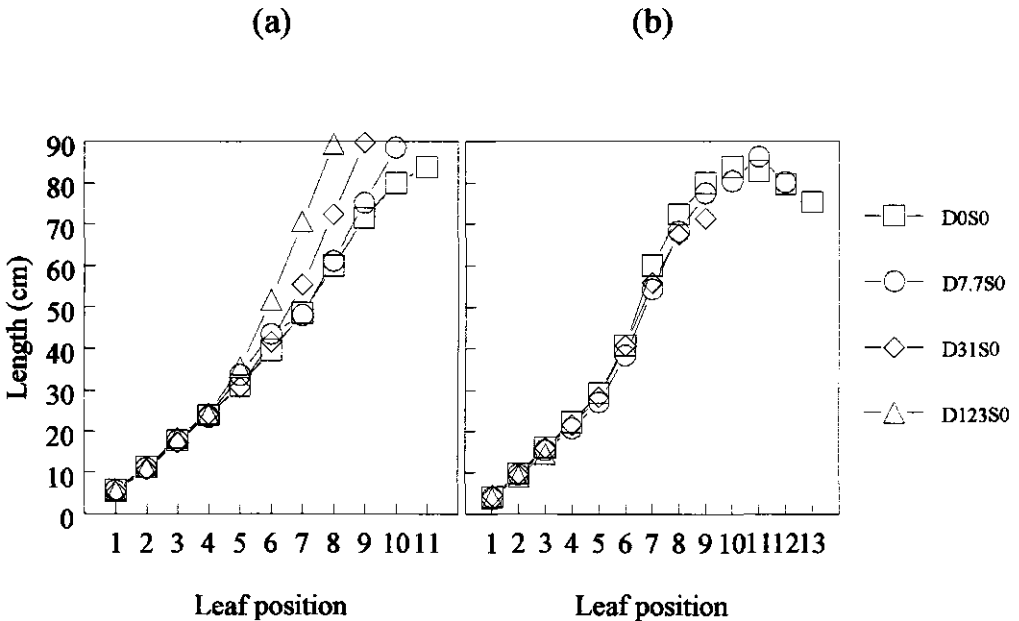


Figure 5. Full-grown leaf length of unshaded (S0) plants grown at different plant densities as a function of position on the plant in (a) the F93 experiment, and (b) the F94 experiment.

Table 2. Full-grown length, LED and LER of Leaf 7 relative to spaced, unshaded plants (D0S0 treatment). Average temperature and growth rate during elongation of Leaf 7 are given.

	Relative length	Relative LED	Relative LER	Average temperature (°C)	Plant growth rate (g appeared leaf ⁻¹)
F93:					
D0S0	1 (= 48.6 cm)	1 (= 104 °C d)	1 (= 0.47 cm °C ⁻¹ d ⁻¹)	16.2	1.99
D7.7S0	0.99	1.11	0.89	16.3	1.97
D31S0	1.14	1.16	0.99	16.4	1.66
D123S0	1.45	1.35	1.07	16.2	0.907
D0S1	1.08	1.19	0.91	16.4	1.90
D7.7S1	1.33	1.22	1.09	16.4	1.69
D31S1	1.54	1.31	1.17	16.2	1.44
D123S1	1.64	1.79	0.91	16.4	1.08
F94:					
D0S0	1 (= 60.1 cm)	1 (= 114 °C d)	1 (= 0.53 cm °C ⁻¹ d ⁻¹)	19.2	1.98
D7.7S0	0.90	0.97	0.93	19.2	1.60
D31S0	0.93	1.16	0.80	19.1	1.48
D123S0	-	-	-	-	-
D0S1	1.23	1.04	1.19	19.0	1.49
D7.7S1	1.11	1.09	1.01	19.1	1.31
D31S1	1.17	1.23	0.95	19.5	0.971
D123S1	1.13	1.33	0.85	19.8	0.496

In all experiments, LED was longer at higher plant densities and for shaded treatments. For wheat, a good relationship existed between LED and leaf appearance interval (Chapter 3). Such a relation also existed between LED and leaf appearance interval of Leaf 7 (Fig. 6). In tillering *Gramineae* species such as barley (Tesařová *et al.*, 1992), tall fescue (Skinner and Nelson, 1995) and wheat (Chapter 3), the growth of successive leaves is related in such a way that on average a constant number of visible leaves (between 1 and 2) is elongating per tiller. For maize, LED of Leaf 7 is four to seven times higher than the leaf appearance interval (Fig. 6). This is in agreement with findings in Chapter 4, where it was found that the number of growing leaves on a maize plant increases during development. Probably there is synchronisation between the growth of successive leaves, but this synchronisation is less simple than in barley, tall fescue or wheat.

Maximum leaf width

For both experimental years, shading significantly decreased the maximum width of leaves that appeared after the shading treatments were started. At higher plant densities, maximum leaf width was also significantly reduced, and already at a lower leaf position at higher plant densities (illustrated for F94 in Fig. 7). This confirms earlier findings for wheat (Chapter 5).

Possibly maximum leaf width is related to the plant growth rate per phyllochron. This measure adjusts for the effect of plant density on LAR and indicates the dry matter produced during one leaf appearance interval. At appearance of Leaf 7, dry matter production per plant and number of appeared leaves per plant were not yet affected by plant density. The plant growth rate per appeared

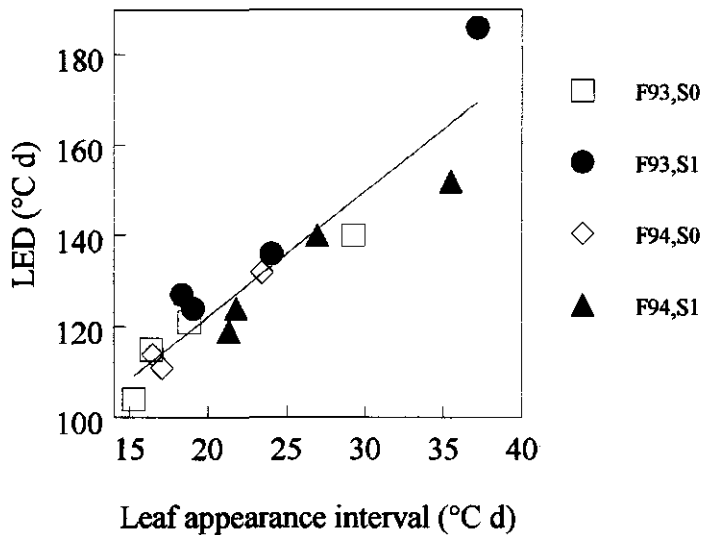


Figure 6. Relation between LED of Leaf 7 and leaf appearance interval, fitted with linear regression. Data from different density treatments.

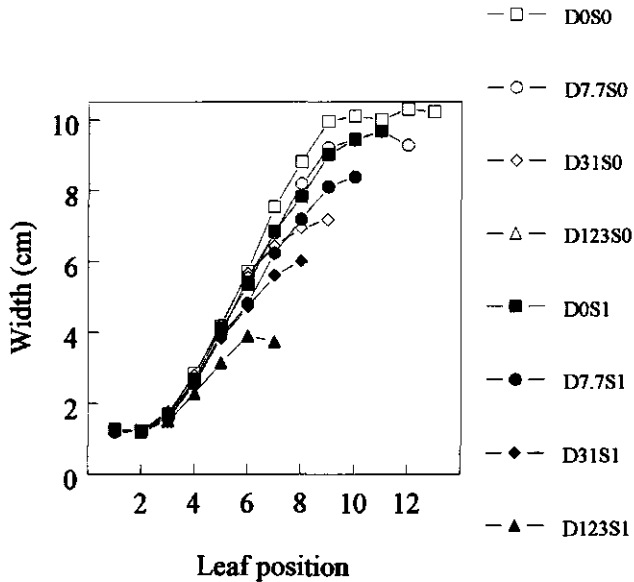


Figure 7. Maximum leaf width of plants grown at different plant densities and shading levels as a function of position on the plant in the F94 experiment.

leaf at appearance of Leaf 7 can therefore not explain the differences in maximum leaf width between plant densities. If the growth rate per appeared leaf is calculated for the period that Leaf 7 is elongating, a good positive relationship was found between maximum leaf width and the growth rate per appeared leaf (Fig. 8). Apparently, if leaf width is determined by growth rate per appeared leaf, maximum leaf width is not set at appearance of the leaf but during elongation.

Leaf shape factor (k)

The leaf shape factor k (Equation 1) decreased from 0.82 for Leaf 1 to 0.69 for Leaf 3 and was between 0.67 and 0.71 up to Leaf 8. Shading nor plant density had a significant effect on the value of k . Sanderson *et al.* (1981) found very small effects of plant density on k . Apparently area per leaf position is determined by the maximum width and length, in a manner which is rather independent of plant density or shading.

Leaf lifespan

There was no significant effect of plant density or shading on the number of dead leaves per plant as a function of DAE within the duration of the experiment (data not shown). At lower densities, old leaves died mainly due to wind, putrefaction (leaves laying on the ground) or penetration of their sheath by crown roots. At high plant densities old leaves mainly died by yellowing.

Conclusions

Plant density affected the leaf area expansion in maize mainly through effects on LAR. The effects on LAR were well related to effects on the plant growth rate per leaf appearance interval.

Appendix. List of abbreviations used

c_m	Maximum growth rate for $t \rightarrow \infty$ (equation 2)
D	Plant density
DAE	Days after emergence
gdd	Growing degree days
LAR	Leaf appearance rate
LAR_0	LAR at $D = 0 \text{ m}^{-2}$ (equation 5)
LED	Leaf elongation duration
LER	Leaf elongation rate
PPFD	Photosynthetic photon flux density
r_m	Initial relative growth rate (Equation 2)
R^2_{adj}	Percentage of variance accounted for
S	Shading treatment (S0: unshaded; S1: 50 % shaded)
t	Time
t_b	Time when the linear growth rate effectively starts (Equation 2)
t_{sh}	Time when the shading treatments started
W	Dry weight above-ground parts per plant
W_{sh}	W at t_{sh}
β	Slope of Equation 5 at $D = 0 \text{ m}^{-2}$

Part III

Simulation

Chapter 7

An object-oriented morphological model of leaf area expansion in wheat

Abstract

A model was developed to simulate plant leaf area expansion of *Gramineae* species. The principles of object orientation were used to obtain maximum flexibility, and the application to modelling foliar development of plants is shown. Plant related processes were strictly simulated at organ level. This implied that some variables, e.g. maximum leaf width, depended on the value of the leaf beneath it, instead of on the position on the plant. Equations and parameter values in the model were derived from earlier published data on spaced wheat plants, and growth was assumed to be sink limited. From these data, all plant processes needed to run the model could be converted to equations and data on organ level, using difference equations for relationships within the plant. The simulations yielded patterns of leaf area expansion that depended on the position of the leaf within the plant. The relative growth rate for leaf area per plant decreased with time. Experimental data were not predicted well, because source limitation was not included and the assumption of a constant leaf appearance rate was not correct. Possible improvements, extensions and applications of the model are discussed.

Introduction

A good prediction of leaf area expansion is crucial to quantify differences in growth between plants or crops (Goudriaan and Van Laar, 1994; Van Loo, 1993). However, relatively few analytical studies have been carried out to understand the mechanisms of leaf area expansion. As a consequence, dynamic crop growth models simulate leaf growth in very different ways.

In SUCROS (Spitters *et al.*, 1989), leaf area growth is divided into two phases. In the first phase, growth is assumed to be sink-limited, and leaf area growth proceeds exponentially with thermal time. In the second phase (Leaf Area Index > 0.75), growth is assumed to be source-limited, and leaf area growth is calculated from the dry weight of the leaves and a predetermined specific leaf area (SLA). However, SLA is strongly affected by environmental factors, especially temperature and photosynthetic photon flux density (PPFD). Therefore, SLA should be an output of a mechanistic growth model, instead of an input (Van Loo, 1993).

Others have tried to simulate leaf area growth completely separately from dry matter production (McMaster *et al.*, 1991; Amir and Sinclair, 1991) or included mechanisms of possible source limitation on tiller appearance and leaf area expansion (Van Loo, 1993). In these models the morphological development of *Gramineae* plants, i.e. tillering, appearance of leaves on a tiller, and individual leaf growth, is included in various degrees. However, a general quantitative concept of morphology is still lacking.

Our Crop Physiology Group introduced a general framework to analyse effects of temperature and PPFD on leaf area growth in wheat (Chapters 2 and 3) and maize (Chapter 4). We used this framework to analyse effects of plant density on wheat (Chapter 5) and maize (Chapter 6). In this paper the framework will be formalised into a mechanistic growth model, in which:

1. sink limited leaf area expansion of wheat is simulated, based upon the variables used for analysing leaf area expansion (Chapters 2 and 3);
2. the mechanisms of regulation of these leaf area variables are included as suggested in Chapters 2 and 3;
3. the resulting model should become very flexible, such that leaf area growth of other plant species can be simulated and source limited growth can be easily introduced.

Theory

Object orientation

To enhance the desired flexibility, object orientation was used in the model. Object orientation can be characterised by the following concepts: objects, member variables, methods, messages, classes, encapsulation, polymorphism and inheritance.

Objects. An object is a representation of a real-world element, for example a particular leaf blade on a specific wheat plant. An object contains member variables and methods (explained below).

Member variables. These are data or other objects stored inside an object (for instance the member variable "Length" is data stored inside a "Leaf Blade" object; the member variable "Seed" is an object stored inside a "Plant" object).

Methods. Methods are functions that belong to an object (for instance the method "Leaf Elongation Rate" in a "Leaf Blade" object calculates the current "Leaf Elongation Rate" depending on, for example, temperature).

Messages. These are the (only) way objects can communicate with each other. An object can send a message to another object. If the message is recognised by one of the methods of the receiving object, an answer will be given. For example, a "Seed" object can send the message: "GiveLength" to a "Leaf Blade" object. If the method "GiveLength" is present in the "Leaf Blade" object, it will execute the code present in that method, and pass the value of the length that is stored in the "Leaf Blade" object to the "Seed" object.

Class. A class is a set of definitions for a uniform group of its derived objects. For example, the class "Leaf Blade" defines that its derived objects contain the member variables "Length" and "Width", and a method "GiveLength". Values of "Length" and "Width" are specific for each of the objects derived from the class.

Encapsulation. Encapsulation prevents that member variables in objects can be retrieved or changed directly by other objects. Objects can only retrieve or change information of other objects by sending messages which are understood by the methods of the receiving object. For example, another object can get the value of the width of a "Leaf Blade" object, only if this "Leaf Blade" object has a method that gives the value of its width.

Polymorphism. Polymorphism allows a program to treat objects derived from different classes as if they were derived from the same class. Thus a certain message can be sent to objects derived from different classes. For example, a "Leaf Blade" object can send a "What is the temperature?" message to an "Abiotic Environment" object. Depending on whether the model is running under growth chamber or field conditions, the "Abiotic Environment" object is derived from class "Growth Chamber" or "Field". Both the "Growth Chamber" and the "Field" class have a method "What is the temperature?", but they can calculate temperature in different ways. In this way, the calculation of temperature is the full responsibility of the "Abiotic Environment" object and hidden from the "Leaf Blade" object.

Inheritance. The concept of inheritance permits objects to be organised in taxons in which specialised objects inherit the member variables and methods of more generalised objects. Similar classes of objects which share member variables and methods can be modeled by specifying a super class, which defines a common part, and then deriving specialised classes (subclasses) from the superclass. For example, the class "Organ" can be seen as a superclass of classes "Root" and "Seed"

("Root" and "Seed" are a kind of "Organ"). "Dry matter" is a member variable that is generic for all organs and can be defined in the "Organ" class. "Nitrogen Uptake" is a member variable specific for "Root" and should be defined in the "Root" class.

Advantages of Object Orientation for modelling morphology. The most important advantage of using Object Orientation for modelling plant morphology is the real-world presentation of objects. With object orientation, the appearance and disappearance of organs on a plant can be simply modeled as the creation and destruction of "Organ" objects. Furthermore, inheritance can be used to describe member variables and methods in one class, while all its subclasses automatically inherit the member variables and methods. For example, if it is decided that all organs should have a new member variable "Nitrogen Content", this new member variable can be defined in the "Organ" class. All subclasses automatically inherit the new member variable "Nitrogen Content", and there is no need to change the code in the subclasses of the superclass "Organ".

Plant morphology

Integration level. In Chapters 2 and 3 a method was developed to calculate the dynamics of numbers of leaf blade organs and the dynamics of individual leaf dimensions for *Gramineae* species. In line with these observations, objects in the simulation model are strictly at organ level and not at a tiller level. Accordingly, leaf area is calculated per individual leaf and not directly per tiller or per plant.

Relationships between organs. Existing simulation models assume simple relations between leaf position and, for example, individual leaf area (McMaster *et al.*, 1991; Amir and Sinclair, 1991).

However, in Chapter 3 it was shown that effects of leaf position differ between tiller types.

Furthermore, it is unrealistic to assume that there is a causal relation between a leaf variable and its position on a tiller. In experiments with Brussels sprouts it was found that newly formed leaves of plants that were supplied with ample nitrogen after a period of a shortage of nitrogen were smaller than comparable leaves on plants supplied with ample nitrogen throughout (Vos *et al.*, 1996). After a while comparable leaves reached equal sizes. These experiments show that both the current environmental conditions and the history of the plant should be taken into account for prediction of leaf area. The history of the plant is probably reflected in the size of the apex (Abbe *et al.*, 1941; Pieters and Van den Noort, 1988, 1990): the size of the apex increases faster under better growth conditions. Mathematically, this can be represented as follows. The value of a certain leaf variable (P_{leaf}) depends on the size of the apex at appearance of Leaf L (A_{leaf}) and environmental conditions (E):

$$P_{leaf} = f_1 (A_{leaf}, E) \quad (1)$$

Apex size changes with every leaf that has appeared:

$$A_{leaf+1} = A_{leaf} + f_2 (A_{leaf}, E) \quad (2)$$

Combining the two equations results in a discrete difference equation for a given leaf variable:

$$P_{leaf+1} = f_3 (P_{leaf}, E) \quad (3)$$

This implies that leaf variable values depend on the values on the leaf beneath it (see also Chapter 3). This mechanism will be used in the model to simulate the change of certain leaf variables with leaf position.

Model description

Plant morphology.

The morphological structure of *Gramineae* plants forms the core of the model. Klepper *et al.* (1982) introduced an identification method for tillers and leaves on wheat seedlings (Fig. 1). The first leaf on a tiller is the prophyll, a non-foliar leaf which is not important for photosynthesis. All leaves (including prophylls) contain a bud which can grow out into a new tiller. Leaves and tillers are counted acropetally: the prophyll is Leaf 0 (L0) on a tiller, the first foliar leaf is Leaf 1 (L1) and so on. Daughter tillers are named after their parent leaf. For example, Tiller t1 is the daughter tiller of

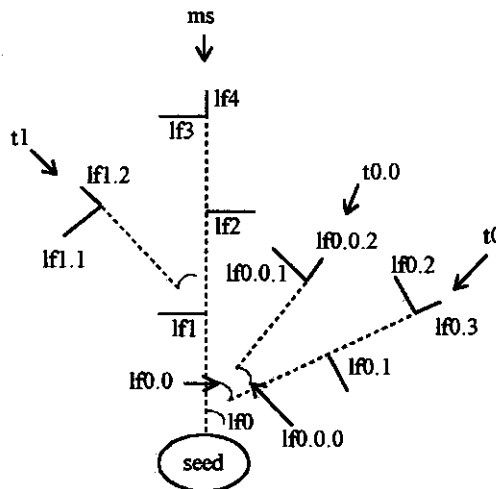


Figure 1. Morphological representation of a *Gramineae* seedling (redrawn from Klepper *et al.*, 1982). lf = leaf, t = tiller, ms = main stem.

Leaf L1 and Leaf L1.2 is the second foliar leaf on Tiller t1 (Fig. 1). In fact Klepper's method gives a morphological representation of leaf positions common for all *Gramineae* plants. Based on the morphological structure of Fig. 1, four variables were derived in Chapter 2 that determine the dynamics of the number of living leaves on a plant:

- i) leaf appearance rate per tiller;
- ii) timing of tiller appearance;
- iii) specific site usage (SSU), i.e. the fraction of existing buds that grow out into a visible tiller;
- iv) timing of leaf death.

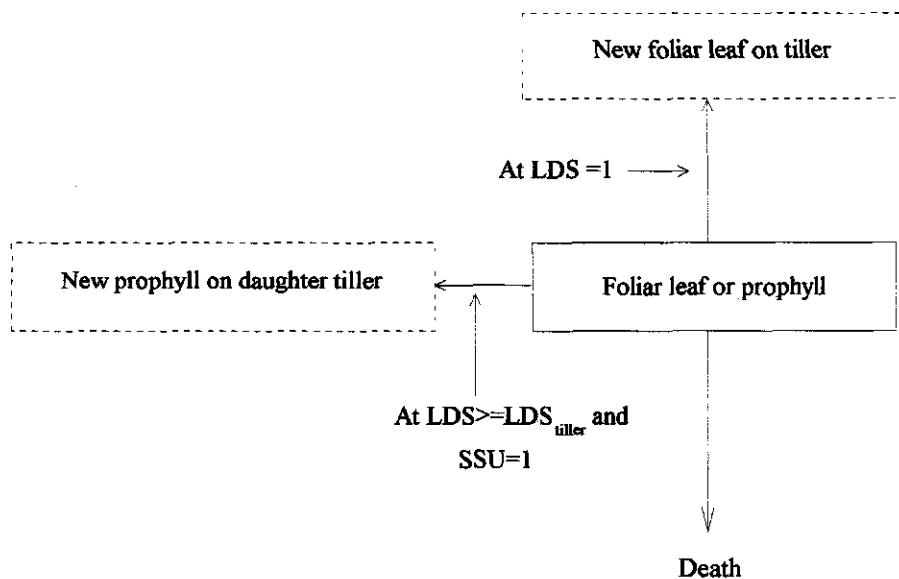


Figure 2. Basic processes of leaf number dynamics in *Gramineae* species.

Table 1. Events which are determined by Leaf Development Stage (LDS).

Value of LDS	Event
0	Foliar leaf appearance
1	Appearance of next leaf on same tiller
LDS_{fg}	Foliar leaf is full-grown; elongation stops
LDS_{tiller}	From this moment onwards, a bud in the axil of a leaf can grow out into the first foliar leaf of the daughter tiller

Processes i), ii) and iii) are at tiller level, which is between organ and plant level. While the model is intended to include processes strictly at organ level, these three processes are converted to organ level. Fig. 2 and Table 1 show the basic processes of leaf formation of *Gramineae* species at organ level. Leaf development stage (LDS) is introduced here to mark the visible appearance of a leaf ($LDS = 0$), the visible appearance of the next leaf on the same tiller ($LDS = 1$), and the moment a leaf is full-grown (ligule is visible) ($LDS = LDS_{fg}$). Leaf development stage also indicates the earliest possible appearance of the first foliar leaf (Leaf 1) on the daughter tiller of the leaf ($LDS = LDS_{tiller}$). The prophyll of the daughter tiller is assumed to appear at one unit of LDS earlier than Leaf 1 on the daughter tiller.

A new set of four variables on leaf level can now be introduced:

- i) leaf development rate (LDR), i.e. the rate of change of LDS;
- ii) LDS_{tiller} : LDS after which the bud in the axil of the leaf can grow out into the first foliar leaf (Leaf 1) on the daughter tiller;
- iii) SSU, now defined as the probability a bud grows out into the first foliar leaf (Leaf 1) on the daughter tiller;
- iv) timing of leaf death.

If the processes in Fig. 2 are iterated with specific values per leaf for LDR, LDS_{tiller} , SSU and timing of leaf death, every possible above-ground leaf arrangement of a *Gramineae* plant can be modelled.

Leaf size

For *Gramineae* species, cell division and expansion of foliar leaves take place within the enveloping leaf sheaths. Therefore, foliar leaf parts that have appeared are full-grown and area expansion of individual foliar leaves can be described with four variables (Chapter 3):

- v) Leaf elongation rate (LER);
- vi) Timing of cessation of elongation;
- vii) Maximum leaf width (MLW);
- viii) Leaf shape variable (k).

Formalisation for sink-limited growth

LDR. LDR (d^{-1}) is equal to leaf appearance rate, because I defined $LDS=0$ at leaf appearance and $LDS=1$ at appearance of the next leaf on the same tiller. Leaf appearance rate on the main stem has been studied extensively, and strong effects of temperature have been found (e.g. Volk and Bugbee, 1991). For spaced plants and high irradiance conditions, leaf appearance rate of tillers is almost equal to that on the main stem (Chapter 2). A linear effect of temperature on LDR independent of leaf type was therefore assumed in the model. Variable LDR is expressed in degree days, with a base

temperature of 0 °C (Chapter 2).

LDS_{tiller} . LDS_{tiller} is equivalent to Haun Stage-delay, a variable introduced in Chapter 2. This variable indicates the timing of tiller appearance relative to the leaf stage of the parent tiller. In Chapter 2 it was found that at high light conditions HS-delay of wheat tillers was independent of temperature, but changed with tiller type. The negative exponential relation found in Chapter 2 was:

$$LDS_{tiller} = 1 + (LDS_{tiller, Leaf 0} - 1) e^{-RDR \times x} \quad (4)$$

where x is the Haun Stage of the main stem at which the tiller appears assuming a maximum site filling of 0.69 (Plant type 1 in Chapter 2), and RDR is the relative decline rate. The current modelling approach requires that the properties of Organ $x+1$ are written as a function of the properties of Leaf x . An appropriate way to achieve this is by using discrete difference equations. Equation 4 can be rewritten into the following discrete difference equation (Edelstein-Keshet, 1988; calculation is given in Appendix I):

$$LDS_{tiller, Leaf+1} = (LDS_{tiller, Leaf} - 1) r_{LDS_{tiller}} + 1 \quad (5)$$

where $r_{LDS_{tiller}}$ is a constant (equal to e^{-RDR}), and $Leaf+1$ is the next younger leaf on the same tiller or the prophyll on the daughter tiller. For $Leaf \rightarrow \infty$ and $-1 < r_{LDS_{tiller}} < 1$, $LDS = 1$, which is the absolute minimum reflecting a site filling of 0.69 (Neuteboom and Lantinga, 1989).

SSU. In principal, all axil buds can grow out into new tillers. If growth is fully sink-limited, *SSU* equals 1.

Timing of foliar leaf death. For spaced wheat plants well supplied with nutrients and water, in Chapter 2 no death of foliar leaves up to HS of the main stem = 7 was found. Therefore, in the current exercise, foliar leaves are assumed not to die within the time-span of canopy construction.

LER. In Chapter 3 it was found that *LER* depends on the position of the leaf on the plant and on temperature with a base temperature of 0 °C:

$$LER = (gT_d - fT_d) (1 - e^{-c(\text{Summed Leaf Position} - 1)}) + fT_d \quad (6)$$

where *Summed Leaf Position* is the sum of all the numbers in the designation of the leaf (e.g. for Leaf 1.0.1 the *Summed Leaf Position* is 2; for Leaf 2.3.0.1 the *Summed Leaf Position* is 6 (Chapter 3)), c is a fitted constant, T_d the mean daily temperature, fT_d the *LER* for *Summed Leaf Position* = 1, and gT_d is the *LER* for *Summed Leaf Position* $\rightarrow \infty$. This relation is split up into two parts here. At a temperature of 10 °C, the relation can be rewritten into the following discrete equation:

$$LER_{T=10^{\circ}\text{C}, \text{Foliar Leaf } +1} = (LER_{T=10^{\circ}\text{C}, \text{Foliar Leaf}} - LER_{\text{max}, T=10^{\circ}\text{C}}) * r_{LER} + LER_{\text{max}, T=10^{\circ}\text{C}} \quad (7)$$

where Foliar Leaf + 1 is the next younger foliar leaf on the same tiller or the first foliar leaf on the daughter tiller, $LER_{\text{max}, T=10^{\circ}\text{C}}$ (cm d^{-1}) is the maximum LER at a temperature of 10°C and Foliar Leaf $\rightarrow \infty$, r_{LER} is a dimensionless constant and $LER_{T=10^{\circ}\text{C}, \text{Foliar Leaf}}$ is the LER at 10°C for a foliar leaf. The effects of temperature on LER are linear (Chapter 3):

$$LER = LER_{T=10^{\circ}\text{C}} * \left(\frac{T - T_{b,LER}}{10 - T_{b,LER}} \right) \quad (8)$$

where $T_{b,LER}$ is the base temperature ($^{\circ}\text{C}$) for LER.

Timing of cessation of elongation. For wheat (Chapter 3), barley (Tesařová *et al.*, 1992), rice (Yin *et al.*, 1995), perennial ryegrass (Van Loo, 1993), and tall fescue (Skinner and Nelson, 1995) leaf elongation duration is proportional to leaf appearance interval. A constant leaf development stage at which the leaf is full-grown (LDS_{FG} , see Table 1 and Fig. 2) is used here to model the timing of cessation of elongation.

MLW. For wheat, maximum leaf width (MLW; in cm) depended on summed leaf position, but not on temperature (Chapter 3):

$$MLW = \frac{MLW_{\text{max}}}{1 + e^{a - b \times \text{Summed leaf position}}} \quad (9)$$

where MLW_{max} (cm) is the maximum MLW for Summed Leaf Position $\rightarrow \infty$, and a and b are fitted constants. This relation is rewritten here as a discrete logistic difference equation:

$$MLW_{\text{Foliar Leaf } +1} = \frac{MLW_{\text{Foliar Leaf}}}{1 + \left(\frac{MLW_{\text{max}}}{MLW_{\text{Foliar Leaf}}} - 1 \right) r_{MLW}} \quad (10)$$

where r_{MLW} is a dimensionless constant.

Leaf shape. The dimensionless leaf shape variable k has been usually determined to calculate full-grown leaf area from maximum leaf width and full-grown leaf length (Chapter 3):

$$k = \frac{\text{Full-grown leaf area}}{\text{Maximum leaf width} * \text{Full-grown leaf length}} \quad (11)$$

Sine functions have been found which describe the width of a leaf at every point (Sanderson *et al*, 1981; Chapter 4). For simplicity, in the model a leaf was assumed to consist of a triangular part from the leaf tip (width=0) to point α (width=MLW), where α is a fraction of the full leaf length. The remaining part (1- α) is assumed to be rectangular with a width of MLW. Parameter α (dimensionless) can be calculated from k:

$$\alpha = 2 - 2k \quad (12)$$

If $LDS < \alpha$, the triangular part of a leaf is appearing. If $LDS \geq \alpha$, the rectangular part is appearing.

Implementation of the model

The model is implemented in C++, which is an object-oriented computer language. Fig. 3 shows the inheritance structure of the model. The classes FOLIAR LEAF and PROHYLL are subclasses of class LEAF (a foliar leaf is a kind of leaf), which means that FOLIAR LEAF and PROPHYLL inherit member variables and methods from their superclass LEAF. LEAF and SEED are subclasses of ORGAN, and GROWTH CHAMBER and FIELD are subclasses of ABIOTIC ENVIRONMENT. Other classes in the model are defined without a superclass. As an example of the use of inheritance, ORGAN has a member variable "Name", which means that every organ (foliar leaf, propyll, or seed) has its own "Name". FOLIAR LEAF has a member variable "Length", which means that this variable is only defined for a foliar leaf, and not for a propyll or a seed.

To connect adjacent organs, pointers are used. A pointer is the computer memory address of

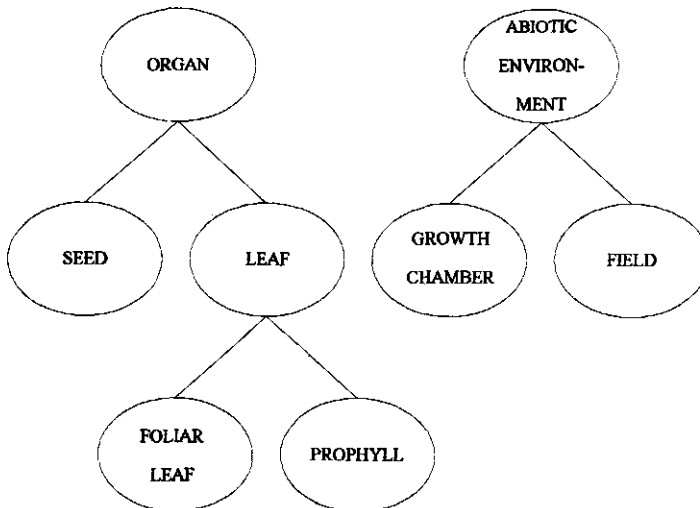


Figure 3. The class inheritance structure of the model.

another object. For example, all objects derived from the class LEAF or its subclasses have a pointer member variable called 'p_younger_leaf', which is the memory address of the next younger leaf on the same tiller. For the foliar leaf L1, p_younger_leaf points to the address of L2. Fig. 4 gives, as an example, the complete pointer structure around leaf 0 (the coleoptile).

At the start of a run (here equal to emergence day), basically the following methods are called:

1. a RUN object (*Run*) is created;
2. *Run* creates an INPUT object (*Input*) and asks *Input* for *Run* member data (e.g. start and finish date of *Run*);
3. *Input* reads required data from a file and hands this over to *Run*;
4. *Run* destroys *Input* and creates a PLANT object (*Plant*);
5. *Plant* creates a SEED object (*Seed*);
6. *Seed* creates a PROPHYLL object (*L0*) and the memory address of *L0* is stored as a pointer member variable in *Seed*;
7. *L0* stores the memory address of *Seed* as a member variable and creates a FOLIAR LEAF object (*L1*). The memory address of *L1* is also stored as a pointer member variable in *L0*; other member variables are initialised (e.g. LDS);
8. *L1* stores the memory address of *L0* as a pointer member variable, creates an INPUT object and asks it for input data (as in 2.); other member variables are initialised (e.g. Length = 0 cm).

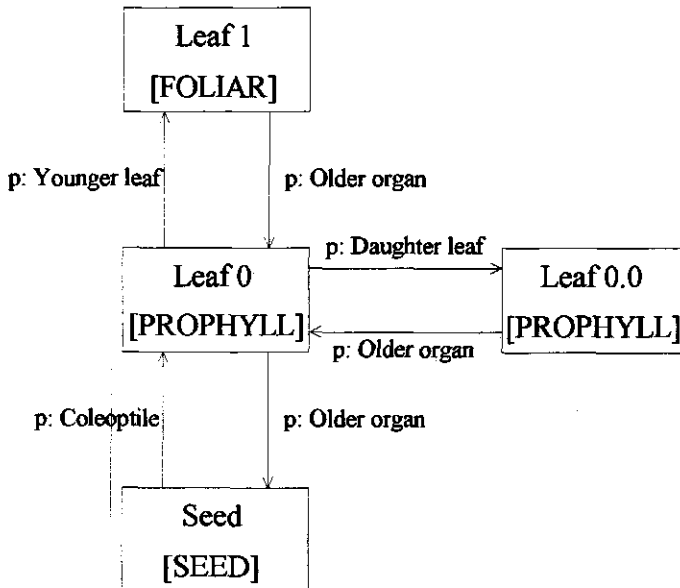


Figure 4. The memory pointer structure of the model. Rectangles are objects, between brackets the class from which the object is derived. "p:..." is a pointer member variable.

As the plant is growing, within one time step sequentially the following methods are called:

1. *Run* asks actual abiotic data from an ABIOTIC ENVIRONMENT object (depending on the choice of the user, this will refer to an object of class GROWTH CHAMBER or FIELD (mechanism of polymorphism));
2. *Run* sends a message to *Plant* to calculate its rates;
3. *Plant* sends a message to *Seed* to calculate its rates; through the pointer structure in Fig. 4 all organs of the plant calculate their rates;
4. *Run* sends a message to *Plant* to calculate its new states;
5. *Plant* sends a message to *Seed* to calculate its new states; using the pointer structure in Fig. 4 all organs of the plant calculate their new states;
6. *Plant* sends a message to *Seed* to form new organs; this message is passed to all other organs using the pointer structure. If a new organ is formed, an object is created, its member variables initialised and the pointer structure adjusted.

At certain intervals file output is produced by objects of the REPORTER class.

This is a very flexible structure: responsibilities per class are such that the functionality is generic: for example the class RUN can be used for all kind of simulations. Using the pointer structure in Fig. 4 a very complex plant structure can be simulated with just a few simple rules.

Calibration

The required numerical values were calculated from data of a growth chamber experiment with spaced spring wheat plants (Chapters 2 and 3). For the closest approximation of sink-limited growth, data from the lowest temperature (13/8 °C) and highest PPFD (286 $\mu\text{mol m}^{-2} \text{d}^{-1}$) treatment were used:

1. LDR is equal to leaf appearance rate: $1/91 = 0.011 \text{ } ^\circ\text{C}^{-1} \text{ d}^{-1}$;
2. $r_{\text{LDS, tiller}}$ is equal to e^{RDR} : $e^{-0.31} = 0.73$;
3. $\text{LDS}_{\text{tiller, Leaf=0}} = 2.2$;
4. $\text{LER}_{\text{max, T=10}^\circ\text{C}} = 0.34 \text{ cm } ^\circ\text{C d}^{-1} * 10 \text{ } ^\circ\text{C} = 3.4 \text{ cm d}^{-1}$;
5. $r_{\text{LER}} = e^{-0.60} = 0.55$;
6. $\text{LER}_{\text{T=10}^\circ\text{C, Foliar Leaf=1}} = 0.17 * 10 = 1.7 \text{ cm d}^{-1}$;
7. $\text{LDS}_{\text{lg}} = 123 / 91 = 1.35$;
8. $\text{MLW}_{\text{Foliar Leaf=1}} = 0.354 \text{ cm}$;
9. $\text{MLW}_{\text{max}} = 2.2 \text{ cm}$;
10. $r_{\text{MLW}} = e^{-0.45} = 0.64$;
11. $\alpha = 2 - 2 * 0.80 = 0.40$.

The base temperature for both leaf appearance and leaf elongation was 0 °C.

Validation

The model was run with hourly time steps at different temperatures (13/8, 18/13 and 23/18 °C) from 0 to 40 days after emergence. Some of the output was compared with growth chamber experiments. Also a sensitivity analysis was performed for all 11 parameters: each parameter was increased 10 % and decreased 10 %, and the effect on leaf area was analysed.

Simulation results

Fig. 5 shows the increase in leaf area for consecutive leaves on the main stem at a temperature regime of 18/13 °C. The leaves appear at regular intervals, caused by a constant LDR. The constant value of LDS_{fg} is reflected in the equal duration of elongation for all leaves. The increase in size of consecutive main stem leaves is completely due to an increased leaf area expansion rate, caused by broader leaves (Eqn. 10) and higher elongation rates (Eqn. 7).

In Fig. 6, the area growth of individual leaves on a selection of tillers is aggregated to tiller level. The interval between appearance of primary tillers t_0 , t_1 , t_2 , t_3 , and t_4 increases up to a constant level, due to Eqn. 5 together with a constant LDR. The increase in leaf area clearly differs between

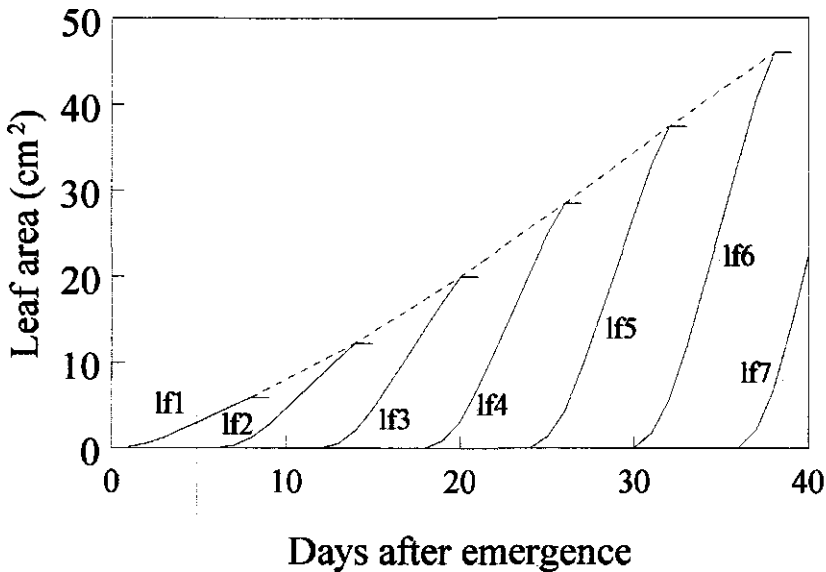


Figure 5. Simulated leaf area growth of consecutive main stem leaves at 18/13 °C. For clarity of presentation, a line is not continued after the leaf is full-grown. The dashed line connects the maximum leaf areas of the leaves.

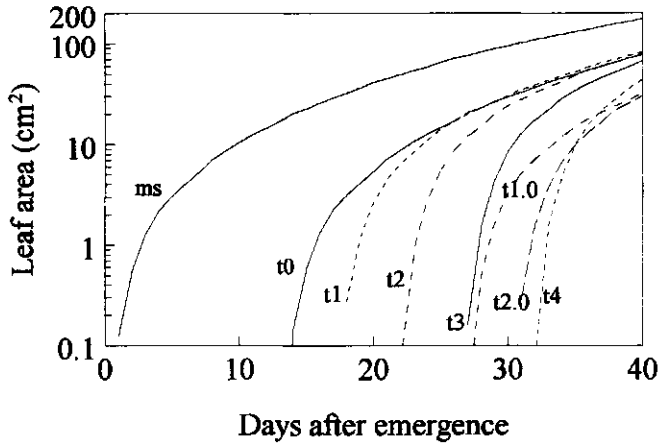


Figure 6. Simulated leaf area growth of a selection of tillers at 18/13 °C.

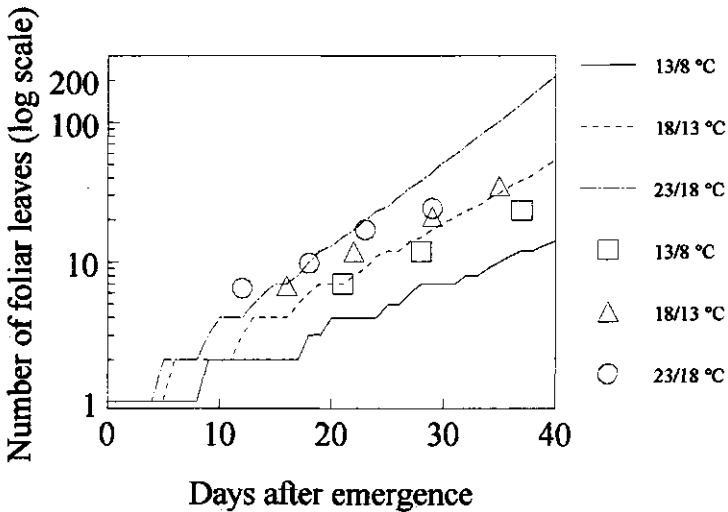


Figure 7. Observed and simulated number of foliar leaves at three temperature regimes.

tiller types, such that even later-appearing tillers have more leaf area than earlier appearing tillers (e.g. compare t_0 and t_1 from 25 days after emergence onwards). Daughter tillers of higher positioned leaves (higher summed leaf position) start with a first leaf which is already quite large (Eqns. 7 and 10) and the interval between appearance of consecutive tillers on the same parent tiller is less than a leaf appearance interval (Eqn. 4). Thus, Leaf 1.1 has the same size as Leaf 0.2, but Leaf 1.1 has appeared earlier (18 days after plant emergence) than Leaf 0.2 (19 days after plant emergence).

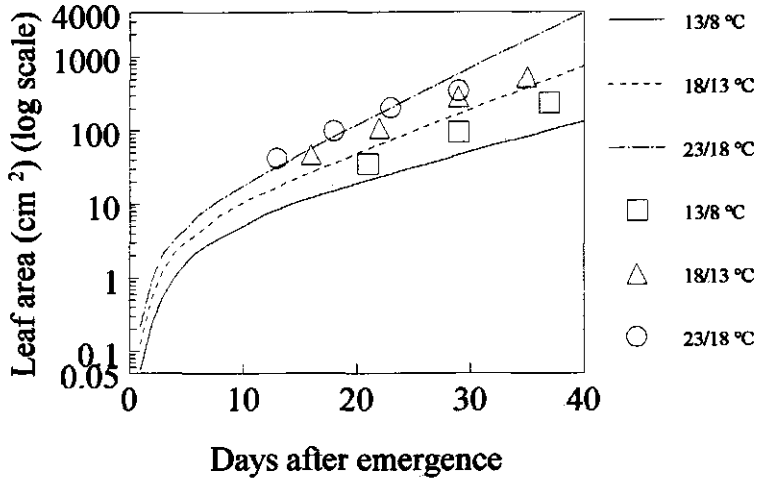


Figure 8. Observed and simulated leaf area per plant at three temperature regimes.

Table 2. Effect of a 10 % decrease or increase of separate plant parameters on leaf area per plant 20 days after emergence relative to standard values for a temperature regime of 23/18 °C. Acronyms and symbols are explained in the text.

Plant parameter	10 % increase	10 % decrease
LDR	+29	-24
$r_{LDS, \text{ tiller}}$	-4	+4
$LDS_{\text{ tiller, Leaf=0}}$	-8	+9
$LER_{\text{ max, T=10}^\circ\text{C}}$	+7	-7
r_{LER}	-3	+3
$LER_{\text{ T=10}^\circ\text{C, Foliar Leaf = 1}}$	+3	-3
$LDS_{\text{ f-g}}$	+5	-6
$MLW_{\text{ Foliar Leaf = 1}}$	+8	-8
$MLW_{\text{ max}}$	+2	-2
r_{MLW}	-11	+12
α	-3	+4

Figs. 7 and 8 show simulation results for three temperature regimes at whole-plant level. The number of leaves increases more or less exponentially, although the curve is not smooth (Fig. 7). Leaf area per plant increases with an decreasing relative growth rate in an early stage and a constant relative growth rate in a later phase (Fig. 8). For both number of leaves and leaf area per plant, the increase is faster at a higher temperature, due to a higher LDR and LER (Eqn. 8). The experimental data are not well predicted by the model. The reasons for this will be discussed below.

Table 2 shows the results of the sensitivity analysis. Small changes in LDR appear to have large impact on leaf area per plant. For the other 10 parameters, the impact is much smaller.

Discussion

In the model, sink limited growth of a young wheat plant was simulated. In one run, more than 400 separate leaves were simulated, each with their individual member variables. It appeared that variables measured at tiller level (e.g. leaf appearance rate) could be converted to individual organ level (LDR). In the model there was no direct relation between leaf position and a leaf variable, because all these relations were successfully converted to discrete equations, in which the leaf variable was related to the equivalent variable of an adjacent leaf. In principle, this is a more mechanistic method than using direct relations with position, because the history of the plant together with the current environmental factors both affect leaf variables.

Object orientation was used to implement the model. Object-oriented programs are potentially more flexible and enhance reusability (Taylor, 1990). Furthermore, plant organs can be viewed as objects that are created and deleted dynamically, just like real organs are. In this way, the model gives a more realistic representation of organ population dynamics and growth on a plant. Also, variables and processes only need to be described at one hierarchical level (e.g. organ, leaf, or foliar leaf), because of the inheritance principle. The organs are held together by the pointer structure. In this way, plants can grow out into a very complex morphological structure, the only boundary being the size of the computer's memory.

The current model is an accumulation of the knowledge on morphology of leaf growth of tillering *Gramineae* species in a vegetative phase. However, only temperature effects are included, and no effects of assimilates or nitrogen. The predictive performance of the model in the current status for predictions is still poor, as can be seen in Figures 5 and 6. There are two main reasons for lack of fit:

1. Variable LDR was measured some time after emergence (Chapter 2), but this value is used here from emergence onwards. It appears that the LDR in a very early stage is underestimated by the model. LDR is also a very sensitive variable for leaf area development (Table 2).
2. At higher temperatures, assimilate availability limits the outgrowth of tiller buds (Chapter 2), so source limitation must be included in the model in order to give better predictions.

Assimilate distribution can be introduced in the model as follows:

1. Calculate photosynthesis, respiration and potential remobilization of assimilates per leaf blade, assuming a certain spatial leaf distribution for photosynthesis calculations.
2. Distribute these assimilates depending on the sink strengths of the neighbouring organs.

Relationships between SLW of parent leaves and the SSU of daughter tillers (Chapter 5) can be introduced to simulate reduced tillering.

When the model is used for simulation of leaf area growth of other *Gramineae* plants, not only parameter values should be adapted, but also the equations need to be changed. For example, in maize LDS_{r_g} is not constant (Chapter 4). To simulate this, a new class should be defined: MAIZE FOLIAR LEAF, which is a subclass of FOLIAR LEAF. The special equation to calculate LDS_{r_g} in MAIZE FOLIAR LEAF overrules the standard equation of the superclass FOLIAR LEAF. However, the basic structure of the model remains the same.

Appendix I. Example of a transformation from a continuous to a discrete equation

Starting point is the following continuous equation:

$$LDS_{tiller} = 1 + (LDS_{tiller,Leaf0} - 1) e^{-RDR \times x} \quad (I.1)$$

where x is the Haun Stage of the main stem at which the tiller appears, assuming a maximum site filling of 0.69 (plant type 1 in Chapter 2). For this plant type, the prophyll in the axil of a leaf develops at the same time as the next leaf on the same tiller. Therefore, the following two equations can be derived (x is replaced by leaf because a leaf appears every Haun Stage unit):

$$LDS_{tiller,Leaf+1} - 1 = (LDS_{tiller,Leaf0} - 1) e^{-RDR \times (Leaf+1)} \quad (I.2)$$

$$LDS_{tiller,Leaf} - 1 = (LDS_{tiller,Leaf0} - 1) e^{-RDR \times Leaf} \quad (I.3)$$

where $Leaf+1$ is the next younger leaf on the same tiller or the prophyll on the daughter tiller. Equation I.2 can be rewritten as:

$$e^{-RDR \times Leaf} = \frac{(LDS_{tiller,Leaf0} - 1) e^{-RDR}}{LDS_{tiller,Leaf+1} - 1} \quad (I.4)$$

and equation I.3 as:

measurements on plant growth.

On the balance, the measurements appeared to be relatively easy to perform. The measurements were done on young plants, but can in principle be continued up to the flag leaf.

Quantifying morphological development

From the morphological measurements, three variables were derived that determine the leaf number dynamics: leaf appearance rate per tiller, specific site usage per tiller and Haun Stage-delay per tiller. To include leaf death, leaf lifespan per leaf should also be measured, but this was left beyond the scope of the study. These variables apply to plants where leaves appear sequentially on a tiller or a branch, when a leaf can have maximally one daughter tiller and tillers always have a parent leaf. These requirements hold for all *Gramineae* species and therefore these variables can be measured on all *Gramineae* species.

Four variables were derived that determine the leaf area growth per individual leaf: leaf elongation rate, leaf elongation duration, maximum leaf width and a leaf shape factor k . The method of measuring leaf elongation rate and leaf elongation duration was different from the usual method. To analyse individual leaf growth, Volenec and Nelson (1982) and Skinner and Simmons (1993) used a radial position transducer. With this method, sheath elongation and blade elongation can be measured separately. This technique was not used here, because the objective of my research was different, namely to analyse leaf area expansion on the whole plant. To avoid complexity in the analysis, blade and sheath elongation were not measured separately.

The total of maximally seven variables was used for the analysis of wheat and maize leaf area expansion, and can be applied to all *Gramineae* species in principle. They form a logical set of variables that relate area growth of individual leaves and leaf number dynamics to plant leaf area expansion. In this thesis, it was shown that effects of temperature, PPFD and plant density on leaf area expansion could be readily analysed with these seven variables. While these seven variables are, from a morphological point of view, logical, these variables also indicate the mechanisms of response of the plant to environmental factors. Effects of other environmental factors on leaf area expansion can also be analysed using these seven variables, and a better insight in the mechanisms that cause their effects on leaf area expansion is obtained. Below, the effects of environmental factors and leaf position on the seven variables are discussed.

Leaf appearance rate

In this thesis, leaf appearance rate of maize and wheat was higher at higher temperatures, higher PPFD levels and lower plant densities (Table 1). Effects of temperature are in line with many previous findings (McMaster and Wilhelm, 1995). The reduction in leaf appearance rate at low PPFD levels is also often found (e.g. Mitchell, 1953). There appeared to be a curvilinear relationship between PPFD and leaf appearance rate for both wheat (Chapter 2) and maize (Chapter 4), in accordance to model assumptions by Volk and Bugbee (1991). Although possible effects of red/far-red ratio can not be ruled out, the effects of plant density on leaf appearance rate are probably caused by reduced PPFD within the crop canopy (Chapter 5 and 6).

Table 1. Effects of temperature, PPFD, and plant density on leaf area variables. (+) indicates that the value of the plant variable is higher at higher values of the environmental factor, (-) indicates the value is lower, and (0) means that there were no or little effects.

Leaf area variable	Maize			Wheat		
	Temperature	PPFD	Plant density	Temperature	PPFD	Plant density
Leaf appearance rate	+	+	-	+	+	0/-
Specific site usage				-	+	-
Haun Stage-delay				0	0	0/+
Leaf elongation rate	+	0	0/-	+	0	0/-
Leaf elongation duration	-	-	+	-	-	0
Maximum leaf width	+/-	+	-	0	0	0/-
k	0	0	0	0	0	0

Haun Stage-delay

Haun Stage-delay was introduced in this thesis as a new plant variable, indicating the timing of tiller appearance relative to the Haun Stage of the parent tiller. Haun Stage-delay appeared to be almost unaffected by temperature, PPFD or plant density (Table 1). However, the effects of tiller bud position were quite large, with late-appearing tillers showing lower values of Haun Stage-delay (Chapter 2). While environmental effects were small, the change of Haun Stage-delay with tiller bud position is under genetic control. The research described in Chapter 2 has shown that this ontogenetic change in Haun-stage delay has large effects on leaf area growth per plant.

Specific site usage

In contrast to the timing of tiller appearance (reflected in the variable Haun Stage-delay), the specific site usage (i.e. the probability that a specific tiller will appear) was greatly influenced by environmental conditions. Specific site usage was clearly higher at lower temperatures, higher PPFD levels and lower plant densities (Table 1), in accordance with previous findings (e.g. Rickman *et al.* (1985); Cannell (1969)). In this thesis, there was evidence that these effects of temperature, PPFD and plant density were well related to assimilate levels locally in the plant. In Chapter 2, for spaced plants, specific site usage was better related to the rate of dry matter production of the parent tiller than to dry matter production of the whole plant. In Chapter 5, in experiments with different plant densities, more evidence was collected for this effect of local assimilates on specific site usage.

For tillering plants, specific site usage is the key variable of response to environmental conditions such as PPFD and plant density. The current findings indicate that young wheat plants can be viewed as a collection of rather individually responding units, instead of one plant unit responding to environmental factors based on whole plant variables.

Leaf elongation rate

For both maize and wheat, leaf elongation rate increased with higher temperatures, and decreased slightly with higher plant densities. This implies that leaf elongation rate is basically temperature driven, and only in extreme conditions there could be an effect of assimilate availability. This is in accordance with research done by Van Loo (1993) with perennial ryegrass plants. There was a clear effect of leaf position on the plant on leaf elongation rate (Chapters 3 and 4).

The combined effects of leaf position on a tiller and position of the tiller on the plant were very different from what was previously assumed. Amir and Sinclair (1991), McMaster *et al.* (1991) and

Van Loo (1993) assumed that there was no effect of tiller position on the plant on leaf area variables. This thesis has shown that there are very large effects of tiller type on leaf elongation rate, and leaf elongation rate was well related to summed leaf position (this is the sum of all the digits in the designation of the leaf). This effect of summed leaf position implies that characteristics such as the elongation rate of a leaf exerts an influence on the elongation rate of the next foliar leaf, regardless whether this next leaf is on the same tiller or is the first leaf on the daughter tiller.

Leaf elongation duration

In wheat, the leaf elongation duration was closely linked to the phyllochron (the inverse of leaf appearance rate), independent of temperature and slightly affected by PPFD (Chapter 3). This strengthens the hypothesis of Tesařová *et al.* (1992) and Skinner and Nelson (1995), that the development of consecutive leaves is synchronised. In maize there was no clear connection between the phyllochron and leaf elongation duration, and the number of growing leaves increases in early growth stages (Chapter 4). Apparently in maize there is no synchronisation or an unknown way of synchronisation, in contrast to wheat and small grasses.

Maximum leaf width

The effects of temperature, PPFD and plant density were small or absent for wheat and more pronounced in maize (Table 1). The effects in maize seem to be caused by effects of assimilate availability, reflected in a good relationship between maximum leaf width and specific leaf weight (Chapter 4). Because wheat has the flexibility to respond to lower assimilate levels with a reduction in specific site usage, an effect on maximum leaf width might be absent in wheat. Just as leaf elongation rate, maximum leaf width was well related to summed leaf position, in contrast to earlier assumptions. This strengthens the hypothesis that leaf characteristics such as elongation rate and maximum width of a leaf has effect on the next foliar leaf (on the same tiller or on the daughter tiller), possibly as a result of the changing size of the apex (discussed in Chapters 3 and 4).

Leaf shape variable: k

Effects of temperature, PPFD, plant density or leaf position on leaf shape variable k were small or absent (Table 1; Chapters 2, 3, 4, 5 and 6). In Chapter 4 the existing model of leaf shape by Sanderson *et al.* (1981) was adjusted. This leaf shape model describing the width depending on the

distance from the leaf tip requires the estimation of two variables. However, for studies on leaf area of the whole plant, one estimate of k together with a certain leaf shape assumption might be sufficient (e.g. leaf consists of a triangular and rectangular part).

Comparison between maize and wheat

In this thesis, both maize, as a representative of a non-tillering *Gramineae* plant, and wheat, as a representative of a tillering *Gramineae* plant were examined. The effects of temperature, PPFD and plant density on the seven leaf area variables are summarised in Table 1. It appears that most of the effects of temperature, PPFD, and plant density are surprisingly consistent for both maize and wheat. The effects of temperature and PPFD were only different for maximum leaf width, which was unaffected in wheat but increased at higher PPFD values and had an optimum value at a temperature of 18/13 - 23/18 °C in maize. Effects of plant density on leaf appearance rate, leaf elongation duration, and maximum leaf width were more pronounced in maize than in wheat. Table 1 shows that for constant conditions and spaced plants, there were almost no differences in effects of temperature or PPFD for maize or wheat. While plants were grown more or less free-standing, every new tiller in wheat is also a free-standing tiller, because competition between tillers for resources was avoided in the experiments. This could explain the lack of difference in effects of temperature and PPFD.

Simulating morphological development

In the simulation model, it was assumed that specific organ variables (e.g. maximum leaf width) are only influenced by its adjacent organs and by abiotic factors. Therefore, the model had two requirements:

1. simulated processes should be strictly on organ level;
2. per organ, variable values should only depend on the values of directly neighbouring organs and on abiotic factors.

Existing morphological models do not comply with these rules. In these models, leaf variables are assumed to depend on the position of the leaf on the tiller (e.g. Van Loo, 1993; McMaster *et al.*, 1991). The initially measured variables in this thesis did also not meet these two requirements. Therefore, new variables were derived from the measured variables. This resulted in a new set of variables, which can be classified into three types:

1. variables indicating initial values (e.g. maximum leaf width of Leaf 1);
2. variables indicating the rate of change compared to the value of the neighbouring organ (e.g. rate

of change in maximum leaf width);

3. variables with constant values (e.g. leaf shape variable k).

Variables of the first type depend mainly on genotype and on seed characteristics: they represent the initial status of the plant. Variables of the second type mainly depend on genotype and environmental conditions. Genotype and environmental conditions determine how fast a certain variable can change from one organ to the other. Variables of the third type only depend on genotype. In this way a set of variables was calculated which complied with the model requirements.

Flexibility of the simulation model

In Part III of this thesis it was claimed that the model was flexible and could be easily extended. To reinforce that claim, possible effects of plant density are introduced into the model (Appendix I) as an example. Some parameter values needed to be guesstimated in this extended model, because no data were available. The example in Appendix I shows that a lot of relationships needed to be included. Most of these relationships could be derived from an existing model (Goudriaan and Van Laar, 1994). The class structure was extended with seed (carbohydrate source), and sheaths and roots (carbohydrate sink). Also several methods and member variables were added in existing classes. However, the basic structure of the model (object orientation, the class structure, the pointer structure, all processes at organ level) was not violated and only specific assimilate features needed to be included.

Possible applications of the simulation model

The simulation model presented in Chapter 7 can be extended for specific applications. For plant breeding, the model can be a tool for analysis of variation in genotypes with respect to leaf area variables. Furthermore, the model can be useful in situations where simpler models do not give enough insight in the processes involved. When different plant species are competing for radiation (intercropping, weeds (Lotz *et al.*, 1996)), or in case of specific management practices (e.g. cutting of plants (Van Loo, 1993)), the simulation technique described in this thesis can be useful for studying the mechanisms that are involved. The model can also be applied to situations where environmental conditions vary during growth of the plants (e.g. fluctuating nitrogen supply (Vos *et al.*, 1996)). The way in which the model is extended depends upon the objective of the study, but the basic principles of the model (object orientation, the class structure, the pointer structure, all processes at organ level) should not be violated.

Conclusions

In this thesis, a method was developed for experimental analysis of leaf area variables of *Gramineae* species. This method was successfully applied to the study of the effects of leaf and tiller position, temperature, PPFD and plant density on a tillering *Gramineae* species, wheat, and a non-tillering *Gramineae* species, maize. Experiments under constant conditions (spaced plants, growth chambers) yielded basic relationships, which were useful in the analysis of environmental effects in field experiments.

A simulation model was created based upon the experimental variables and relationships. To obtain maximum flexibility in the model, object orientation was used and processes were strictly simulated at organ level. Because of time constraints, only a part of the knowledge was summarised in the model. However, it was shown that the model could be extended without violating the basic structure.

Appendix I. An example of an extension of the model: effects of plant density.

In this appendix, the existing simulation model (Chapter 7) is extended to include effects of plant density on leaf area growth in wheat. In this example, it is assumed that the effects of plant density are only caused by effects of assimilate availability on SSU (Chapter 5). For this purpose, the class structure needed to be extended with seed, sheath, and root (Fig. I.1).

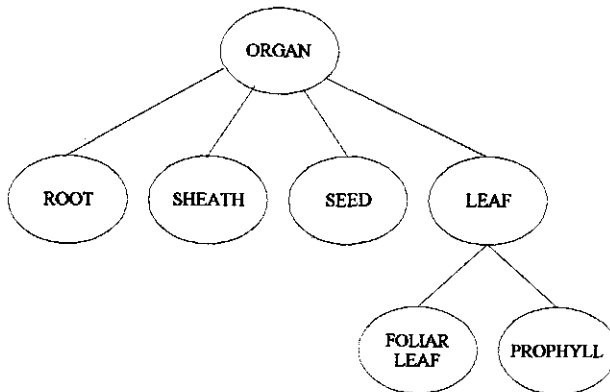


Figure I.1. The new hierarchial class structure in the extended model.

Effects of assimilates on SSU.

In Chapters 2 and 5 it was shown that SSU more likely depends on local assimilate availability than on assimilate availability of the whole plant. In the model it is assumed that the amount of assimilates of the organ from which bud the tiller appears (parent organ), determines the specific site usage (SSU). If the parent organ is a prophyll, the parent organ of that prophyll is considered. The parent organ can be a leaf blade or the seed. This results in the following equations:

$$\begin{aligned}SSU &= 0 \quad \text{if } A < A_{\min} \\SSU &= 1 \quad \text{if } A \geq A_{\min}\end{aligned}$$

with A the amount assimilates available (g) and A_{\min} the minimum amount of assimilates required for outgrowth of a tiller bud (g). A is calculated as follows:

$$A = (DM_{\text{parent organ}} - DM_{\min, \text{parent organ}}) * CF_{DM \text{ of parent organ} \rightarrow CH_2O}$$

where $DM_{\text{parent organ}}$ is the dry weight of the parent organ, $DM_{\min, \text{parent organ}}$ is the minimum dry weight of the parent organ (thus not available for conversion to CH_2O), and $CF_{DM \text{ of parent organ} \rightarrow CH_2O}$ the conversion factor from dry matter to CH_2O . This implies that all dry weight of a parent organ above a minimum can become available for depending organs.

If a leaf blade is the parent organ, it is assumed that there is a minimum SLW (SLW_{\min}), because a leaf has a minimum amount of structural material (Van Loo, 1993):

$$DM_{\min} = SLW_{\min} * \text{Area of leaf blade}$$

If the seed is the parent organ, it is assumed that a certain fraction of the seed can not be converted to CH_2O ($f_{\text{structural, seed}}$):

$$DM_{\min} = DM * (1 - f_{\text{structural, seed}})$$

To calculate dry weights of organs, assimilate formation, distribution, losses and conversion to dry matter must be calculated. This is described below.

Photosynthesis. Photosynthesis was calculated per leaf. Leaves were assumed to be vertically layered as shown in Fig. I.2. For every layer photosynthesis was calculated with three-point Gaussian integration and a negative exponential relation between absorbed PPFD and photosynthesis as was done in SUCROS for the whole crop canopy (Goudriaan and Van Laar, 1994). Incoming PPFD for a layer was equal to the PPFD that was transmitted through the layer above it.

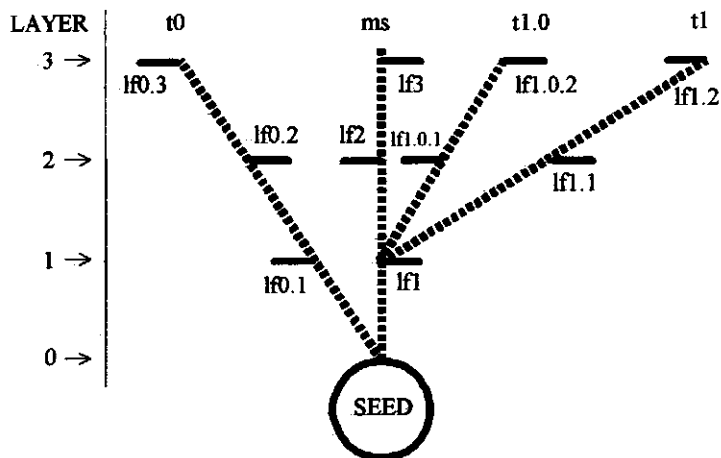


Figure I.2. The layering of leaves in the model.

Assimilate distribution. Assimilates are distributed as shown in Fig. I.3. This figure shows eight flows:

1. Leaf photosynthesis as was explained before, not applicable for seed.
2. A part of the dry matter in the leaf blade or seed can be redistributed (see above). The amount of assimilates that is potentially redistributed per time interval is simulated as:

$$\frac{dCH_2O}{dt} = A * f_{redistributed} * LDR$$

where $f_{redistributed}$ the fraction of A that is redistributed per leaf appearance interval ($leaf^{-1}$) and LDR is the leaf development rate.

The CH_2O is distributed between the dependent leaf, sheaths, roots and the leaf blade itself depending on the sink strengths of these organs:

$$\frac{dDM_{organ}}{dt} = \frac{dCH_2O(flow\ 1,2)}{dt} * \frac{SS_{organ}}{\sum SS_{all\ organs}} * CF_{CH_2O-DMOrgan}$$

where SS is the sink strength (no dimension).

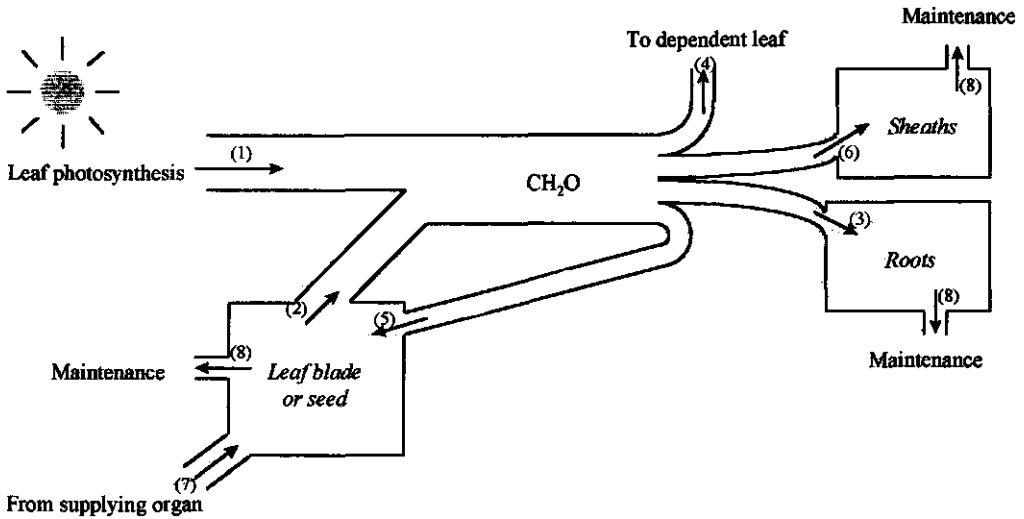


Figure I.3. Assimilate flows in the model. Details are explained in the text.

3. Because it is the relative sink strength that is important (strength of one sink compared to the other sink), one sink strength can be treated as a constant. The sink strength of the roots is taken as reference and therefore constant.
4. The sink strength of a leaf blade is modelled as:

$$SS_{Blade} = \frac{SLW_{max} - SLW}{SLW_{max} - SLW_{min}}$$

where SLW_{max} is the maximum SLW. This equation implies that the sink strength of blades is higher if the SLW is lower. The dependent leaf is defined as the most recently appeared leaf that is connected with the pointer structure to the considered leaf or seed without any other leaf blades in between. Dependent leaf of L1 can be L2, L1.1, L1.0.1 etc.

5. The sink strength of the leaf blade itself is calculated as for the dependent leaf (flow 4).
6. While sheath/blade ratios are rather constant, SS_{sheath} was calculated as:

$$SS_{sheaths} = f_{sheaths} * (SS_{blade} + SS_{depending\ blade})$$

where $f_{sheaths}$ is the sink strength of the sheaths relative to the leaf blades.

7. The flow from the supplying organ is comparable to the flow to the dependent leaf. The difference is that the considered leaf is the dependent leaf for the flow from the supplying organ.

8. Maintenance respiration was calculated as in SUCROS (Goudriaan and Van Laar, 1994).

Calibration and results

Estimates of parameter values are shown in Table I.1. The model was run for 35 days, starting at plant emergence, at plant densities of 1, 10, 100, or 1000 plants m⁻² under the following conditions:

Temperature	=	15	°C
Photosynthetic photon flux density	=	200	μmol m ⁻² s ⁻¹
Daylength	=	12	hours day ⁻¹
Seed weight	=	0.04	g DM

Table I.2 shows results of the tillering pattern, which is clearly influenced by plant density. The tillering trends are the same as reported in Chapter 5, only the coleoptile tiller (t0), appeared more frequently than measured in the experiments.

Table I.1. Calibration of parameters used in the simulation model. If no source is mentioned, the value was roughly estimated.

Parameter	Dimension	Estimated value	Source
A_{min}	g CH ₂ O	0.015	-
AMAX (maximum rate of photosynthesis)	g CH ₂ O m ⁻² h ⁻¹	2.73	Goudriaan and Van Laar (1994)
CF _{DM → CH₂O}		1.43	Goudriaan and Van Laar (1994)
CF _{CH₂O → DM}		0.70	1 / CF _{DM → CH₂O}
EFF (initial light use efficiency)	(g CH ₂ O m ⁻² h ⁻¹) / (μmol m ⁻² s ⁻¹)	0.00667	Goudriaan and Van Laar (1994)
$f_{redistributed}$		0.20	-
f_{sheath}		0.50	It is assumed that sink strength of sheaths is half the sink strength of the leaf blades
$f_{structural, seed}$		0.20	-
KDIF (extinction coefficient diffuse light)		0.70	Goudriaan and Van Laar (1994)
MAINTLVS (maintenance leaf blades)	g CH ₂ O g ⁻¹ DM day ⁻¹	0.030	Goudriaan and Van Laar (1994)
MAINTSH (maintenance sheaths)	g CH ₂ O g ⁻¹ DM day ⁻¹	0.015	Goudriaan and Van Laar (1994)
MAINTRT (maintenance roots)	g CH ₂ O g ⁻¹ DM day ⁻¹	0.015	Goudriaan and Van Laar (1994)
MAINTSD (maintenance seed)	g CH ₂ O g ⁻¹ DM day ⁻¹	0.015	Goudriaan and Van Laar (1994)
Q10 (maintenance respiration)		2.0	Goudriaan and Van Laar (1994)
REFTEMP (maintenance respiration)	°C	25	Goudriaan and Van Laar (1994)
SCV (scattering coefficient)		0.2	Goudriaan and Van Laar (1994)
SLW _{min}	g DM m ⁻²	20	-
SLW _{max}	g DM m ⁻²	50	-
SS _{root}		0.50	Set as reference value

Table I.2. Simulated appearance of tillers at four different plant densities.

Plant density (m ⁻²)	Primary tillers appeared	Secondary tillers appeared	Tertiary tillers appeared
1	t0, t1, t2, t3, t4	t0.0, t0.1, t0.2, t1.0, t1.1, t2.0, t3.0	t0.0.0
10	t0, t1, t2, t3, t4	t0.2, t1.0, t1.1, t2.0, t3.0	-
100	t0, t2, t3, t4	t2.0, t3.0	-
1000	t0	-	-

Summary

Leaf area expansion is an important factor for the understanding of plant and crop growth. In this thesis, leaf area expansion was analysed for two representatives of the *Gramineae* family: wheat and maize.

Existing assumptions of mechanisms of plant leaf area expansion can be divided into three groups:

1. plant leaf area expansion is an exponential function of accumulated degree days;
2. availability of assimilates determines plant leaf area expansion;
3. the morphology of the plant (e.g. number and individual sizes of leaves) is the basis for plant leaf area expansion.

Application of the third hypothesis gives the best insight in the mechanisms, but a general morphological framework is lacking and more and better experimental data are needed.

The objective of this research was to present a morphological analysis of the mechanisms of leaf area expansion in *Gramineae*. The approach for the analysis was the following:

1. determine general morphological variables for leaf area expansion of *Gramineae*;
2. in experiments, compare two *Gramineae* species that clearly differ in their morphology (wheat: tillering plant; maize: non- or rarely-tillering plant);
3. perform the first basic experiments at constant environmental conditions (growth chambers, spaced plants), to avoid complexity in the basic analysis;
4. analyse the effects of some important environmental conditions (temperature, photosynthetic photon flux density (PPFD), and plant density) on the morphological variables;
5. summarise the knowledge in a simulation model, which should be easily extendable to other species and environmental conditions.

In Part I the morphological model was introduced. This model consisted of seven variables:

1. leaf appearance rate per tiller;
2. specific site usage, which is the fraction of buds that ultimately develop into a visible tiller at a specific site;
3. HS-delay, which is the difference in Haun Stage (HS) between the parent tiller and the daughter tiller above the point where the daughter tiller appears;
4. leaf elongation rate;
5. leaf elongation duration;
6. maximum leaf width;
7. a leaf shape factor: k .

The effects of temperature and photosynthetic photon flux density (PPFD) on these seven variables

were analysed on two contrasting *Gramineae* species: wheat and maize. These experiments were carried out in growth chambers at daily mean temperatures of 10.5, 15.5, 20.5, and 25.5 (maize only) °C and at PPFD values of approximately 110, 190, and 280 $\mu\text{mol m}^{-2} \text{s}^{-1}$.

For wheat, effects of temperature and PPFD on leaf appearance rate were well described by equations already reported in literature. Specific site usage was higher at lower temperatures and higher PPFD values and was related to tiller position. It was proposed that these effects on specific site usage reflect differences in local availability of assimilates for tiller appearance. HS-delay of a tiller was lower if the tiller appearance, calculated with a maximum site filling of 0.69, was later and was only slightly affected by PPFD or temperature. Effects of leaf position and tiller type on maximum leaf width and leaf elongation rate could be explained by a new assumption, that maximum leaf width, and leaf elongation rate, of a leaf depend on the values for the previous foliar leaf on the same tiller, or on the parent tiller. Leaf elongation rate increased linearly with temperature and was not affected by PPFD, whereas maximum leaf width was not influenced by temperature or PPFD. Leaf elongation duration was closely related to phyllochron (i.e. the inverse of leaf appearance rate) expressed in days, although this relation was slightly modified by PPFD. Equations formulated for each leaf area variable accounted for 90% of the variation in leaf area between different leaf types, temperatures and PPFD values.

In maize, tillering was absent, and therefore no effects on specific site usage or HS-delay were measured. At 10.5 °C, a high proportion of the plants died due to prolonged exposure to cold stress. Both high temperatures and high PPFD values increased leaf appearance rate. Maximum leaf width was highest at intermediate temperatures (20.5 °C) and high PPFD values, and was strongly related to specific leaf weight ($R^2_{\text{adj}} = 0.88$). At higher temperatures leaf elongation rate was greater and leaf elongation duration was lower, resulting in a maximum final leaf length at 20.5 °C. At lower PPFD values leaves were slightly longer, caused by a prolonged leaf elongation. Leaf shape was described with new functions; the functions for Leaves 1 and 2 differed from the one for higher positioned leaves.

In Part II, the effects of plant density on the seven variables which were derived in Part I were analysed for spring wheat and maize at ample supplies of water and nutrients. Also, it was analysed which environmental factor (PPFD, red/far-red (R/FR) ratio or temperature) was responsible for the plant density effects.

For spring wheat, plants were grown in different plant densities (0 - 494 m^{-2}) in the field and in growth chambers. Ratios of R/FR were manipulated by using different combinations of lamps (growth chamber) or adding red light to the base of the plant with diodes (experiments outdoors). At early growth stages, leaf properties and tillering were not affected by plant density. However, specific site usage of later appearing tillers was reduced at higher plant densities. For late tillers, leaf appearance rate was slower and HS-delay was longer at higher plant densities. Furthermore,

maximum leaf width and full-grown leaf length of high positioned leaves on the main stem were significantly smaller. Plant density effects occurred at lower leaf and tiller number the higher the plant density. A dynamic model was used to evaluate the relative importance of effects of plant density on the seven variables determining leaf area growth per plant. The model analysis showed that the effect of plant density on SSU was by far the strongest determinant of density-dependent changes in leaf area per plant during early growth of wheat. The effects of plant density on specific site usage could not be fully explained by temperature differences, plant growth rate or R/FR effects. The variable specific site usage appeared to be well related to the specific leaf weight of the parent leaf (i.e. the leaf from which the tiller is appearing) at the time of tiller appearance, independent of R/FR ratio. While specific leaf weight of a single leaf depends on local assimilate supply, it was proposed that specific site usage is regulated by local assimilate supply.

For maize, plants at a wide range of plant densities ($0 - 123 \text{ m}^{-2}$) were grown in the field for two years. Half of the plots were shaded (50 % transmittance). Leaf appearance rates were lower at higher plant densities and under shade. These effects were not caused by the small differences in canopy temperature observed, but were closely associated with reductions in the growth rate per individual plant. Leaf length was higher under shade than with full light; effects of plant density on leaf length were inconsistent over the two years, associated with inconsistent effects on leaf elongation rate. Leaf elongation duration was longer at higher plant densities in both experimental years. The crop-ecological analysis showed that plant density affected leaf area expansion of maize mainly through effects on leaf appearance rates, and that these effects were closely related to density effects on plant growth rate per leaf appearance interval.

In Part III, a simulation model was developed for wheat based upon the morphological framework presented in Part I. The principles of object orientation were used to obtain maximum flexibility, and the application to modelling foliar development of plants is shown. Plant related processes were strictly simulated at organ level and growth was assumed to be sink-limited. All plant processes needed to run the model could be converted to equations and data on organ level, using difference equations for relationships within the plant. The simulations yielded patterns of leaf area expansion that depended on the position of the leaf within the plant. The relative growth rate for leaf area per plant decreased with time. Experimental data were not predicted well, because source limitation was not included in the model and the assumption of a constant leaf appearance rate was not in agreement with reality.

In the general discussion, the morphological measurement techniques were evaluated and the usefulness of the seven variables that determine leaf area expansion were discussed. Furthermore, the effects of leaf and tiller position, temperature, PPFD and plant density on the seven variables and the differences between wheat and maize were analysed. In maize, at higher temperatures leaf

appearance rate and leaf elongation rate were higher, and leaf elongation duration was shorter. At higher PPFD values, leaf appearance rate and maximum leaf width were higher and leaf elongation rate was lower. In wheat, the effects of temperature and PPFD were qualitatively equal to those in maize, except there was no effect of PPFD on maximum leaf width. In wheat, specific site usage was higher at lower lower temperatures and higher PPFD values. The morphological framework can be used for experimental analysis of leaf area growth, revealing mechanisms regulating leaf area growth of plants.

It was shown that the simulation model was extendable with an example, that included plant density effects in the simulation model. The simulation model is flexible and can be easily extended for different environmental conditions and plant species.

Samenvatting

Bladoppervlakteuitbreiding is een belangrijk proces voor de analyse van plant- en gewasgroei. In dit proefschrift wordt de bladoppervlakteuitbreiding geanalyseerd voor twee soorten van de *Gramineae* familie: tarwe en maïs.

Bestaande veronderstellingen over de mechanismen van bladoppervlakteuitbreiding van een plant vallen in drie categorieën:

1. bladoppervlakteuitbreiding van een plant is een exponentiële functie van de temperatuursom;
2. de beschikbaarheid van assimilaten bepaalt de bladoppervlakteuitbreiding van een plant;
3. de bladoppervlakteuitbreiding is gebaseerd op de onderliggende morfologische processen, zoals de aantalsdynamiek van bladeren en vertakkingen (spruiten).

De derde hypothese geeft het meeste inzicht in de mechanismen van bladoppervlakteuitbreiding, maar is nog onvoldoende uitgewerkt.

Het doel van dit onderzoek was het kwantitatief analyseren van de mechanismen van bladoppervlakteuitbreiding van *Gramineae* soorten op basis van de morfologie. Voor de analyse werd de volgende benadering gekozen:

1. bepaal algemene morfologische variabelen voor bladoppervlakteuitbreiding van *Gramineae*;
2. vergelijk twee *Gramineae* soorten die duidelijk verschillen ten aanzien van hun morfologie (tarwe: uitstoelende plant; maïs: niet of weinig uitstoelende plant) in experimenten;
3. voer de basis-experimenten uit onder constante omgevingsfactoren (fytotroncellen, vrijstaande planten) om complexiteit te voorkomen tijdens de basis-analyses;
4. analyseer de effecten van enige belangrijke omgevingsfactoren (temperatuur, lichtsterkte en plantdichtheid) op de morfologische variabelen;
5. vat de kennis samen in een simulatiemodel, dat eenvoudig uit te breiden is naar andere soorten of omgevingsfactoren.

In deel I werd het morfologische model geïntroduceerd. Dit model bestond uit zeven variabelen:

1. bladverschijningssnelheid per spruit;
2. specifieke knopbenutting; dit is het gedeelte van de okselknoppen dat uitgroeit tot een zichtbare spruit op een specifieke plek in de plant;
3. HS-delay, dit is het verschil in Haun Stage (HS) tussen de ouder-spruit en de dochter-spruit boven het punt waar de dochter-spruit tevoorschijn komt;
4. bladstrekkingssnelheid;
5. bladstrekkingduur;
6. maximale bladbreedte;

7. een bladvormvariabele: k.

De effecten van temperatuur en lichtsterkte op deze zeven variabelen werden geanalyseerd in twee contrasterende *Gramineae* soorten: tarwe en maïs. Deze experimenten werden uitgevoerd in fytoncellen met gemiddelde etmaaltemperaturen van 10.5, 15.5, 20.5 en 25.5 (alleen voor maïs) °C en lichtsterktes van ongeveer 110, 190 en 280 $\mu\text{mol m}^{-2} \text{s}^{-1}$.

In tarwe werden de effecten van temperatuur en lichtsterkte op bladverschijningsnelheid goed beschreven met vergelijkingen uit bestaande literatuur. Specifieke knopbenutting was hoger bij lagere temperaturen en hogere lichtsterktes, en was gerelateerd aan de positie van de spruit aan de plant. Deze effecten op specifieke knopbenutting kunnen samenhangen met de lokale beschikbaarheid van assimilaten voor spruitverschijning. HS-delay van een spruit was lager wanneer de verwachte verschijning van de spruit later was en werd weinig beïnvloed door lichtsterkte en temperatuur. Bladpositie- en spruittypen-effecten op maximale bladbreedte en bladstrekkingsnelheid konden worden verklaard door een nieuwe hypothese. Deze hypothese luidde dat maximale breedte en strekkingssnelheid van een blad afhangen van de waardes van het vorige blad op dezelfde spruit of op de ouder-spruit. De bladstrekkingsnelheid nam lineair toe met de temperatuur en werd niet beïnvloed door lichtsterkte. De maximale bladbreedte werd door lichtsterkte noch temperatuur beïnvloed. De bladstrekkingsduur was sterk gerelateerd aan het bladverschijningsinterval, uitgedrukt in dagen. Deze relatie werd lichtelijk beïnvloed door lichtsterkte. De vergelijkingen die geformuleerd werden voor elke bladoppervlaktevariabele verklaarden 90 % van de variatie in bladoppervlakte tussen de verschillende bladtypes, temperaturen en lichtsterktes.

Omdat maïs niet uitstoelt, konden effecten op specifieke knopbenutting en HS-delay niet worden geanalyseerd voor maïs. Bij een temperatuur van 10.5 °C stierf een groot percentage van de planten door de langdurige blootstelling aan koudstress. Hoge temperaturen en hoge lichtsterktes versnelden de bladverschijningsnelheid. De maximale bladbreedte was het grootst bij gemiddelde temperaturen en hoge lichtsterktes en was sterk gerelateerd aan het specifiek bladgewicht ($R^2_{\text{adj}} = 0.88$). De bladstrekkingsnelheid was hoger en de bladstrekkingsduur was korter bij hogere temperaturen. Het bleek dat de langste bladeren werden gevormd bij een temperatuur van 20.5 °C. Bij lagere lichtsterktes werden de bladeren iets langer, als gevolg van een langere bladstrekkingsduur. De bladvorm werd beschreven met een nieuwe vergelijking en was verschillend voor de eerste twee bladeren van een plant en de hoger gepositioneerde bladeren.

In deel II werden de effecten van plantdichtheid op de zeven variabelen, die bepaald werden in deel I, geanalyseerd voor zomertarwe en maïs bij een voldoende water- en nutriëntenvoorziening. Ook werd geanalyseerd welke omgevingsfactor (lichtsterkte, rood/verrood (R/VR) verhouding of temperatuur) de plantdichtheidseffecten veroorzaakte.

Zomertarweplanten werden opgekweekt bij verschillende plantdichtheden (0 - 494 m^{-2}) in veld- en fytonproeven. De R/VR-verhouding werd beïnvloed door het gebruik van verschillende

lampcombinaties (fytotron) of door het toevoegen van rood licht aan de plantbasis door middel van diodes (veldproeven). Blad- en spruitvariabelen werden niet beïnvloed tijdens de allereerste begingroei. De specifieke knopbenutting van spruiten die later verschenen, werd gereduceerd bij een hogere plantdichtheid. Ook de maximale breedte en de lengte van volgroeide bladeren die hoger gepositioneerd waren in het gewas waren significant kleiner. De effecten van plantdichtheid werden zichtbaar bij lagere blad- en spruitposities naar mate de plantdichtheid hoger was. Om het relatieve belang van de zeven bladoppervlaktevariabelen met betrekking tot effecten van plantdichtheid op bladoppervlakte per plant te bepalen werd een dynamisch model gebruikt. Deze modelanalyse toonde aan dat de effecten van plantdichtheid op de specifieke knopbenutting duidelijk het belangrijkste waren om de verschillen in bladoppervlakte tussen de verschillende plantdichtheden te verklaren. Deze effecten van plantdichtheid op de specifieke knopbenutting konden niet volledig worden verklaard door temperatuur, groeisnelheid van de plant of R/VR-verhouding. De specifieke knopbenutting bleek wel goed gerelateerd te zijn aan het specifieke bladgewicht van het ouderblad (dit is het blad vanuit wiens okselknop de spruit ontstaat) op het moment van spruitverschijning en onafhankelijk van de R/VR-verhouding. Omdat het specifieke gewicht van een blad afhangt van de lokale assimilatenvoorziening, werd verondersteld dat de specifieke knopbenutting gereguleerd wordt door de lokale assimilatenvoorziening.

Maisplanten werden opgekweekt bij verschillende plantdichtheden ($0 - 123 \text{ m}^{-2}$) in veldproeven in twee jaren. De helft van de veldjes werd 50 % beschaduwd. De bladverschijningssnelheid was lager bij hogere plantdichtheden en bij beschaduwing. Deze effecten werden niet veroorzaakt door temperatuurverschillen, maar waren sterk gerelateerd aan de reductie in groeisnelheid van de plant. Bladeren werden langer bij beschaduwing; effecten van plantdichtheid op bladlengte waren echter inconsistent over de twee jaren, wat gerelateerd was aan de inconsistente effecten op bladstrekkingssnelheid. Bladstrekkingduur was langer bij hogere plantdichtheden in beide jaren. De gewasecologische analyse toonde aan dat plantdichtheid de bladoppervlaktetoename in mais voornamelijk beïnvloedde door effecten op bladverschijningssnelheid. Deze effecten op bladverschijningssnelheid waren sterk gerelateerd aan de groeisnelheid van de plant per bladverschijningsinterval.

In deel III werd een simulatiemodel ontwikkeld op basis van het morfologische raamwerk van deel I. De principes van object-oriëntatie werden gebruikt om een maximale flexibiliteit van het model te bewerkstelligen. Plantprocessen werden strikt gesimuleerd op het niveau van het orgaan. Verder werd verondersteld dat de groei niet afhankelijk was van externe bronnen als lichtsterkte, water of nutriënten. Alle plantprocessen die benodigd waren werden geconverteerd naar vergelijkingen op het niveau van het orgaan door gebruik te maken van differentievergelijkingen. De simulaties lieten patronen van bladoppervlakteuitbreiding zien die afhingen van de positie van het blad aan de plant. De relatieve groeisnelheid van bladoppervlakte nam voorts af tijdens de groei. Experimentele

gegevens werden niet goed voorspeld door het model, omdat er geen effecten van assimilaten waren ingebouwd en omdat bladverschijningsnelheid in werkelijkheid niet constant is, zoals wel werd verondersteld in het model.

In de algemene discussie werden de morfologische metingen geëvalueerd en het nut van de zeven bladoppervlaktetoenamevariabelen bediscussieerd. Verder werden ook de effecten van blad- en spruitpositie, temperatuur, lichtsterkte en plantdichtheid op de zeven variabelen, en de verschillen tussen tarwe en maïs geanalyseerd. Bij een hogere temperatuur waren in maïs de bladverschijningsnelheid en de bladstrekkingssnelheid hoger en de bladstrekkingduur korter. Bij grotere lichtsterktes waren de bladverschijningsnelheid en de maximale bladbreedte groter, maar de bladstrekkingssnelheid was lager. In tarwe waren deze effecten van temperatuur en lichtsterkte kwalitatief gelijk aan die van maïs, alleen was er geen effect van lichtsterkte op maximale bladbreedte. In tarwe was verder de specifieke knopbenutting groter bij lagere temperaturen en hogere lichtsterktes. Dit morfologische raamwerk kan dus worden gebruikt voor proefondervindelijke analyse van bladoppervlakteuitbreiding, waarbij inzicht wordt verkregen in de mechanismes voor bladoppervlakteuitbreiding van een plant.

Het simulatiemodel dat gebaseerd was op object oriëntatie en waarin alle processen op het nivo van het orgaan gemodelleerd werden, was flexibel. Deze flexibiliteit werd succesvol getest door het uitbreiden van het model met plantdichtheidseffecten.

References

- Abbe EC, Randolph LF, Einset J. 1941.** The developmental relationship between shoot apex and growth pattern of leaf blade in diploid maize. *American Journal of Botany* **28**: 778-784.
- Allard G, Nelson CJ, Pallardy SG. 1991.** Shade effects on growth of tall fescue: I. Leaf anatomy and dry matter partitioning. *Crop Science* **31**: 163-167.
- Amir J, Sinclair TR. 1991.** A model of temperature and solar-radiation effects on spring wheat growth and yield. *Field Crops Research* **28**: 47-58.
- Barnes C, Bugbee B. 1991.** Morphological responses of wheat to changes in phytochrome photoequilibrium. *Plant Physiology* **97**: 359-365.
- Boone MYL, Rickman RW, Whisler FD. 1990.** Leaf appearance rates of two winter wheat cultivars under high carbon dioxide conditions. *Agronomy Journal* **82**: 718-724.
- Borrill M. 1959.** Inflorescence initiation and leaf size in some Gramineae. *Annals of Botany* **23**: 217-227.
- Borrill M. 1961.** The developmental anatomy of leaves in *Lolium temulentum*. *Annals of Botany* **25**: 1-11.
- Cannell RQ. 1969.** The tillering pattern in barley varieties. I. Production, survival and contribution to yield by component tillers. *Journal of Agricultural Science, Cambridge* **72**: 405-422.
- Cao J, Hesketh JD, Zur B, Reid JF. 1988.** Leaf area development in maize and soybean plants. *Biotronics* **17**: 9-15.
- Cao W, Moss DN. 1989.** Temperature effect on leaf emergence and phyllochron in wheat and barley. *Crop Science* **29**: 1018-1021.
- Carberry PS, Muchow RC, Hammer GL. 1993.** Modelling genotypic and environmental control of leaf area dynamics in grain sorghum. II. Individual leaf level. *Field Crops Research* **33**: 311-328.
- Casal JJ, Deregibus VA, Sanchez RA. 1985.** Variations in tiller dynamics and morphology in *Lolium multiflorum* Lam. Vegetative and reproductive plants as affected by differences in red/far-red irradiation. *Annals of Botany* **56**: 553-559.
- Casal JJ, Sanchez RA, Deregibus VA. 1986.** The effect of plant density on tillering: the involvement of R/FR ratio and the proportion of radiation intercepted per plant. *Environmental and Experimental Botany* **26**: 365-371.
- Casal JJ, Sanchez RA, Deregibus VA. 1987.** Tillering responses of *Lolium multiflorum* plants to changes of red/far-red ratio typical of sparse canopies. *Journal of Experimental Botany* **38**: 1432-1439.

- Casal JJ, Sanchez RA, Gibson D. 1990.** The significance of changes in the red/far-red ratio, associated with either neighbour plants or twilight, for tillering in *Lolium multiflorum* Lam. *New Phytologist* **116**: 565-572.
- Charles-Edwards DA, Beech DF. 1984.** On the ordered development of plants. 3. Branching by the grain legume *Cyamopsis tetragonoloba* (Guar). *Annals of Botany* **54**: 673-679.
- Cook MG, Evans LT. 1978.** Effect of relative size and distance of competing sinks on the distribution of photosynthetic assimilates in wheat. *Australian Journal of Plant Physiology* **5**: 495-509.
- Dale JE. 1988.** The control of leaf expansion. *Annual Review of Plant Physiology and Plant Molecular Biology* **39**: 267-295.
- Davies A. 1965.** Carbohydrate levels and regrowth in perennial ryegrass. *Journal of Agricultural Science, Cambridge* **65**: 139-144.
- Davies A. 1974.** Leaf tissue remaining after cutting and regrowth in perennial ryegrass. *Journal of Agricultural Science, Cambridge* **82**: 165-172.
- Deregibus VA, Sanchez RA, Casal JJ. 1983.** Effects of light quality on tiller production in *Lolium* spp. *Plant Physiology* **72**: 900-902.
- De Wit CT. 1960.** *On Competition*. Verslagen van Landbouwkundige Onderzoekingen No. 66.8. Pudoc, Wageningen.
- Dwyer LM, Stewart DW. 1986.** Leaf area development in field-grown maize. *Agronomy Journal* **78**: 334-343.
- Eames AJ. 1961.** *Morphology of the angiosperms*. McGraw-Hill Book Company, New York, USA.
- Edelstein-Keshet L. 1988.** *Mathematical models in biology*. New York: Random House.
- Ellis RH, Summerfield RJ, Edmeades GO, Roberts EH. 1992.** Photoperiod, temperature, and the interval from sowing to tassel initiation in diverse cultivars in maize. *Crop Science* **32**: 1225-1232.
- Forde BJ. 1966.** Effect of various environments on the anatomy and growth of perennial ryegrass and cocksfoot. 1. Leaf growth. *New Zealand Journal of Botany* **4**: 455-468.
- Friend DJC, Helson VA, Fisher JE. 1962.** Leaf growth in marquis wheat, as regulated by temperature, light intensity, and daylength. *Canadian Journal of Botany* **40**: 1299-1311.
- Friend DJC, Pomeroy ME. 1970.** Changes in cell size and number associated with the effects of light intensity and temperature on the leaf morphology of wheat. *Canadian Journal of Botany* **48**: 85-90.
- Gallagher JN. 1979.** Field studies of cereal leaf growth I. Initiation and expansion in relation to temperature and ontogeny. *Journal of Experimental Botany* **30**: 625-636.
- Gmelig Meyling HD. 1973.** Effect of light intensity, temperature and daylength on the rate of leaf appearance of maize. *Netherlands Journal of Agricultural Science* **21**: 68-76.

- Goudriaan J, Van Laar HH. 1994.** *Modelling potential crop growth processes*. Dordrecht: Kluwer Academic Publishers.
- Grant RF. 1989.** Simulation of maize phenology. *Agronomy Journal* **81**: 451-457.
- Grant RF, Hesketh JD. 1992.** Canopy structure of maize (*Zea mays* L.) at different populations: simulation and experimental verification. *Biotronics* **21**: 11-24.
- Guiamet JJ, Willemoes JG, Montaldi ER. 1989.** Modulation of progressive leaf senescence by the red:far-red ratio of incident light. *Botanical Gazette* **150**: 148-151.
- Harper JL. 1989.** Canopies as populations. In: Russell G, Marshall B, Jarvis DG, eds. *Plant canopies: their growth, form and function*. Cambridge: Cambridge University Press, 105-128.
- Haun JR. 1973.** Visual quantification of wheat development. *Agronomy Journal* **65**: 116-119.
- Hay RKM, Tunnicliffe Wilson G. 1982.** Leaf appearance and extension in field-grown winter wheat plants: the importance of soil temperature during vegetative growth. *Journal of Agricultural Science, Cambridge* **99**: 403-410.
- Hay RKM, Walker AJ. 1989.** *Introduction to the physiology of crop yield*. Longman Group UK Limited, Harlow, UK.
- Hesketh JD, Warrington IJ. 1989.** Corn growth response to temperature: rate and duration of leaf emergence. *Agronomy Journal* **81**: 696-701.
- Ito M, Nakayama S, Tsubota Y. 1987.** Morphological studies on tillering habits in temperate herbage grasses. V. Patterns of tillering and tiller bud development of some grasses under contrasting light regimes. *Journal of Japanese Society of Grassland Science* **33**: 163-174.
- Jewiss OR. 1966.** Morphological and physiological aspects of growth of grasses during the vegetative phase. In: F.L. Milthorpe and J.D. Ivins (Eds.), *The growth of cereals and grasses*. Butterworths, London, UK, 39-54.
- Kalt-Torres W, Huber SC. 1987.** Diurnal changes in maize leaf photosynthesis. III. Leaf elongation rate in relation to carbohydrates and activities of sucrose metabolizing enzymes in elongating leaf tissue. *Plant Physiology* **83**: 294-298.
- Kasperbauer MJ, Karlen DL. 1986.** Light-mediated bioregulation of tillering and photosynthate partitioning in wheat. *Physiologia Plantarum* **66**: 159-163.
- Keating BA, Wafula BM. 1992.** Modelling the fully expanded leaf area of maize leaves. *Field Crops Research* **29**: 163-176.
- Kemp DR, Blacklow WM. 1980.** Diurnal extension rates of wheat leaves in relation to temperatures and carbohydrate concentrations of the extension zone. *Journal of Experimental Botany* **31**: 821-828.
- Kemp DR. 1981a.** The growth rate of wheat leaves in relation to the extension zone sugar concentration manipulated by shading. *Journal of Experimental Botany* **32**: 141-150.

- Kemp DR. 1981b.** Comparison of growth rates and sugar and protein concentrations of the extension zone of main shoot and tiller leaves of wheat. *Journal of Experimental Botany* **32**: 151-158.
- Kirby EJM. 1973.** The control of leaf and ear size in barley. *Journal of Experimental Botany* **24**: 567-578.
- Kirby EJM, Appleyard M, Fellowes G. 1985.** Leaf emergence and tillering in barley and wheat. *Agronomie* **5**: 193-200.
- Klepper B, Rickman RW, Peterson CM. 1982.** Quantitative characterization of vegetative development in small cereal grains. *Agronomy Journal* **74**: 789-792.
- Klepper B, Rickman RW, Belford RK. 1983.** Leaf and tiller identification on wheat plants. *Crop Science* **23**: 1002-1004.
- Kropff MJ. 1993.** Mechanisms of competition for light. In: Kropff MJ and Van Laar HH, eds. *Modelling crop-weed interactions*. Wallingford: CAB international, 33-62.
- Lawlor DW. 1987.** *Photosynthesis: metabolism, control and physiology*. Longman Scientific and Technical Publishers, New York..
- Lotz LAP, Christensen S, Cloutier D, Fernandez Quintanilla C, Légère A, Lemieux C, Lutman PJW, Pardo Iglesias A, Salonen J, Sattin M, Stigliani L, Tei F. 1996.** Prediction of the competitive effects of weeds on crop yield based on relative leaf area of weeds. *Weed Research* **36**: 93-101.
- Masle J. 1985.** Competition among tillers in winter wheat: consequences for growth and development of the crop. *NATO advanced study institutes series. Series A. Life sciences* **86**: 33-54.
- Masle-Meynard J, Sebillotte, M. 1981.** Etude de l'hétérogénéité d'un peuplement de blé d'hiver. II. Origine des différentes catégories d'individus du peuplement; éléments de description de sa structure. *Agronomie* **1**: 217-224.
- McCullagh P, Nelder JA. 1989.** *Generalized linear models*. London: Chapman and Hall.
- McMaster GS, Klepper B, Rickman RW, Wilhelm WW, Willis WO. 1991.** Simulation of shoot vegetative development and growth of unstressed winter wheat. *Ecological Modelling* **53**: 189-204.
- McMaster GS, Wilhelm WW. 1995.** Accuracy of equations predicting the phyllochron of wheat. *Crop Science* **35**: 30-36.
- Mitchell KJ. 1953.** Influence of light and temperature on the growth of ryegrass (*Lolium* spp.) I. Pattern of vegetative development. *Physiologia Plantarum* **6**: 21-46.
- Montgomery DC, Peck EA. 1982.** *Introduction to linear regression analysis*. Wiley, New York, USA.
- Munier-Jolain N, Ney B, Duthion C. 1996.** Analysis of branching in spring-sown white lupins (*Lupinus albus* L.): the significance of the number of axillary buds. *Annals of Botany* **77**: 123-131.

- Neuteboom JH, Lantinga EA. 1989.** Tillering potential and relationship between leaf and tiller production in perennial ryegrass. *Annals of Botany* **63**: 265-279.
- Peacock JM. 1975.** Temperature and leaf growth in *Lolium perenne*. I. The thermal microclimate: its measurement and relation to crop growth. *Journal of Applied Ecology* **12**: 99-114.
- Peterson, CM, Klepper B, Rickman RW. 1982.** Tiller development at the coleoptilar node in winter wheat. *Agronomy Journal* **74**: 781-784.
- Pieters GA. 1986.** Dimensions of the growing shoot and the absolute growth rate of a poplar shoot. *Tree Physiology* **2**: 283-288.
- Pieters GA, Van den Noort ME. 1988.** Effect of irradiance and plant age on the dimensions of the growing shoot of poplar. *Physiologia Plantarum* **74**: 467-472.
- Pieters GA, Van den Noort ME. 1990.** Adaption of growth rate of *Populus euramericana* to light and nitrate proceeds via the vascular system. In: Van Beusichem ML, Ed. *Plant nutrition - Physiology and applications*. Dordrecht: Kluwer Academic Publishers, 61-67.
- Porter JR. 1984.** A model of canopy development in winter wheat. *Journal of Agricultural Science, Cambridge* **102**: 383-392.
- Porter JR. 1985.** Approaches to modelling canopy development in wheat. *NATO Advanced Study Institutes Series. Series A.: Life Sciences (USA)*: 69-81.
- Rawson HM, Hofstra G. 1969.** Translocation and remobilization of ^{14}C assimilated at different stages by each leaf of the wheat plant. *Australian Journal of Biological Sciences* **22**: 321-331.
- Reid JF, Zur B, Hesketh JD. 1990.** The dynamics of a maize canopy development. 2. Leaf area growth. *Biotronics* **19**: 99-107.
- Rickman RW, Klepper B, Peterson CM. 1985.** Wheat seedling growth and developmental response to incident photosynthetically active radiation. *Agronomy Journal* **77**: 283-287.
- Robson MJ. 1973.** The growth and development of simulated swards of perennial ryegrass. I. Leaf growth and dry weight change as related to the ceiling yield of a seedling sward. *Annals of Botany* **37**: 487-500.
- Robson MJ, Ryle GJA, Woledge J. 1988.** The grass plant - its form and function. In: M.B. Jones and A. Lazenby (Eds.), *The grass crop. The physiological basis of production*. Chapman and Hall, London, UK, 25-83.
- Sambo EY. 1983.** Leaf extension rate in temperate pasture grasses in relation to assimilate pool in the extension zone. *Journal of Experimental Botany* **34**: 1281-1290.
- Sanderson JB, Daynard TB, Tollenaar M. 1981.** A mathematical model of the shape of corn leaves. *Canadian Journal of Plant Science* **61**: 1009-1011.
- Schnyder H, Nelson, CJ. 1989.** Growth rates and assimilate partitioning in the elongation zone of tall fescue leaf blades at high and low irradiance. *Plant Physiology* **90**: 1201-1206.

- Scholte K. 1987.** Relationship between cropping frequency, root rot and yield of silage maize on sandy soils. *Netherlands Journal of Agricultural Science* **35**: 473-486.
- Skinner RH, Nelson CJ. 1992.** Estimation of potential tiller production and site usage during tall fescue canopy development. *Annals of Botany* **70**: 493-499.
- Skinner RH, Nelson CJ. 1994.** Effects of tiller trimming on phyllochron and tillering regulation during tall fescue development. *Crop Science* **34**: 1267-1273.
- Skinner RH, Nelson CJ. 1995.** Elongation of the grass leaf and its relationship to the phyllochron. *Crop Science* **35**: 4-10.
- Skinner RH, Simmons SR. 1993.** Modulation of leaf elongation, tiller appearance and tiller senescence in spring barley by far-red light. *Plant, Cell and Environment* **16**: 555-562.
- Smith H. 1982.** Light quality, photoperception, and plant strategy. *Annual Review of Plant Physiology* **33**: 481-518.
- Spitters CJT, Van Keulen H, Van Kraalingen DWG. 1989.** A simple and universal crop growth simulator: SUCROS87. In: Rabbinge R, Ward SA and Van Laar HH, Eds. *Simulation and systems management in crop protection*. Wageningen: Pudoc, 147-181.
- Steiner AA. 1984.** The universal nutrient solution. *Proceedings of the VIth International Congress on Soilless Culture*, pp. 633-650.
- Stewart DW, Dwyer LM. 1994.** Appearance time, expansion rate and expansion duration for leaves of field-grown maize (*Zea mays* L.). *Canadian Journal of Plant Science* **74**: 31-36.
- Struik PC. 1983.** The effects of short and long shading, applied during different stages of growth, on the development, productivity and quality of forage maize (*Zea mays* L.). *Netherlands Journal of Agricultural Science* **31**: 101-124.
- Taylor DA. 1990.** Object-oriented technology: a manager's guide. Alameda: Servio.
- Tesařová J, Seidlová F, Nátr L. 1992.** Relationships between the blade and sheath growth in the same leaf and successive leaves of winter barley. *Biologia Plantarum* **34**: 325-333.
- Thiagarajah MR, Hunt LA. 1982.** Effects of temperature on leaf growth in corn (*Zea mays*). *Canadian Journal of Botany* **60**: 1647-1652.
- Tollenaar M, Daynard TB, Hunter RB. 1979.** Effect of temperature on rate of leaf appearance and flowering date in maize. *Crop Science* **19**: 363-366.
- Van Arkel H. 1978.** Leaf area determinations in sorghum and maize by the length-width method. *Netherlands Journal of Agricultural Science* **26**: 170-180.
- Van Keulen, H, Seligman, NG. 1987.** Simulation of water use, nitrogen nutrition and growth of a spring wheat crop. Wageningen: Pudoc.
- Van Loo EN. 1992.** Tillering, leaf expansion and growth of plants of two cultivars of perennial ryegrass grown on hydroponics at two water potentials. *Annals of Botany* **70**: 511-518.

- Van Loo EN, Schapendonk AHCM, De Vos ALF. 1992.** Effects of nitrogen supply on tillering dynamics and regrowth of perennial ryegrass populations. *Netherlands Journal of Agricultural Science* **40**: 381-400.
- Van Loo EN. 1993.** *On the relation between tillering, leaf area dynamics and growth of perennial ryegrass (Lolium perenne L.)*. Wageningen: PhD thesis.
- Volenc JJ, Nelson CJ. 1982.** Diurnal leaf elongation of contrasting tall fescue genotypes. *Crop Science* **22**: 531-535.
- Volk T, Bugbee B. 1991.** Modeling leaf emergence rate in wheat and barley. *Crop Science* **31**: 1218-1224.
- Vos J, Biemond H, Struik PC. 1996.** Dynamics of change of leaf attributes of Brussels sprouts in response to switches between high and low supply of nitrogen. *Netherlands Journal of Agricultural Science* **44**: 31-42.
- Warrington IJ, Kanemasu ET. 1983.** Corn growth response to temperature and photoperiod. II. Leaf-initiation and leaf-appearance rates. *Agronomy Journal* **75**: 755-761.
- Wilhelm WW, McMaster GS, Rickman RW, Klepper B. 1993.** Above-ground vegetative development and growth of winter wheat as influenced by nitrogen and water availability. *Ecological Modelling* **68**: 183-203.
- Wilhelm WW, McMaster GS. 1995.** Importance of the phyllochron in studying development and growth in grasses. *Crop Science* **35**: 1-3.
- Williams WA, Loomis RS, Lepley CR. 1965.** Vegetative growth of corn as affected by population density. I. Productivity in relation to interception of solar radiation. *Crop Science* **5**: 211-215.
- Wilson D, Cooper JP. 1969a.** Apparent photosynthesis and leaf characteristics in relation to leaf position and age, among contrasting *Lolium* genotypes. *New Phytologist* **68**: 645-655.
- Wilson D, Cooper JP. 1969b.** Effect of light intensity during growth on leaf anatomy and subsequent light-saturated photosynthesis among contrasting *Lolium* genotypes. *New Phytologist* **68**: 1125-1135.
- Yin X, Kropff MJ, McLaren G, Visperas RMA. 1995.** A nonlinear model for crop development as a function of temperature. *Agricultural and Forest meteorology* **77**: 1-16.
- Yin X, Kropff MJ. 1996.** The effect of temperature on leaf appearance in rice. *Annals of Botany* **77**: 215-221.
- Yin X, Kropff MJ, Ellis RH. 1996.** Rice flowering in response to diurnal temperature amplitude. *Field Crops Research* **48**: 1-9.

Curriculum Vitae

Huibert Jan Bos werd geboren op 9 februari 1968 te Rotterdam. Na het behalen van het diploma Gymnasium aan het Fioretti College te Lisse in 1986, studeerde hij Landbouwplantenteelt aan de Landbouwwuniversiteit te Wageningen. In juni 1992 studeerde hij af met als afstudeervakken Theoretische Produktie-Ecologie, Graslandkunde en Statistiek. In het kader van een stage werkte hij van augustus 1991 tot en met februari 1992 in Victoria, Australië, aan de Melbourne University, het Victorian Institute for Dryland Agriculture in Horsham en het Mallee Research Station in Walpeup. Vanaf mei 1992 tot en met december 1996 werkte hij als assistent in opleiding / gastmedewerker bij de vakgroep Agronomie van de Landbouwwuniversiteit. Bij deze vakgroep werd het onderzoek voor dit proefschrift uitgevoerd binnen het onderzoeksprogramma van de onderzoeksschool Produktie Ecologie. Vanaf januari 1997 is hij werkzaam bij Panfox, een adviesbureau in de informatietechnologie. Sinds mei 1997 is hij voor Panfox ingezet bij KPN Telecom als Designer.